Surficial Geologic Map of the Owlshead Mountains 30' x 60' Quadrangle, Inyo and San Bernardino Counties, California

By Christopher M. Menges and Pamela M. Cossette

Pamphlet to accompany

Scientific Investigations Map 3496

2023

U.S. Department of the Interior
U.S. Geological Survey

U.S. Geological Survey, Reston, Virginia: 2023

Suggested citation:
Menges, C.M., and Cossette, P.M., 2023, Surficial geologic map of the Owlshead Mountains 30' x 60' quadrangle, Inyo and San Bernardino Counties, California: U.S. Geological Survey Scientific Investigations Map 3496, pamphlet 46 p., 2 sheets, 1:62,500, https://doi.org/10.3133/sim3496.

Assodicated data for this publication:
Menges, C.M., and Cossette, P.M., 2023, Digital database for surficial geologic map of the Owlshead Mountains quadrangle, Inyo and San Bernardino Counties, California: U.S. Geological Survey data release, https://doi.org/10.5066/P9LSW65B.

ISSN 2329-132X (online)

Cover. View to southeast of the southern margin of southern Death Valley along the base of the northeastern range front of the Avawatz Mountains. At left and center are series of ridges within an uplifted fault-bounded block along the Southern Death Valley basin margin containing exposures of light-colored, steeply dipping, lower Quaternary to upper Tertiary alluvial sediments unconformably capped by very gently sloping darker-colored mid-Pleistocene alluvial-fan deposits, also visible in foreground. In the right and upper center of the image, the Southern Death Valley Fault Zone and associated transpressive thrust faults form the primary structural and physiographic boundary between this alluvial-basin fault block on left and the bedrock range front on right. This basin block itself is uplifted along large fault propagation folds on blind thrust faults adjacent to the southern boundary of the alluvial basin of Southern Death Valley just beyond the left margin of this view.

Contents

Figures

Surficial Geologic Map of the Owlshead Mountains 30' x 60' Quadrangle, Inyo and San Bernardino Counties, California

By Christopher M. Menges and Pamela M. Cossette

Introduction

The surficial geologic map of the Owlshead Mountains 30' x 60' quadrangle depicts the distribution and characteristics of surficial-deposit materials and neotectonic deformation for an area of approximately 5,000 square kilometers (km^2) located in the western Basin and Range Province of eastern California. The map represents a new compilation of the surficial geology that encompasses deposits within the late Pliocene to Quaternary. The map is based primarily on new mapping conducted between 2001 and 2009. Map compilation was supported by field observations distributed across the map area, combined with reference to several published and unpublished mapping sources that mostly emphasized neotectonic deformation. The surficial-deposit units included in the map follow a classification scheme that systematically denotes depositional process, relative age, and any secondary sedimentologic or morphologic characteristics. Identification, correlation, and age estimation of map units are based primarily on the relative degree of development of certain time-dependent characteristics such as surface morphology, including local dissection and surface preservation, surface clast modification, and degree of soil development; these characteristics are implicitly incorporated into unit designations. The map represents a detailed and regionally uniform synthesis of the late Neogene geology for this large area that provides a framework applicable to many interpretative studies, such as regional patterns of deposition and dissection; surface drainage development and evolution; and the distribution, style, and timing of neotectonic deformation.

The primary products of this publication are the digital and plottable renditions of the surficial geologic map and associated documentation that includes a complete listing and correlation of all map units. This pamphlet presents complete descriptions of all map units, in addition to overview descriptions of the physiography and geology of the map area, data sources used in map compilation, and summaries of select surficial-deposit and deformational features on the map. This map publication additionally includes an ArcGIS-based digital geodatabase that contains linkages of map elements to supportive locational, nomenclatural, and descriptive geologic data. The digital data components of this map compilation are contained in a separate data release platform (Menges and Cossette, 2023).

Physiographic and Geologic Setting

The Owlshead Mountains 30' x 60' quadrangle encompasses an area commonly associated with the Mojave Desert area of eastern California (fig. 1). However, the quadrangle extent actually straddles a key physiographic and tectonic transition between the western Basin and Range Province, which includes central Death and Panamint Valleys to the north, and the north-central and northeastern Mojave Desert region to the south. The central physiographic feature in the map area is the northwest-trending lowland of southern Death Valley (fig. 2). This is the southernmost extension of the overall regional Death Valley system, although the southern part of the valley in the map area is a gently sloping trough surrounded by low- to moderate-relief highlands that contrast with the low-elevation salt-encrusted valley floors and steep, rugged, and higher-altitude mountains that surround the better known central Death Valley basin to the north (for example, Slate and others, 2000; Workman and others, 2002a, b; Slate and others, 2009). Southern Death Valley merges to the south and east into Valjean and Silurian Valleys within the northeastern Mojave Desert province. To the northeast of the axial valley of southern Death Valley lie a series of upland basins and intervening ranges that extend northwestward from the southwestern Great Basin region of the southernmost Nevada and east-central California border region. This area includes, from west to east, the southern sections of the Greenwater, Chicago, and California Valleys and Tecopa valley. These valleys are separated by the intervening southern parts of the southern Black Mountains, the Ibex Hills, the Dublin Hills, the southern Resting Spring and Nopah Ranges, and the western Kingston Range. The actual physiographic boundary between these basins and ranges relative to southern Death Valley to the southwest follows a topographically continuous highland area that comprises the southernmost Kingston Range, Sperry Hills, and southern Ibex and Black Mountains and intervening valleys informally termed the “Tecopa hump” (McMackin, 1997, 2001; Miller and others, 2007). Southern Death Valley is bordered on the west, southwest, and south by several mountainous highlands including the southern Panamint Range, the Owlshead Mountains, and the western and central Avawatz Mountains. Each of these highlands is separated by and (or) includes

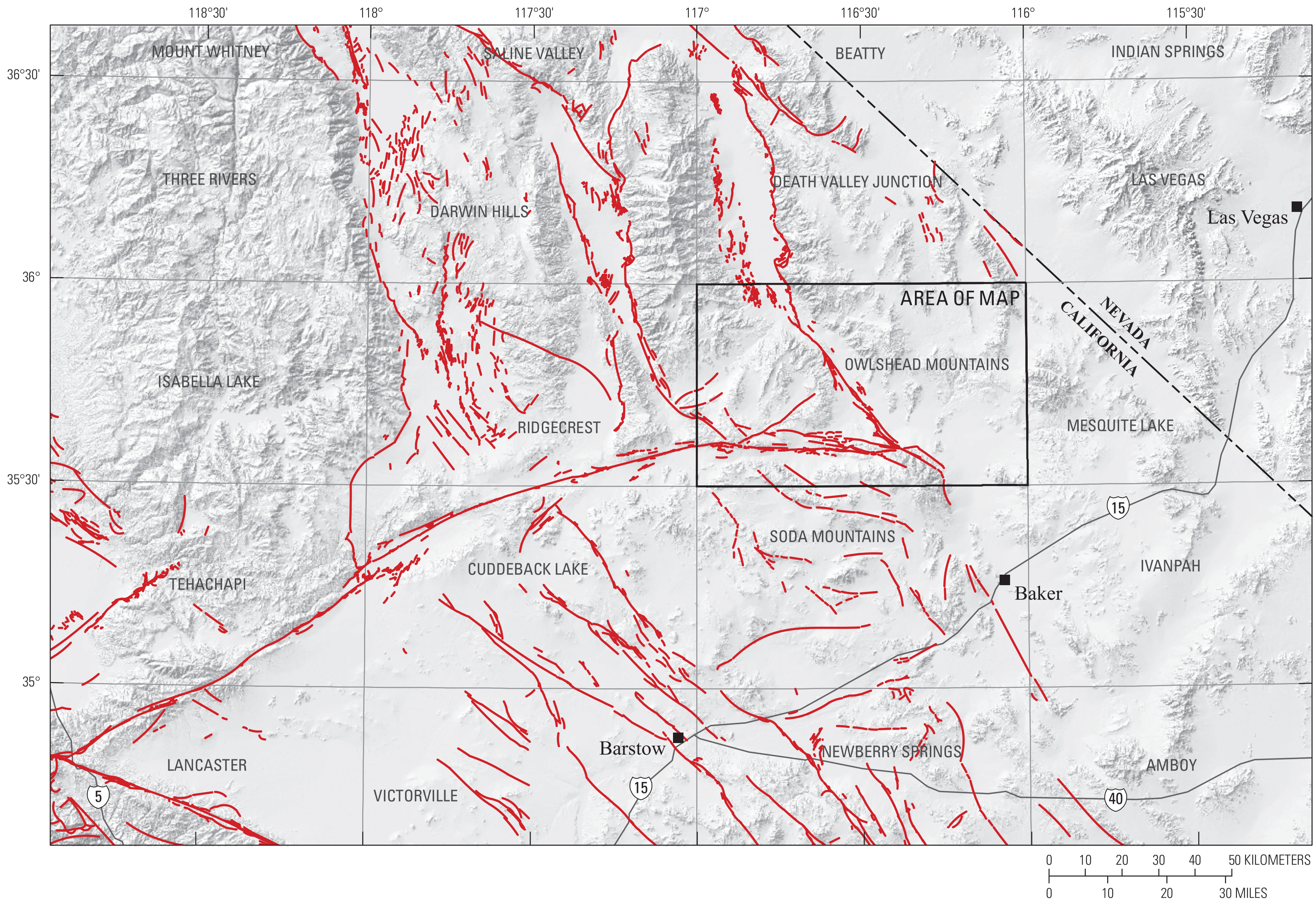

Figure 1. Shaded-relief map showing the location of Owlshead Mountains 30' x 60' quadrangle (black outline), California, relative to surrounding 30' x 60' quadrangles (gray outlines and labels), as well as regional Quaternary faults (red lines; from Bryant, 2005) and select major highways and cities. 10 meter shaded-relief base from U.S. Geological Survey, The National Map (available at https://www.usgs.gov/core-science-systems/national-geospatial-program/national-map).

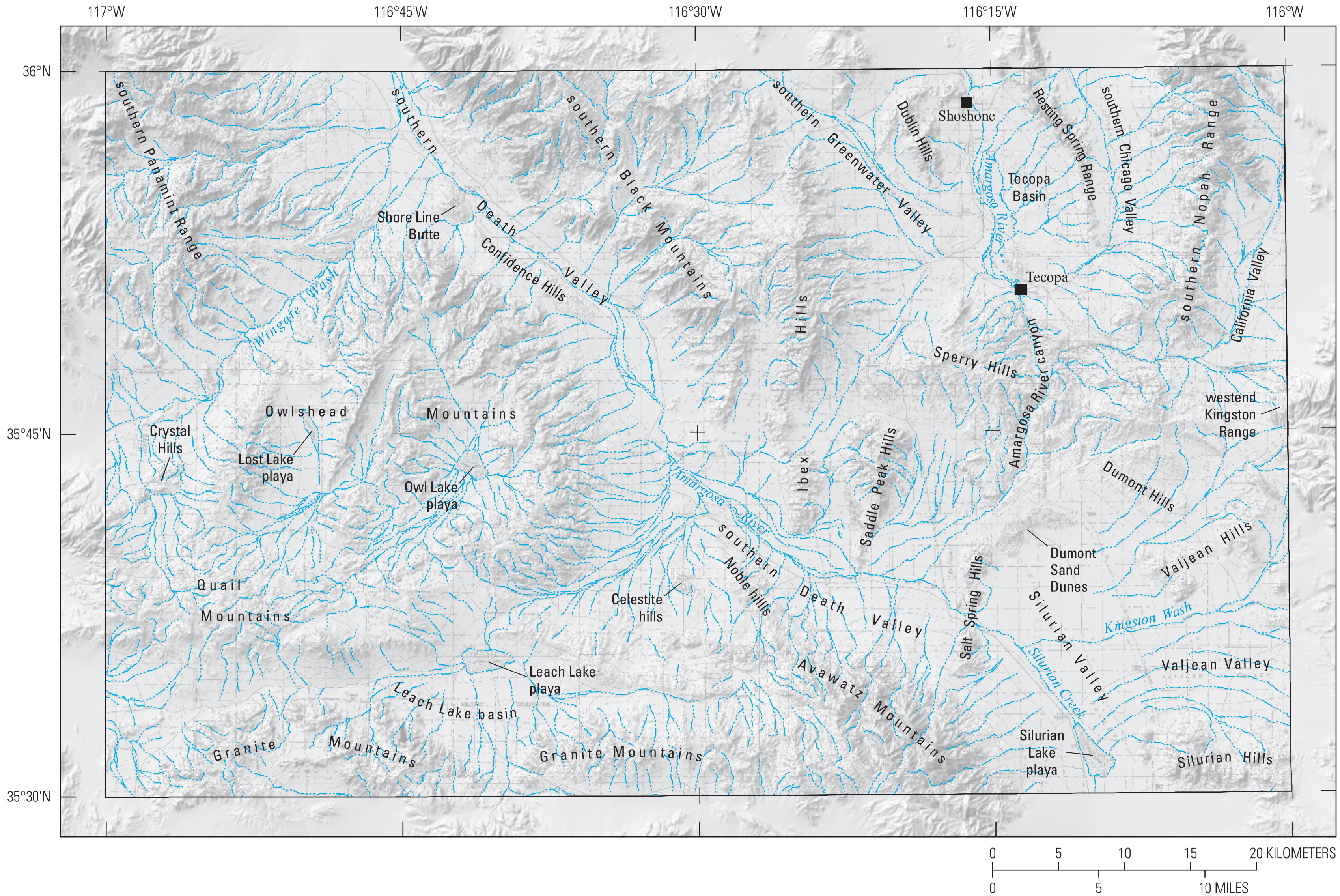

Figure 2. Shaded-relief map of the Owlshead Mountains 30' x 60' quadrangle, California, showing the names of selected physiographic features, towns, and intermittent hydrographic stream network (blue). 10 meter shaded-relief base from U.S. Geological Survey, The National Map (available at https://www.usgs.gov/core-science-systems/national-geospatial-program/national-map).

several lowland areas that, other than Wingate Wash and eastern Leach Lake basin in the southwestern area, are relatively small, isolated, and internally drained subbasins.

Altitudes in the map area vary from 1,876 meters (m; North American Vertical Datum [NAVD] 88) in the eastern Avawatz Mountains to –50 m along the axis of southern Death Valley. However, most of the map area outside of southern Death Valley occupies altitudes exceeding 500 m. The average climate ranges from arid, with extremes of hyperarid in the lowest altitudes of axial southern Death Valley, to semiarid in the higher elevation part of mountain ranges (Ries and others, 2017). Precipitation in the area lies within a gradational boundary between Mojave (winter polar jet stream) and Sonoran (mixed winter polar jet stream and summer monsoonal) climatic patterns, although most of the rainfall typically occurs in the winter months (Hereford and others, 2003, 2006).

The physiography and geology of the Owlshead Mountains quadrangle reflects its position straddling the boundaries among three late Neogene tectonic provinces. The series of north- to northeast-trending valleys in the northeastern part of the map area lie within the southern Walker Lane deformational belt of the southern Great Basin section of the Basin and Range Province. This belt is dominated by mostly Miocene to Pliocene, but locally Quaternary, range-bounding normal faults intermixed in places with Miocene to Quaternary strike-slip faults that are mostly located to the northeast of the map (Workman and others, 2002b). Many of the basins formed by extension during the Pliocene to Miocene along normal faults that produced variably deep bedrock basins defined by potential-field geophysical surveys (Blakely and others, 1999; Blakely and Ponce, 2001) and seismic reflection data (Serpa and others, 1988; Scheirer and others, 2010). The southeastern part of the map (for example, Silurian Valley, Silurian Hills, and Valjean Hills) is in the mostly tectonically inactive northeast section of the eastern Mojave Desert (Dokka and Travis, 1990; Bedford and others, 2010).

The major valleys and ranges in the central and western parts of the map (including southern Death Valley, the southern Black Mountains, and ranges to the west and south) lie within the tectonically active eastern section of the northwest-trending Eastern California Shear Zone (ECSZ). This zone is characterized both geologically and geodetically by significant active right-lateral shear (Dokka and Travis, 1990; Miller and others, 2001; Dixon and others, 2003). The ECSZ within the map area may be subdivided into two tectonic subprovinces across a boundary defined by the eastern section of the Garlock Fault Zone. The south-central and southwestern-most areas of the map to the south of the Garlock Fault Zone lie within the northeastern Mojave Desert subprovince, a distinct region in the northeastern Mojave Desert characterized by a series of east-striking left-lateral transcurrent faults that show secondary transpressive deformation (Schermer and others, 1996; Pavlis and others, 1998; Miller and Yount, 2002; Miller and others, 2014). The area to the north of the eastern Garlock Fault Zone is contained within the southwestern Basin and Range subprovince, which is a major extensional to transtensional zone characterized by a series of interacting systems of north-northeast- to north-northwest-trending normal faults and northwest-trending dextral transcurrent faults that collectively produce the large alluvial basins of Death and Panamint Valleys between intervening bedrock ranges of the Black, Panamint, and Owlshead Mountains.

The western part of the map to the north of the Garlock Fault Zone lies within that part of the southwestern Basin and Range subprovince located within the eastern margin of the ECSZ. Neotectonic deformation in this area has traditionally been associated with a series of right-lateral strike-slip faults, locally associated with secondary transpressive and extensional deformation, that is concentrated in southern Death Valley (Brady, 1984, 1986; Troxel, 1986a; Brogan and others, 1991; Knott, 1999; Knott and others, 2005). An exception occurred in the Wingate Wash area, however, where Luckow and others (2005) and Pavlis and others (2012) showed that deformation consisted of a complex mix of sinistral, dextral, normal, and contractional faults that varied in activity over time. New data presented in this map indicate that the complex deformation described by Luckow and others (2005) and Pavlis and others (2012) in the Wingate Pass area is a more regionally pervasive characteristic of neotectonic deformation throughout most of the area of the ECSZ within the western and southeastern Owlshead Mountains quadrangle (Menges and others, 2005, 2006). The regional contraction component is expressed not only by discrete contractional structures, such as folds, fault-related folds, and thrust faults commonly occurring along or adjacent to strike-slip fault systems, but also by diffuse zones of uplift commonly localized near intersections of large translational faults (for example, north-central Avawatz Mountains and southern Quail Mountains) and regional areas of active downwarping and arch-like uplift such as southern Death Valley trough and Tecopa hump (Miller and others, 2007).

A number of previous studies have defined the pre-Quaternary geologic history of the map area (for example, Muehlberger, 1954; Noble and Wright, 1954; Wright, 1954, 1976a, b; Wright and Troxel, 1954, 1967, 1973, 1984, 1999; Jennings and others, 1962; Noble and others, 1963; Brady, 1984, 1986; Troxel, 1986a; Thompson and others, 1999; Serpa and Pavlis, 1996; Workman and others, 2002a, b; Luckow and others, 2005; Miller, 2005; Fridrich and Thompson, 2011; Pavlis and others, 2012, 2014). The pre-Quaternary geology for some areas of the map was primarily derived from unpublished maps by B. Troxel (California Geological Survey and University of California, Davis, 1980–1995), L.A. Wright (Pennsylvania State University, 1980–1995), R.H. Brady, III, (University of California, Davis, 1980–1985, and California State University, Fresno, 1985–2000), and M.R. McMackin (Lettis Consultants International, 1999–2005). These studies and maps collectively document a complex assemblage of metamorphic and igneous rocks forming the early Proterozoic basement that is in places overlapped by a variably metamorphosed sequence of upper Proterozoic carbonate and siliciclastic strata. Deposition of a thick series of unmetamorphosed marine carbonate and siliciclastic sedimentary rock continued throughout the late Proterozoic to Permian and represents a long-lived miogeoclinal passive margin present during this time. These miogeoclinal strata are folded and thrust-faulted by probable early to late Mesozoic regional crustal shortening events. The early stages of development of a magmatic arc are represented in places by a sequence of Triassic to possibly Jurassic metavolcanic rocks. This early developmental stage was followed by intrusion of Jurassic to Cretaceous plutonic rocks ranging from diorites to granites that marked the development of the roots of the main Sierran magmatic arc. After Late Cretaceous tectonic extension and a subsequent long interval of early Tertiary(?) uplift and erosion, major localized areas of sedimentation and (or) volcanism began in the middle to late Tertiary. Volcanism consisted of intermixed lava flows, ash-flow tuffs, and local extrusive centers, ranging from silicic to intermediate in composition, that were coeval with intrusion of Miocene granitic intrusive rocks at relatively shallow mid- to upper-crustal depths. The area experienced major regional-scale low-angle detachment faulting, extension, and tectonic denudation that in places exposed Tertiary granites and mid-crustal ductile fabrics. Most of the Tertiary basins and volcanic centers also experienced varying, but commonly significant, amounts of coeval to post-formational extensional deformation characterized by complex networks of normal to strike-slip faults. Our mapping demonstrates that some localized areas such as southern Death Valley and adjoining highlands experienced a variable, but locally significant and even dominant, contractional component of deformation as well.

Previous Quaternary Studies

Surficial Deposits

A relative paucity of published studies in the map area incorporates consistent and detailed mapping of surficial deposits, compared to those focused on pre-Quaternary geology. Most of these few works are located in the eastern and northeastern section of the Owlshead Mountains map area, including Chicago Valley, Tecopa basin, and parts of California Valley (for example, Hillhouse, 1987; McKittrick, 1988). Green (2009) completed a detailed map of surficial deposits as part of a thesis study along a section of the southern Death Valley Fault northwest of the Noble hills. Yount and others (1994) developed the original classification scheme for surficial deposits in the Valjean and Silurian Valleys that forms the basis for surficial mapping throughout the map area. Miller, D.M., and Yount, J.L., (U.S. Geological survey, unpublished mapping, 1985–2000) subsequently applied their classification scheme to detailed unpublished surficial mapping of the area, which we simplified further in that part of the southeastern corner of the map area. Most of the other geologic investigations in the area emphasized older, pre-Quaternary rocks with only generalized depiction of Quaternary units; however, several studies did present important stratigraphic and map data on select Pliocene to Quaternary stratigraphic units in various parts of the Tecopa basin (Morrison, 1999) and southern Death Valley (Wright and Troxel, 1984; Troxel, 1986a, b; Beratan and others, 1999; Green and others, 2007; Green, 2009; Knott and others, 2018). The regional mapping of Workman and others (2002a) included a generalized and simplified scheme of surficial deposits across the entire map area. Several 30’ x 60’ geologic maps adjacent to or near the map area contain detailed surficial-deposit mapping generally comparable to or even similar to this quadrangle mapping in level of detail and unit classification schemes (Slate and others, 2000, 2009; Bedford, 2003; Page and others, 2005; Schmidt and McMackin, 2006; Bedford and others, 2010).

Neotectonic Studies

Neotectonic (late Pliocene to Pleistocene) deformation has been examined in much greater detail relative to surficial deposits within the Owlshead Mountains map area. Many of the early studies were conducted in the 1970s and 1980s and focused on neotectonic deformation along the northern range front of the Avawatz Mountains and the Southern Death Valley Fault Zone, in and adjacent to southern Death Valley, as well as in the eastern section of the Garlock Fault (Clark, 1972; Davis and Burchfiel, 1973; Spencer, 1981, 1990a, b; Brady, 1984, 1986; Butler, 1984; Wright and Troxel, 1984; Troxel, 1986a, b; Butler and others, 1988). Much additional subregional-scale unpublished mapping by B. Troxel (California Geological Survey and University of California, 1980–1990), R.H. Brady, III, (University of California, Davis, 1980–1990), and P.R. Butler (University of California, Davis, 1975–1985) delineated neotectonic deformation on these structures. These studies collectively documented Quaternary tectonic activity on strike-slip and normal faults in this area but also demonstrated a significant component of contractional deformation, including thrust faults, transpressive structures, and folding within southern Death Valley proper that is anomalous relative to regional deformation patterns dominated by significant extension in terrain to the north and west. A number of more recent studies have emphasized definition of the location, deformation patterns, and timing relations for the most recent surface ruptures on the major active fault zones in the map area, such as the Avawatz Mountains Thrust Fault system (Stroud and McGill, 1994; Mendonca, 2007; Miller and others, 2007), the Southern Death Valley Fault Zone and normal faults in Death Valley to the north (Wills, 1989a, b; Brogan and others, 1991; Dooley and McClay, 1996; Klinger, 1999; California Geological Survey, 2000a–e; Miller and others, 2007; Sohn and others, 2007; Menges, 2008; Green, 2009; Caskey and others, 2010), and the eastern Garlock Fault Zone (McGill, 1994a, b; California Geological Survey, 2000f–k). Other previous works have examined the structural framework and character of surface deformation of less-well-known faults and folds in the map area, including in Chicago Valley (McKittrick, 1988), the Tecopa hump (McMackin, 1997, 2001; Miller and others, 2007), the Tecopa basin (Morrison, 1999), the western and northern Owlshead Mountains (Luckow and others, 2005; Pavlis and others, 2012), and the northern Granite Mountains and basins in the northeastern Mojave Desert to the south (Schermer and others, 1996; Pavlis and others, 1998; Miller and Yount, 2002; Miller and others, 2014). These investigations have documented the widespread distribution and complexity of neotectonic deformation in the area and, particularly, in southern Death Valley and regions to the west that provide a foundation for the regional mapping and compilation of these features shown on this map.

Mapping Methods

This map (map sheet 1) is derived from new mapping, compiled at a scale of 1:62,500, focusing on Neogene to Quaternary surficial geology, including both time-stratigraphic surficial map units and neotectonic structures in the 30' x 60' Owlshead Mountains quadrangle. Pre-Pliocene bedrock units are mapped as substrate classified into nine generalized rock types that are influential in the production and transport of detritus incorporated into the surficial deposits in the region. Pre-neotectonic structures that appear primarily associated with earlier deformation were not compiled as part of this map. Our primary mapping method consisted of a combination of original mapping and compilation of units and structures, supported in many areas by field traverses and, supplemented with published and unpublished data sources where available in selected sections of the map.

More specifically, map features were initially photogrammetrically identified on aerial photography using uniform coverage by National High Altitude Photography (NHAP) black-white aerial photography imagery at 1:60,000 nominal scale. This mapping was then digitally compiled manually using standard ArcGIS software (ESRI, 2009, ArcMap, ver. 9.3.1) on a georeferenced, orthophoto-quadrangle base map provided by a digital mosaicked suite of standard photorectified black and white Digital Orthophoto Quarter Quadrangle imagery. Supplemental reference during map compilation was made to: (a) specially processed Landsat 7 imagery, specifically natural-to near-Infra red color images processed by National Agriculture Imagery Program imager, with procedures applied and developed by Dohrenwend (2001), that was available only for the San Bernardino County area in the central and southern sections of the map; (b) a standard mosaicked suite of 10-m Digital Elevation Models (DEMs) derived from standard national DEM data; and (c) selected locations of augmented high-resolution lidar-derived DEM data within restricted strip maps along several major faults (for example, eastern Garlock and Owl Lake Fault Zones) from Earthscope Southern & Eastern California LiDAR project, 2009. All contacts between surficial units, including stratigraphic, topographic, and structural boundaries, were digitized in original form at typical expanded-screen scales of 1:10,000 to 1:20,000, although larger scales to 1:2,000 to 1:3,000 were used locally to determine the relation of surface deformation to specific surficial deposits.

Several published and unpublished maps, reports, and articles were used as references in the digitization of structures in some areas primarily located in the central and western part of the map area (see figure 3 for mapping sources). However, no single referenced structural features were directly scanned and incorporated in original form digitally into the map but, instead, were used only as guides for interpreting the originally digitized structure within the map compilation. Some structures shown on original sources were modified, adjusted, and (or) reinterpreted to varying degrees during the digitization process for this map on the basis of either interpreted relations on imagery and (or) field observations for given or nearby similar features. All the pre-Quaternary bedrock substrate units and structures were compiled in a more generalized manner, relative to the more detailed and independent interpretations of all surficial deposits on this map. The compilations of these pre-Quaternary rocks primarily were based on reference to the outside sources, which in most cases consisted of relevant sources depicted in figure 3, supplemented in the remaining uncovered areas by the regional map compilation of Workman and others (2002a). Unit boundaries for some of these pre-Quaternary units were modified to varying, but usually minor, degrees based on reference to other remote-sensing data such as processed Landsat 7 or derivative DEM imagery.

The primary map compilation of surficial map units and neotectonic deformation relied strongly on field observations at sites along a series of traverses distributed throughout most of the map area, with a major exception located in extremely remote and inaccessible regions in the west-central and northwestern map areas (fig. 4). At each field site, data were collected at detailed to reconnaissance levels on surficial deposits and, where present, any neotectonic deformation. A variety of field data was collected on surficial deposits at a given site, usually with reference to associated aerial photography and relevant remote-sensed imagery. These data included relations to adjacent units; development and depth of internal and external drainages; textures and compositions of clast lithologies; sedimentological textures; unit thicknesses, where observable; characteristics of original and (or) modified surfaces (for example, development of bar and swale topography, pavements, varnishing, and physical weathering of surface clasts); horizonation, characteristics, and depth of soil development; and type and distribution of associated vegetation. Data on near-surface soils and sedimentology were collected systematically in shallow pits dug on undisturbed surfaces at most field sites; additional observations of deposits, surface soils, and buried paleosols were taken at greater depths where naturally exposed along nearby wash banks or surface-unit margins. Field observations on surface deformation, and especially faults, included structural data on geometry and kinematics, morphology of associated tectonic landforms, displacement characteristics, relations to other structures, and identification of affected and unaffected surficial deposits that could be applied to define the style, amounts, and age relations of the deformation. All field-site locations were recorded by portable Global Positioning System (GPS) units to a spatial accuracy of ±5 to 10 m. All field data were directly integrated (1) as input to constrain and calibrate the classification and age estimation of surficial-deposit map units and deformation features during map compilations and (2) to provide the basis for supportive materials such as the correlation scheme, map listing, and description of map units.

Basis for Mapping Surficial Units

Surficial map units are classified and mapped on the basis of genesis (including depositional process) and relative age assignments. Most of these map units are surficial deposits, although a few are erosional features commonly associated to some degree with overlying surficial deposits. These basic mapping classification schemes have been developed over many years for surficial-deposit mapping in semiarid to arid regions, as summarized by Bull (1991). The first unit characteristic, genesis, or process of formation is commonly assessed for a given depositional or erosional surficial map unit on the basis of several physical characteristics, including sedimentology (texture, fabric, layering), geomorphologic morphology, stratigraphic relations, and landscape or geomorphic position. These characteristics are used to infer

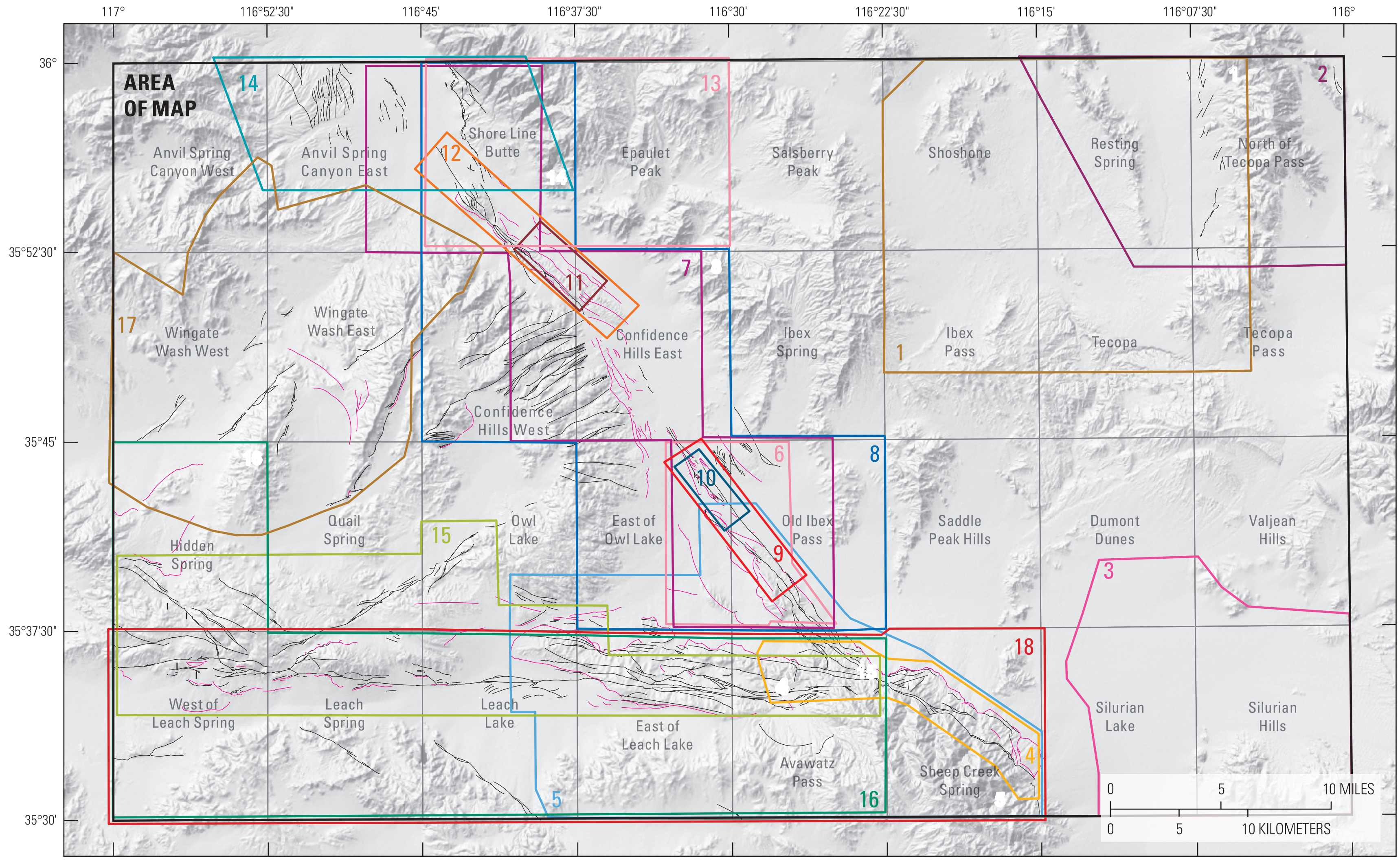

EXPLANATION

Mapping sources

1 Hillhouse, 1987
2 McKittrick, 1988
3 Miller, D.M., and Yount, J.L., U.S. Geological Survey., unpublished mapping, 1985–2000
4 Troxel, B.W., California Geological Survey and University of California, Davis, and Butler, P.R., (Unitversity of California, Davis), unpublished mapping, 1980–1988
5 Brady, R.H.,III, San Jose State University in University of California,1986
6 Troxel, B.W.,California Geological Survey and University of California, Davis, unpublished mapping, 1980–1988
7 Wills, 1989a
8 California Geological Survey, 2000a–e
9 Green, 2008
10 Troxel, B.W.,California Geological Survey and University of California, Davis, 1986
11 Troxel.B.W.,California Geological Survey and University of California, Davis), and Butler, P.W. (Unitversity of California, Davis, 1986a
12 Dooley and McClay, 1996
13 Wright and Troxel, 1984
14 Brogan and others, 1991
15 Clark, 1972
16 California Geological Survey, 2000f–k
17 Luckow and others, 2005
18 Schermer and others, 1996

Figure 3. Shaded-relief map with structures (red folds, black faults) from current study showing area coverage of published and unpublished maps that served to guide compilation of surficial geology (mostly neotectonic deformation) in the Owlshead Mountains 30' x 60' quadrangle, California. Quadrangle boundaries and labels (gray) of 7.5' quadrangle maps are labeled as follows: 10 meter shaded-relief base from U.S. Geological Survey, The National Map (available at https://www.usgs.gov/core-science-systems/national-geospatial-program/national-map).

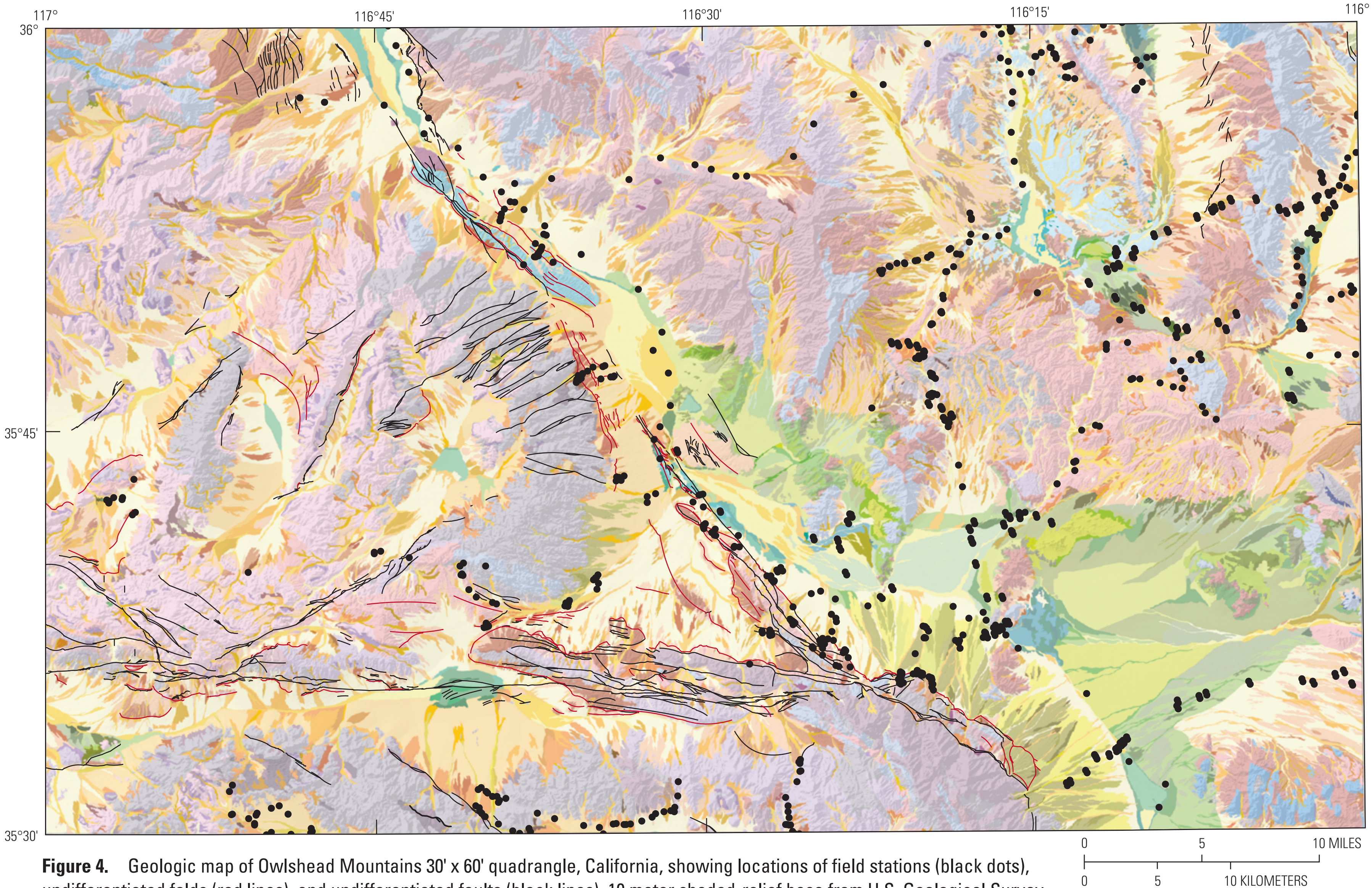

Figure 4. Geologic map of Owlshead Mountains 30' x 60' quadrangle, California, showing locations of field stations (black dots), undifferentiated folds (red lines), and undifferentiated faults (black lines). 10 meter shaded-relief base from U.S. Geological Survey, The National Map (available at https://www.usgs.gov/core-science-systems/national-geospatial-program/national-map).

the primary mode of deposition and formational environment for surficial deposits, which provide the initial hierarchical component in the unit classification scheme. The second unit characteristic, general age classification, is estimated primarily for depositional units on the basis of specific recognizable physical characteristics and associated features that have at least a partial time-dependent progression in their mode and degree of development. Chief among these are (1) surface characteristics, such as preservation and (or) degree of modification of original depositional form or microtopography, development of desert pavement and vesicular A (Av) horizons, degree of varnishing, and amount of physical weathering of clasts (Bull, 1991) and (2) the degree of soil development, focusing on key soil properties and characteristics that can be interpreted in the field for post-depositional age of desert soils (for example, degree of alteration of parent material; accumulation of secondary materials such as eolian sand and silt, illuvial clay, and (or) pedogenic carbonate or silica; and profile depth and horizonation characteristics [Birkeland, 1999]). Many of these soil and surface characteristics are also sensitive to other controlling factors such as parent material, climate, vegetation, and topography; however, the effects of time can commonly be extracted to estimate at least approximate deposit ages (Bull, 1991; Birkeland, 1999).

Many studies present stratigraphic and geochronologic data for surficial deposits within the region surrounding the Owlshead Mountains quadrangle (for example, Reheis and others, 1989; Wells and others, 1990; Menges and others, 2001; Workman and others, 2002a; Mahan and others, 2007; Menges and Miller, 2007; and Slate and others, 2009). These investigations provide valuable regional stratigraphic context, including local and regional patterns of depositional characteristics and process, geomorphic surface development, and soil stratigraphy, for the surficial-deposit units in the map. Many studies also contribute numerical age data for surficial deposits using several geochronologic techniques such as radiocarbon, luminescence dating, cosmogenic exposure, and uranium series methods. The undated surficial deposits in the map area are assigned to the generalized age ranges by careful property-based correlations of these deposits with these reference-dated sequences. Available age control is specifically cited in the map unit descriptions. Several of these studies lie within the map area, including Tecopa basin (Morrison, 1999; Nelson and others, 2001), the Amargosa Canyon reach of the Amargosa River (Anderson, 2005); southern Death Valley (Anderson and Wells, 2003a; Sohn and others, 2007; Green, 2009); Salt Spring Hills groundwater-discharge site (Anderson and Wells, 2003b; Bright and Anderson, 2007); and Valjean, Silurian, and California Valleys (Yount and others, 1994; Green and others, 2007; Mahan and others, 2007; Menges and Miller, 2007; Schmidt and Menges, 2007; Smith, 2007). Many others lie outside the map in the surrounding region (Reheis and others, 1989; McDonald and others, 1995; Bedford, 2003; Wells and others, 2003; Whitney and others, 2004; Jayko, 2005, 2009; Page and others, 2005; Frankel and others, 2007, 2015; Jayko and others, 2008; Machette and others, 2008; Bedford and others, 2010). Some studies have applied stratigraphic, paleomagnetic, and (or) tephrochronologic methods for Pliocene and Quaternary stratigraphic sequences in and near the map area (Sarna-Wojicicki and others, 1984; Troxel and others, 1986; Hillhouse, 1987; Beratan and others, 1999; Knott, 1999; Morrison, 1999; Knott and others, 2005, 2018; Green, 2009).

Explanation of Map Units

The basic system of map units follows previous work and mapping by Yount and others (1994), Schmidt and McMackin (2006), Menges and Miller (2007), and Bedford and others (2010). This system is similar to the map-unit schemes used by other published mapping studies in the region (for example, Menges and others, 2001), although it does add several features such as composite units, erosional surfaces, and secondary characteristics not generally used by many other schemes.

Singular Map Units

The fundamental type of surficial-deposit unit included in this map is the singular unit that contains only one unit designation per mapped area. The nomenclature for basic singular-unit labels sequentially identifies the age, depositional process, and any select secondary characteristics (for example, grain size, composition, depositional form) for that unit. The first one to two characters in the unit label denote the time period (Q or QT), the next character refers to relative age (a, active; y, young; i, intermediate; o, old), the next one to two characters indicate depositional-process type, depending on whether the unit includes a single or mixed process type (a, alluvial fan; e, eolian; ae, mixed alluvial and eolian) and, in some cases, a final character denotes secondary characteristics (g, composed of grus; d, debris flow; r, sand ramp). The singular units are assigned to groups based on the depositional-process category, including both unique and mixed-process types. Individual units are then arranged within each primary grouping—first by relative age and then followed by any secondary characteristics.

Composite Map Units

This map defines three categories of composite units that are combinations of the singular map units, represented as a single unit label for a given map area. Two categories are applied to surficial deposits: (1) veneered composite units indicate a thin veneer or mantle of a given surficial deposit, listed to the left of a slash (/), followed to the right of the slash by an underlying surficial deposit or substrate material (for example, units Qye/Qia, Qha/fp) and (2) combined units include a linked series of two singular units. They are applied to map areas with at least two singular units that are either too small in size and (or) complexly intermixed to be identified individually at map scale. The resulting combined unit label consists of each individual unit separated by a plus (+) sign; the dominant unit (as much as 80 percent of the area) is listed first, followed by the secondary unit (as little as 20 percent of the area). For example, unit Qya+Qia denotes an area containing a mixture of both unit Qya and unit Qia deposits, with Qya deposits spatially dominant relative to Qia but with no other deposits exceeding 20 percent coverage. The many combinations of singular map units identified on this map produce a large number of combined units. These composite units are arranged in the Correlation of Map Units and the Description of Map Units within four subgroups based on the relative age ranges of the individual components: combined surficial-deposit map units that have approximately similar age ranges (for example, unit Qia+Qig); combined surficial-deposit map units that have approximately sequential age ranges with no detectable age-range gaps (for example, unit Qaw+Qya); combined surficial-deposit map units that have different age ranges with at least one discernible age-range gap (unit Qya+Qoa); and one surficial-deposit map unit combined with discontinuous exposures of an underlying pre-Quaternary substrate material (unit Qia+fv). (3) A third category of composite unit is used to delineate pediment erosional surfaces that are commonly associated with variably discontinuous thin exposures of overlying surficial deposits. These surfaces are defined by two-unit labels separated by a hyphen (-). The first label defines the general age (Q undifferentiated) followed by the degree of incision of the pediment and any surficial-deposit veneers; whereas, the second unit label indicates the type of substrate material beveled by the pediment. Thus, unit Qpi-fp indicates a partially exposed and incised pediment surface cut across felsic plutonic rocks.

Substrate Units

Substrate materials refer to exposed pre-Quaternary rocks that are not identified by specific formation or age but rather by nine general rock types considered important to the production and transport of source material for mapped surficial deposits. Unit labels for the substrate materials listed in boxes without color in the Correlation of Map Units and the List of Map Units (map sheet 2) indicate the basic bedrock rock types underlying mapped surficial units. On the map itself, the substrate units are combined as components of either a veneered or combined composite unit; the map unit shows the color of the surficial cover unit.

Neotectonic Deformation

This geologic map depicts a complex and diverse pattern of neotectonic deformation that includes a complicated array of dozens of discrete fault and fold structures (fig. 5). Much of this deformation is complexly distributed throughout the southern and western part of the map area, with a pronounced concentration in both density and complexity of deformation in southern Death Valley and the areas to the south and west between Wingate Wash and the Avawatz Mountains (figs. 2 and 5) along the eastern margin of the ECSZ. Many of the structures in this region are transcurrent faults with both right-lateral and left-lateral senses of slip. However, this mapping has confirmed not only the presence of significant contractional strain indicated by thrust faults and folds as described in previous studies (for example, Brady, 1984; Wright and Troxel, 1984; Troxel, 1986a, b; Spencer, 1990a, b; Pavlis and others, 1998; Luckow and others, 2005; Menges and others, 2005, 2006; Caskey and others, 2010), but it has expanded the spatial extent, scale, and complexity of the contractional features across the region. In contrast, the north-central and northeastern parts of the map to the east and north of the Tecopa hump border of southern Death Valley contain only relatively minor neotectonic deformation that is limited to a few spatially restricted sets of normal faults in the northeasternmost corner of the map (fig. 5).

Several meso- to regional-scale neotectonic structures depicted in this map were originally identified in previous studies, although the character and tectonic framework of many of these features have been reinterpreted in this study. Some new deformational elements were identified during the course of mapping as well. The final structural scheme for neotectonic deformation in the map area consists of four major categories of faults and three types of fold structures that are commonly arranged along discrete zones or corridors distributed throughout the western and southern parts of the map area (fig. 5). Major types of faults include (1) dextral and dextral-oblique transcurrent fault zones, commonly steeply dipping (≥70–90°) with northwest average strike azimuths (300–330°), that are included or are subparallel to the Southern Death Valley and southern Panamint Valley Fault Zones; (2) sinistral and sinistral-oblique transcurrent faults, also similarly steeply dipping (≥70–90°), but with contrasting east-southeast to northeast strike azimuths (45–110°) that are commonly, but not uniquely, associated with the eastern Garlock and Owl Lake Fault Zones; (3) normal faults with moderate to steep dips and mostly north-northwest to north strike azimuths (330–360°) located mainly in a few concentrated zones in southern Death Valley and eastern Chicago Valley in the northwest and northeast corners of the map; and (4) thrust and reverse faults, with variable strikes and shallow to steep dips, commonly distributed adjacent to and (or) between major transcurrent fault zones. A variety of fold structures include many zones of fault-generated anticlinal folds, commonly asymmetric in profile with sinuous branching axes that locally overlie exposures of subjacent shallowly buried blind-thrust to reverse faults; a few independently formed, mostly upright and symmetric anticlinal folds structures; and elongate homoclinal blocks of tilted sedimentary deposits, with steep to moderate cross-sectional dips and variably striking laterally truncated upper and lower boundaries, that collectively resemble the rotated limbs of fault-dismembered folds. Many of these major structures are additionally associated with complex, spatially variable zones of smaller-scale deformation that commonly indicate locally significant areas of secondary transpression. Stratigraphic and tectonic geomorphic relations in some areas suggest isolated to interlinked zones of diffuse subregional uplift and subsidence that, although interspersed among some of the larger discrete deformational zones described above, are not themselves clearly linked structurally to any specific mappable surface structures. Each of these major groups of structures is summarized below relative to key areas of primary development.

The ages of many structures compiled in this map are directly constrained by stratigraphic constraints related to the presence or absence of deformation observed in various surficial units of known or estimated age along the feature. Many of these structures also are associated with tectonic landforms such as fault scarps, stream deflections, popup structures, and (or) shutter ridges that indirectly can be used for estimation of the age of surface deformation. Other fault-related structures that have no direct age control are less reliably included within the map compilation on the basis of their spatial and (or) geometric association with neotectonic structures that have better age control.

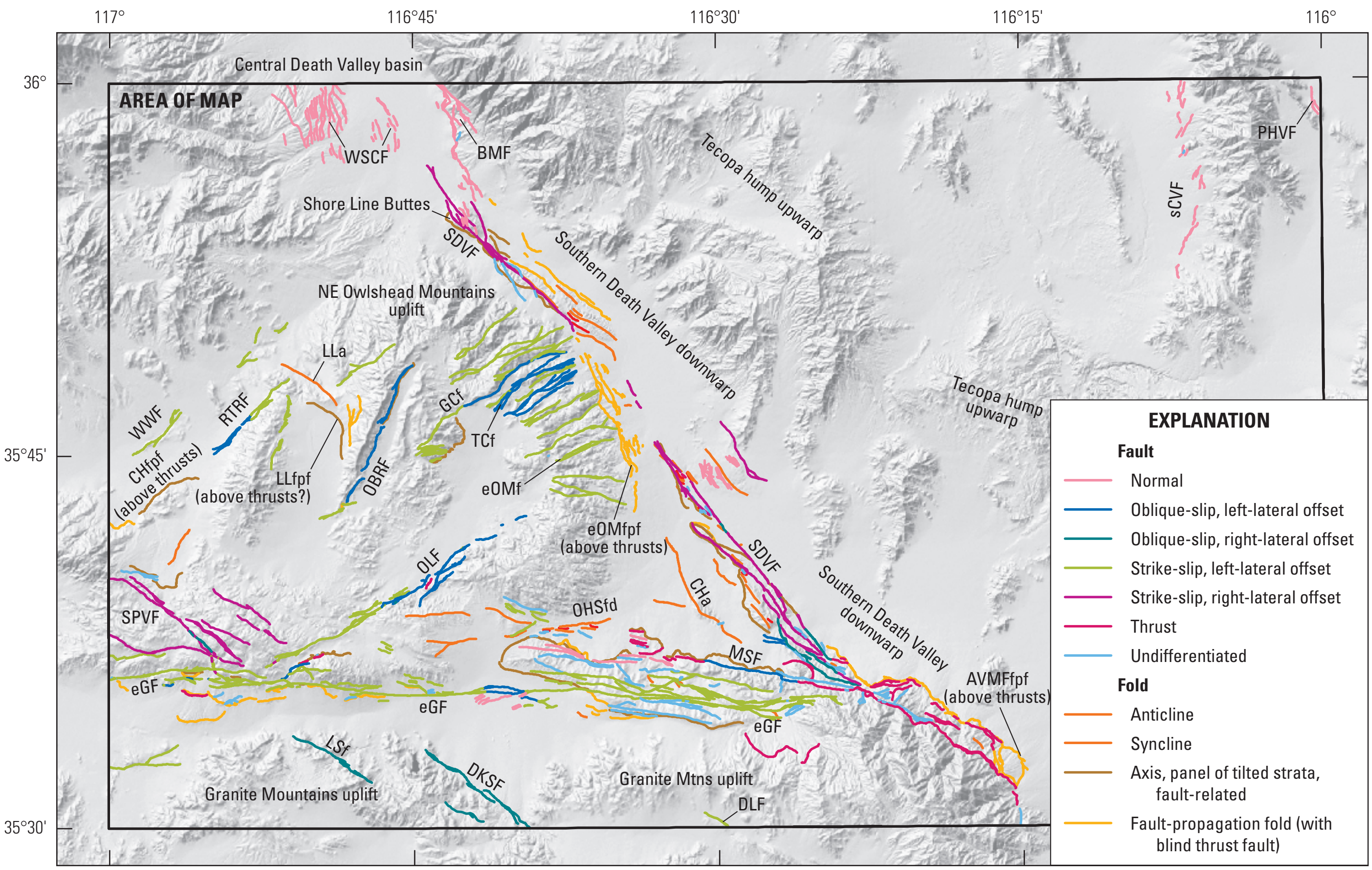

Figure 5. Shaded-relief map showing neotectonic deformation in the Owlshead Mountains 30' x 60' quadrangle, California, focusing on the location and types (color coded) of faults and folds. Regional features of uplift and downwarping are also labeled. Abbreviations for structure labels: AvMFfpf, Avawatz Mountains Thrust Fault Zone fault propagation folds (fpf, above thrusts), with AvMF from Brady (1984, 1986), Wright and Troxel (1984), and new mapping (this study) and fpf from new mapping (this study); BMF, south end, Black Mountains Fault Zone, from Brogran and others (1991), Klinger (1999), Machette and others (2001), new mapping (this study); CHa, Celestite Hills anticline, from Brady (1984, 1986), new mapping (this study); CHfpf, Crystal Hills thrust faults fault-propagation folds (fpf, above thrusts), from new mapping (this study); DKSF, Desert King Spring Fault, from Schermer and others (1996), Miller and Yount (2001), new mapping (this study); DLF, Drinkwater Lake Fault Zone, from Schermer and others (1996); eGF, eastern Garlock Fault Zone, from Clark (1972), Schermer and others (1996), Brady (1984, 1986), new mapping (this study); eOMf, east Owlshead Mountains faults, new mapping (this study); eOMfpf, east Owlshead Mountains thrust faults-fault-propagation folds (above thrusts), new mapping (this study); GCf ,Granite Canyon fault zone, from new mapping (this study); LLa, Lost Lake anticline, from Luckow and others (2005), from new mapping (this study); LLfpf, Lost Lake thrust faults-fault propagation folds (fpf, above thrusts), from new mapping (this study); LSf, Leach Spring Fault, from new mapping (this study); MSF, Mule Spring Fault, from Brady (1984, 1986), new mapping (this study); OBRF, Owl Beak Range Fault, from Luckow and others (2005), new mapping (this study); OHSfd, Owl Hole Spring folds,from new mapping (this study); OLF, Owl Lake Fault Zone, from Clark (1972), Serpa and Pavlis (1996), Guest and others (2003), new mapping (this study); PhVF, Pahrump Valley Fault Zone (Stateline Fault), west strand, from McKittrick (1988); RTRF, Radio Tower Range Fault, from Luckow and others (2005), new mapping (this study); sCVF, southern Chicago Valley Fault, from McKittrick (1988), new mapping (this study); SDVF, Southern Death Valley Fault Zone, from Brady (1984, 1986), Wright and Troxel (1984),Troxel and Butler (1986b), Green (2008), new mapping (this study); SPVF, Southern Panamint Valley Fault, from Muehlberger (1954), Clark (1972), Andrew (2000, 2007), new mapping (this study); TCf, Through Canyon fault zone, from new mapping (this study); WSCF, Warm Spring Canyon Faults, from Brogan and others (1991), new mapping (this study); WWF, Wingate Wash Fault Zone, from Luckow and others (2005), new mapping (this study). 10 meter shaded-relief base from U.S. Geological Survey, The National Map (available at https://www.usgs.gov/core-science-systems/national-geospatial-program/national-map).

Dextral and Dextral-Oblique Fault Zones

One of the most prominent set of structures consists of steeply dipping (70–90°), northwest-trending (300–330° azimuths) dextral and dextral-oblique transcurrent faults aligned approximately subparallel to the overall orientation of the ECSZ and the GPS-determined dominant sense of regional shear, as reported by Dokka and Travis (1990), Miller and others (2001), and Dixon and others (2003). Within this set are two major fault zones in the ECSZ north of the Garlock Fault, including (1) the entire Southern Death Valley Fault Zone, which represents the southern section of the regional Death Valley Fault System (Klinger, 1999; Machette and others, 2001; Workman and others, 2002b; fig. 5), and (2) the southeastern end of the southern Panamint Valley Fault Zone (Muehlberger, 1954; Clark, 1972; Andrew, 2000, 2007; fig. 5). Also included in this set of faults are two faults, including the Desert King Springs Fault (Schermer and others, 1996; Miller and Yount, 2002; Miller and others, 2014) and Leach Spring fault, a newly recognized fault with similar orientation and structural style, that both lie in the northern Granite Mountains south of the Garlock Fault (fig. 5).

Southern Death Valley Fault Zone

The Southern Death Valley Fault Zone is an especially prominent, 50-kilometer-long fault zone that traverses southeast along the axis and western part of southern Death Valley between Shore Line Butte and the western Avawatz Mountains (fig. 5). The north end of the fault zone disappears to the northwest beneath the Recent to latest Holocene channel and floodplain deposits of the Amargosa River and adjacent latest Holocene alluvium in the floor of Death Valley north of Shore Line Butte. However, a trace of the fault zone obliquely continues northeastward from Shore Line Butte across the Amargosa River and floor of Death Valley into a system of normal faults that merges with the south end of the Black Mountains Fault Zone of central Death Valley (Wright and Troxel, 1984; Serpa and others, 1988; Klinger, 1999; Machette and others, 2001). The Southern Death Valley Fault Zone merges to the southeast at the northwest corner of the Avawatz Mountains with several other fault systems that have oblique-transcurrent and reverse-thrust senses of displacement. These include the northernmost sinistral-oblique (reverse) strand of the eastern Garlock Fault bounding the west-central part of the Avawatz Mountains (the Mule Spring Fault of Brady, 1984, 1986; Troxel and Butler, 1986b) and the southernmost of a series of reverse and thrust faults that form the boundary structures of the northeastern Avawatz Mountain range front (see Northern and Eastern Avawatz Mountain Range Front, below). Whether this transition represents a termination of the dextral southern Death Valley Fault Zone or a transition into a fault zone with a different slip sense remains unresolved at present. However, the latter interpretation is more compatible with a general overall continuation in the northwest orientation of the Southern Death Valley Fault through the interior of the Avawatz Fault Zone and the reemergence of a dextral fault on the southeastern and southern margin of the Avawatz Mountains (Spencer, 1990a, b; D. Miller, U.S. Geological Survey, oral commun., 2005; Green and others, 2007). The total amount of right-lateral displacement across the Southern Death Valley Fault Zone is not well constrained. Previously published estimates vary widely from 8 to 40 kilometers (km) based on differing interpretations of reference piercing points (Wright and Troxel, 1967; Butler and others, 1988; Pavlis and Trullenque, 2021), although the latest mapping does support the larger displacement estimate and Caskey and others (2010) suggest an even smaller cumulative displacement amount of 0.6 km.

The main surface trace of the southern Death Valley Fault is complex and discontinuous in detail and consists of numerous subparallel fault strands commonly associated along strike with gaps, overlap zones, deflections in orientation, and en-echelon stepovers (fig. 5; Brady, 1984, 1986; Wright and Troxel, 1984; Troxel, 1986b; Green, 2009). Several strands within the Southern Death Valley Fault Zone are associated with discrete topographic escarpments that suggest a persistent vertical (reverse) slip component within a regime of oblique-dextral transcurrent slip. Furthermore, most of the fault zone is located within linear zones of uplift associated with internal folding, warping, and marginal fold structures, such as fold scarps and zones of rotated strata interpreted as fault propagation folds and fault-truncated tilt blocks related to subsurface boundary thrust faults. These secondary features are especially prominent in the Confidence Hills and the Noble hills sections of the southern Death Valley Fault, which have been interpreted in most studies, including this work, as representing contractional transpressive strain that is localized in positive flower structures persistently developed along the fault zone (see Fault-Generated Folds Associated with Major Transcurrent Fault Zones, below; Brady, 1984, 1986; Wright and Troxel, 1984; Dooley and McClay, 1996; Menges and others, 2005, 2006). However, Caskey and others (2010), in contrast, have proposed an alternative interpretation whereby the folding predates and is structurally discontinuous with superposed strike-slip faulting in the Confidence Hills. Limited reconnaissance geologic and geomorphic mapping conducted in the area as part of this study supports the former transpressive strike-slip structural model for this deformation.

Stratigraphic relations along the most active trace of the fault within and northwest of the Noble hills, as identified by Wills (1989b), Green (2009), and original mapping in this study (map sheet 1), indicate rupture of middle to late Holocene surficial units (Qya and Qyag). These relations suggest a middle to late Holocene age for the most recent surface rupture for most, if not all, of this fault zone between the Shore Line Butte area and the northwestern Avawatz Mountains. This relation may explain the large gap observed in the mapped surface trace of this fault zone between major fault-zone exposures in the Confidence Hills and the area northwest of the Noble hills, because the trace of the fault zone is likely a continuous right-stepping or right-bending fault zone primarily buried beneath the pervasive, very young late to latest Holocene and recent active distal alluvial-fan sediments (units Qyag, Qaag, and Qaw) deposited between the Noble hills and Confidence Hills in this area.

Southern Panamint Valley Fault Zone

The Owlshead Mountains quadrangle includes only a small part of the southern Panamint Valley Fault Zone, where it continues to the southeast from the southernmost end of Panamint Valley across the southwestern Quail Mountains north of its junction with the eastern Garlock Fault Zone (fig. 5; Muehlberger, 1954; Clark, 1972; Andrew, 2000, 2007). Several surface-fault traces in the broad southern Panamint Valley Fault Zone of this area are well defined by a series of truncated bedrock ridges and small fault-bounded valleys with local sag-pond playas. The age of the most recent rupture is not well constrained but appears localized on the southwesternmost fault traces of the composite zone and is likely late Quaternary, based on potential displacement of middle to late Pleistocene units Qiw and Qia and possibly Holocene units Qyw and Qya in some of the fault-controlled valleys and canyons.

Northern Granite Mountains Area

Three moderate-length (6 to 10 km long), northwest-striking dextral faults, the Desert King Springs Fault, an adjacent smaller fault (Schermer and others, 1996; Miller and Yount, 2002; Miller and others, 2014), and the Leach Spring Fault (identified in this study), are located in the southwestern part of the map area on the north-central and northwestern flank of the Granite Mountains (fig. 5). All these faults lie south of the Garlock Fault Zone and the Leach Lake basin and, thus, represent the northernmost fault zones in the northeastern Mojave Desert tectonic province. These faults, however, have anomalous west-northwest strikes and dextral-oblique slip that is more typical of fault zones to the north of the tectonic boundary of the Garlock Fault Zone, relative to the more dominant set of east-trending sinistral faults to the south in the Fort Irwin area of the northeastern Mojave Desert neotectonics province. Cumulative lateral slip on the Desert King Springs Fault is poorly constrained as <5 km (Schermer and others, 1996); the amount of slip is unknown, but probably has a similar magnitude to both the nearby short fault adjacent to the southwest and the Leach Spring Fault farther to the west. The surface trace of each of these fault zones is relatively narrow and contains structural and geomorphic evidence for some right slip, as mapped by Schermer and others (1996); however, these fault traces are complex in detail, with several, mostly left-stepping jogs and deflections that form multiple discrete individual fault strands. Evidence shows at least middle to late Pleistocene activity on these faults, because early and middle Pleistocene units (Qoa and some older Qiag and Qia) appear deformed, although there is no evidence for surface displacements of younger Holocene units (Qyag and Qya).

Sinistral and Sinistral-Oblique Fault Zones

Sinistral and sinistral-oblique transcurrent faults form another major set of structures in the Owlshead Mountains quadrangle. Most of these sinistral faults strike to the east or northeast, transverse or at high angles to the general northwest structural grain of both dextral faults (fig. 5) and the regional northwest-oriented dextral shear orientations measured by GPS for the ECSZ described in the previous section on Physiographic and Geologic Setting. The dominant sinistral fault in the map area is the eastern end of the Garlock Fault Zone, a major regional fault zone that forms a transverse tectonic boundary between the northern Mojave Desert and the southwestern Basin and Range neotectonic domains of the ECSZ (Davis and Burchfield, 1973). However, there are several shorter sinistral faults in the western part of the quadrangle. Many of these are in the Owlshead Mountains, including the Owl Lake Fault in the southern part of the range, a sequence of overlapping to southeastward-stepping en echelon faults in upper Wingate Wash and the northern section of the range, and a series of overlapping to juxtaposed faults that transect the eastern front of the range. The map area also includes the northwestern end of the sinistral Drinkwater Lake Fault, which primarily lies in the northeastern Mojave Desert neotectonic subdomain to the south of this quadrangle and strikes subparallel to the Desert King Springs and Leach Springs Faults described in the previous section on dextral faults in the northern Granite Mountains area. These contrasts between orientations and senses of slip of these two sets of faults suggest a possible and somewhat unusual transitional structure between the two major structural domains north and south of the eastern Garlock Fault in the map area.

Eastern Garlock Fault Zone

A 50-km-long section of the eastern Garlock Fault passes along the north side of Leach Lake basin and the south side of the Avawatz Mountains (fig. 5). The eastern Garlock Fault Zone in the map area is a direct continuation of the 250-km-long Garlock Fault from the west and southwest. Maximum estimates of cumulative late Tertiary to Quaternary displacements for the central part of the Garlock Fault is estimated as ~48–67 km, although there is uncertainty whether this amount applies to the east end of the fault within the map area (Monastero and others, 1997; Ganev and others, 2012; Andrew and others, 2015; Hatem and Dolan, 2018). From west to east across the map area, the eastern Garlock Fault bounds the southern margin of the Quail Mountains and continues eastward across central Leach Lake basin and playa into the southwest corner of the Avawatz Mountains. The exact nature and location of the eastern termination of the fault zone has been a subject of debate. Early compilations indicated that the southern Death Valley Fault terminated against the eastern Garlock Fault Zone (Jennings and others, 1962), which at least may have continued beneath the Quaternary alluvium of southern Death Valley into Miocene sediments exposed to the south of the Kingston Range (Davis and Burfield, 1973; Davis, 2018). Subsequent studies, however, have proposed that the reverse is true and at least the youngest active Quaternary trace of the eastern Garlock Fault terminates to the west of the southern Death Valley Fault (Brady, 1984, 1986; Pavlis and others, 1998; this study). Brady (1984) noted that the Mule Spring Fault strand on the northern edge of the eastern Garlock Fault Zone along the northwest margin of the Avawatz Mountains merges directly into the Southern Death Valley Fault Zone, which appears to continue to the east as an interior strand of the Avawatz Mountain thrust system (see subsections, Southern Death Valley Fault Zone, above, and Northern and Eastern Avawatz Mountain Range Front, below). All the other fault strands of the eastern Garlock Fault Zone with evidence for Quaternary activity terminate in a series of fault splays in the Avawatz Mountains behind and west of the proposed continuation of the Southern Death Valley Fault Zone in the Avawatz Mountain thrust system.

The surface trace of the eastern Garlock Fault Zone is complex, consisting of several to numerous subparallel fault strands commonly associated along strike with gaps, overlap zones, deflections in orientation, and en echelon stepovers. The zone is particularly wide and complex in the southwestern and central Avawatz Mountains and in the south-central Quail Mountains (Brady, 1984, 1986) near the area of intersection with the southern Panamint Valley and Owlshead Lake Fault Zones from the north. Some of the fault strands in the Avawatz Mountain section of the eastern Garlock Fault Zone, including the Mule Spring Fault strand described above, are also associated with significant topographic relief on the south and southwest sides of the structure that suggests a persistent vertical component of oblique sinistral slip, an inference confirmed by observed striae that have plunges ≥20° on some fault surfaces. Much of the fault zone is also associated with highland areas bounded by fold structures, including fault-propagation and (or) homoclinal-tilt fault blocks interpreted as generated by subsurface thrusts bordering positive flower-structure uplift zones. This transpressive strain is most strongly developed on the margins of the western Avawatz Mountains and on the southern piedmont of the Quail Mountains. One notable exception in the center of the eastern Garlock Fault Zone is a prominent set of normal-oblique and normal faults associated with a pull-apart graben formed at a distinct left step in the fault zone in Leach Lake playa.

Abundant geomorphic and stratigraphic evidence for Pleistocene–Holocene activity is visible on the eastern Garlock Fault Zone in the map area. High-resolution lidar imagery delineates topographic features (fault scarps, stream deflections, and offset landforms) indicative of Pleistocene to Holocene surface rupture on a core set of fault strands embedded in the larger fault zone similar to the rupture identification of Clark (1972), McGill and Sieh (1991), and McGill (1994b). These features appear to displace younger elements of Holocene units (Qya and Qyw), suggesting a middle to late Holocene age for the most recent rupture, consistent with preliminary estimates of late Holocene surface ruptures by McGill (1994b) for the east end of the fault zone.

Owl Lake Fault

The Owl Lake Fault is a 15- to 20-km-long sinistral transcurrent fault that cuts northeastward from its south end at the southeast edge of the Quail Mountains through the southeast corner of the Owlshead Mountains (fig. 5). The north end of the Owl Lake Fault structurally defines the southeast margin of Owl Lake alluvial basin in the eastern part of the Owlshead Mountains range. In the southwest, the fault approaches and abuts at an oblique angle against the cross-cutting eastern Garlock Fault Zone near where it truncates the southeast end of the southern Panamint Valley Fault Zone at the south-central structural and topographic margin of the Owlshead Mountains. The Owl Lake Fault has been identified and shown in more generalized structural form in relation to several regional studies of neotectonic faulting, mainly in relation to its structural association with the Garlock Fault (Clark, 1972; Serpa and Pavlis, 1996; Guest and others, 2003; Ganev and others, 2012). In detail, the surface trace of the Owl Lake Fault Zone is relatively narrow but displays an internal structural complexity that increases markedly toward its northeast end. The fault consists of a sequence of mostly aligned fault segments in the southern portion that transitions into a more complex pattern of obliquely branching splays to the north. The simpler geometry of the southern trace of the fault defines linear fault-controlled valleys that suggest mainly transcurrent slip. This contrasts with the persistent topographic relief and absence of consistent horizontal slip indicators along the north section of the fault, which implies a more significant and perhaps dominant vertical component of oblique slip on the topographically higher terrain on the southeast side along the central and northern sections of the fault. Some published information suggests Quaternary activity on the Owl Lake Fault (Muehlberger, 1954; McGill, 1994a, b), an interpretation confirmed by field observations during this study that indicate surface displacements of latest Pleistocene to middle Holocene deposits (Qia and older Qya units).

Wingate Wash and Northwestern, Northern, and Central Owlshead Mountains Areas

Discontinuous, relatively short (3 to 10 km long), sinistral and sinistral-oblique transcurrent faults define a diffuse structural boundary on the northwest, north, and northeast borders of the Owlshead Mountains (fig. 5; Luckow and others, 2005; Pavlis and others, 2012). This structural boundary begins on the northwest with a series of short sinistral faults (including the Wingate Wash Fault in upper Wingate Wash) and progressively steps to the east and southeast along a series of sinistral-oblique to sinistral faults in the northern part of the Owlshead Mountains (fig. 5). Several of the larger faults in the northern Owlshead Mountains, including the Radio Tower Range, Owl Beak, and Granite Canyon Faults (fig. 5), structurally bound all or parts of internal subranges in this area. These faults may represent neotectonic sinistral-oblique reactivation of earlier late Miocene normal to normal-oblique faults originally mapped in the area by Luckow and others (2005) and Pavlis and others (2012). Many of these faults contain topographic and structural evidence for secondary transpression during at least the neotectonic component of deformation, although previous mapping indicates a predominance of transtension during the earlier late Miocene deformational interval (Guest and others, 2003; Luckow and others, 2005; Pavlis and others, 2012). The cumulative lateral displacement across the structural zone in upper Wingate Wash is estimated at between 7 km and 15 km on the basis of pre-Quaternary piercing-point markers (Luckow and others, 2005). The surface trace of each individual fault zone commonly is complex in detail, with many curvilinear sequences of overlapping to splayed individual fault stands. Evidence for neotectonic deformation on these faults consists of probable fault-controlled topographic features such as scarps, linear valleys, and truncated ridges and spurs that are located on many faults largely formed in bedrock. Late Quaternary surface ruptures are indicated by deformation of late Pleistocene surficial deposits (units Qia and Qiag) on several of these faults and, on at least one fault (Wingate Wash Fault), by displacement of Holocene deposits (unit Qya).

Northeastern and Eastern Margin of Owlshead Mountains Area

A complicated array of subparallel northeast-trending linear features interpreted as traces of sinistral faults transect the band of bedrock forming the northeast and east margin of the Owlshead Mountains between Owl Lake basin and the eastern range front. Many individual faults are geometrically complex and display numerous splays, fault branches, and en echelon overlaps and step-overs. The Granite Canyon and the Through Canyon Faults (defined herein) are the most prominent structures in this fault set, and both are associated with fault scarps and displaced alluvium along the base of topographic escarpments that suggest sinistral-oblique slip. Most of the other structures are developed primarily in bedrock, but an active fault origin is strongly suggested by geometric similarity to the Granite Canyon and Through Canyon Faults and association with many fault-controlled features such as bedrock scarps, linear valleys, truncated ridges, and sharply bounded alluvial flat.

Northeastern Mojave Desert Area

The south-central margin of the map contains the northwest tip of the Drinkwater Lake Fault, a structure that is primarily located in the southeastern Granite Mountains area to the south of the map (fig 5). This fault zone is the northernmost element of a series of east- to east-northeast-trending sinistral to oblique-sinistral faults originally identified in the northeast corner of the Mojave Desert subprovince of the ECSZ by Schermer and others (1996), Pavlis and others (1998), Miller and Yount (2002), and Miller and others (2014). The section of the Drinkwater Lake Fault at and south of the map boundary is a steeply dipping to subvertical southeast-oriented transcurrent fault that sinistrally displaces a late Quaternary surficial deposit and associated landforms along the northeast margin of a low-relief linear bedrock ridge.

Thrust Faults and Associated Fault-Related Folds

Earlier workers have identified the presence of active Quaternary thrust faults that displace bedrock over alluvium along the north and east range front of the Avawatz Mountains (Spencer, 1981, 1990a, b; Brady, 1984, 1986). More recent work, including this study, supports this conclusion. This new mapping expands the extent of this contraction and refines the timing of Quaternary deformation on the Avawatz Mountain Thrust Fault system (fig. 5; McGill, 1994b; Stroud and McGill, 1994; Mendonca, 2007; Miller and others, 2007). These recent studies identify tectonic scarps associated with surface rupture of middle to uppermost Pleistocene surficial deposits, development of fault-propagation folds above shallowly buried blind thrusts, and the geometry and migration patterns of multiple stacked reverse and thrust faults. Also, this study has identified several previously unrecognized sets of fault-related folds probably related to similar thrust-fault systems along the base of the eastern range front and several interior subranges in the eastern, western, and northwestern Owlshead Mountains (fig. 5).

Northern and Eastern Avawatz Mountains Range Front

A complex system of thrust faults defines the tectonically active structural boundary of the northern and eastern Avawatz Mountains at the southeast margin of southern Death Valley and the northwest margin of Silurian Valley (figs. 2, 5). The fault system displays a general northwest trend of fault traces grossly aligned with the Southern Death Valley Fault Zone to the northwest. In detail, however, the faults form a broad, arcuate, outwardly convex and basinward-directed salient that is centered on and structurally defines the northeast corner of the Avawatz Mountains. The surface trace of the fault zone is more complex in detail, consisting in map view of many subparallel, arcuate strands that branch and merge laterally along the range front to produce a series of elongate to lozenge-shaped fault blocks that collectively form an outwardly convex frontal fault system. As a result, the range front is a complex landform of recesses and salients in the range front. In cross section, most of these faults dip steeply to moderately to the southwest toward the innermost strand of this imbricate fault system in the range-block interior. Brady (1984), among others including this author, has interpreted this strand as a relatively older, possibly pre-Quaternary deflected continuation of the Mule Spring Fault strand of the eastern Garlock Fault incorporated within the Avawatz Mountain Thrust Fault system.

A close correspondence exists between the surface traces of individual faults in the thrust stack and the overall stepped topography associated with the range front. That is, successive fault zones within the bedrock range front commonly occur at the base of steeply sloping topographic steps or escarpments varying in height from 20 to 400 m. The fault blocks between successive fault strands and associated escarpments generally underlie subhorizontal to gently sloping benches that vary from 0.1 to 3 km in width. The stratigraphic and geomorphic relations along each of the individual fault strands indicate that, at a given location, the youngest surface ruptures occur on the outermost basin-bounding strand and that many of the interior fault strands have been deactivated, uplifted and back-rotated, and incorporated into the range front above the subjacent youngest active thrusts. These patterns indicate progressive encroachment and migration of the loci of thrust faulting and uplift into the basin that is most strongly developed at the range-front salients.

Quaternary activity of these range-bounding thrust faults is well documented by exposures of bedrock thrusts above Quaternary alluvium at several locations along the range front (Brady, 1984; Spencer, 1990a, b; Miller and others, 2007). These and other workers have identified many tectonic scarps developed in alluvium along the fault system (for example, McGill, 1994b; Stroud and McGill, 1994). More recent work has revealed that these features are not directly related to surface fault rupture but rather are fold scarps related to shallowly buried blind thrust faults. That is, the folds are geometrically related to subjacent thrust faults that terminate below and are shallowly buried by the overlying folded sediments within the scarp. Typically, both scarp morphology and the degree of fold development is directly related to the amount and relative age of displacement on the underlying thrust fault, shown by the highest and steepest scarps and folds with the highest amplitudes and steepest profiles that occur above the oldest faults with the greatest demonstrable bedrock displacement. These relations indicate that the folds and associated scarps resemble fault-propagation folds that are directly and progressively generated by near-surface ruptures on the underlying thrust faults (fig. 5; Mendonca, 2007; Miller and others, 2007). The fault-propagation folds and underlying thrust faults deform all Pleistocene (Qia) and possibly some latest Pleistocene to early Holocene (Qyao) units along the range front, although younger middle to late Holocene (Qya) units are not affected by the structures; these relations indicate at least a late Pleistocene through, perhaps, latest Pleistocene to Holocene age range for the youngest displacements on the Avawatz Mountains Thrust Fault system.

Eastern Owlshead Mountains Range Front

Another set of fault-propagation folds is in the proximal piedmont below and northeast of the eastern range front of the Owlshead Mountains (fig. 5). These structures are defined at the surface by fold scarps underlain by northeast-vergent folded surficial deposits that closely resemble the morphology, geomorphic position, and structural setting of fold scarps and fault-propagation folds associated with buried thrust faults that are observed along the Avawatz Mountain range front. These features are interpreted as developed above subjacent northeast-vergent blind-thrust faults that dip southwestward beneath the east margin of the Owlshead Mountains, although no thrust faults are exposed at this location. Boundary thrust faults are, thus, uplifting and displacing the Owlshead Mountain block northeastward into the central section of the southern Death Valley trough. This zone of thrusting into the valley coincides closely with the zone of apparent right deflection in the projected trace of the Southern Death Valley Fault Zone between the northern Noble hills and Confidence Hills sections of the fault. This geometry suggests that the deflection is a kink or deformation bend in the fault trace produced by valleyward motion of the Owlshead Mountain block on the east boundary thrusts. It also spatially coincides with a northeastward deflection and local gradient increase of a reach in the Amargosa River in the adjacent axis of the southern Death Valley basin (Menges, 2008). In plan view, this 10-km-long zone of fault-propagation fold scarps consists of a lateral series of multiple, commonly overlapping and branching, individual features at most several kilometers in length. The fault-propagation folds uplift and deform all Pleistocene (Qia) units along the range front but do not appreciably disturb latest Pleistocene to Holocene (Qyao or Qya) units in the area, which establishes middle to late Pleistocene minimum ages for surface deformation on the structures. Successive fold scarps decrease in height and involve progressively younger units in a basinward direction from the base of the bedrock range front. These relations are consistent with a northeastward propagation of younger, and possibly more actively developing, thrust-related deformation into the west flank of southern Death Valley.

Western and Northern Owlshead Mountains Area

Four other distinct topographic scarps (three sets of scarps and an individual scarp) occur along the base of subranges in the western and northwestern Owlshead Mountains. Luckow and others (2005) and Pavlis and others (2012) described some of these features, but this study provides more complete evaluation of structures with evidence for deformation of Quaternary deposits and landforms. These features are interpreted as several types of fault-related fold scarps tectonically generated by subjacent blind thrust faults. One set of northeast-oriented scarps has developed along the northwest base of the Crystal Hills (CHfpf, fig. 5). These scarps are interpreted as fault-related folds developed above a subjacent southeast-dipping blind thrust fault bounding and uplifting the range on the northwest flank (fig. 5). These scarps are thought to be generated by fault-propagation anticlinal folds that are developed along the mostly underlying buried and locally exposed thrust faults. These fault-generated folds transition and continue northeastward into elongate blocks of homoclinally tilted surficial deposits and associated scarps that display the same orientation and structural-physiographic position of the fault-generated folds. The strata in these blocks are rotated steeply basinward above similarly dipping scarps, but the blocks are truncated above and below across very narrow deflection zones that more closely resemble bounding faults than the more gently dipping limbs and wider crestal inflection zone typically observed in distinct fault-propagation folds. Thus, these tilted blocks are interpreted to represent the structural and topographic expression of tightly rotated forelimbs of fault-truncated folds. These features lack the discrete axes and back limbs of fault-propagation folds because of fault dismemberment of extremely narrow flexure zones with very tight radii of curvature at the base and crest of tilted sediments and (or) older uplifted rocks caught between the underlying blind thrust and the overriding structurally intact range block. To the south of these structures bounding the Crystal Hills, a second scarp is similarly interpreted as thrust-generated homoclinal tilt blocks developed along the curvilinear base of the northwestern Quail Mountains. A third set of north- to northwest-oriented scarps parallel the northern and northeastern margin of the Lost Lake basin in the northwestern Owlshead Mountains (LLfpf, fig. 5), features clearly recognized and mapped by Luckow and others (2005) and Pavlis and others (2012). A fourth curvilinear set of northeast to north-trending scarps associated with southeast- to east-dipping tilted fault blocks are located along the basal corner of the interior subranges on the northwest flank of the Owl Lake basin in the northeast corner of the Owlshead Mountains (fig. 5). All of these scarps are similarly interpreted as either fault propagation folds or homoclinal tilted-block folds related to a series of north-, northeast-, to east-dipping blind to locally exposed thrust faults. The timing of deformation on all these fold and fault structural zones in the western and northern Owlshead Mountains is not well constrained, but they definitely involve surficial deposits as old as Pliocene and early Pleistocene (unit QToa) and as young as middle to late Pleistocene (unit Qia). Collectively these structures demonstrate a significant northwest-southeast-directed neotectonic component of contraction in the west corner of the Owlshead Mountains.

Folds

The Owlshead Mountains quadrangle contains a diverse array of folds in addition to the fault-generated folds associated with blind-thrust fault systems described above. These fold structures are primarily located in the more highly deformed western and southern parts of the area. Many, but not all, of these structures progressively deform various ages of surficial deposits and were actively forming in the middle to late Quaternary. Neotectonic folding in the quadrangle includes (1) isolated to multiple groups of anticlines and synclines co-located within and, at least in some locations, apparently genetically related to zones of complex faulting in highland areas; (2) several types of fault-related folding generated by transpressive strain along major transcurrent and oblique-transcurrent fault zones; and (3) single to multiple series of doubly plunging anticlines developed in surficial deposits within alluvial basins.

General Folds

A series of anticlines and synclines have been mapped by previous workers in many areas within the Owlshead Mountains quadrangle, including (1) the northeastern range front of the Avawatz Mountains, (2) several sites along the Southern Death Valley Fault Zone, including the Noble hills proper, low hills to the north and northwest of the Noble hills, and the Confidence Hills, and (3) a series of east-trending fold ridges on the southeast and south-central flanks of the Owlshead Mountains to the north and northwest of the Garlock Fault and the Leach Lake basin (fig. 5; Brady, 1984, 1986; Troxel, 1986a, b; Troxel and Butler, 1986a; Dooley and McClay, 1996; Green, 2009; Caskey and others, 2010). These folds are typically open to tight and locally nearly isoclinal, with subhorizontal to gently plunging fold axes. They typically formed predominantly in either upper Tertiary sediments (substrate unit pc) or in the Pliocene to middle Quaternary unit QToal surficial deposits; however, these folded sediments are unconformably truncated or overlapped by undeformed younger middle to late Quaternary surficial deposits. The folds at all localities except the southeastern Owlshead Mountain site are located within fault-bounded blocks within the Avawatz Mountain Thrust Fault system, or secondary deformation within or adjacent to the Southern Death Valley Fault Zone. Most previous workers, as well as this study, attribute most of the folds in the Southern Death Valley Fault Zone to secondary transpression related to positive flower structures or transpressive step-over zones, although Caskey and others (2010) consider this folding as predating and disconnected from later development of superposed dextral faulting.

Fault-Generated Folds Associated with Major Transcurrent Fault Zones

Many of the linear highland areas centered along sections of the southern Death Valley and eastern Garlock Fault Zones, including the Mule Springs Fault stand, (SDVf, eGf, and MSf, fig. 5) are bounded by a series of topographic scarps commonly defined by folded or basinward-rotated surficial deposits and (or) underlying sediments of units QToal or by unit pc substrate. These features are especially prominent along the base of the upland areas of the Noble hills, the Confidence Hills, and the northwest and west range fronts of the Avawatz Mountains. These features are interpreted as the fault-propagation folds or homoclinally rotated tilt blocks developed above subjacent blind-thrust faults similar to those described above (in section Thrust and Associated Fault-Related Folds). However, this group of fault-related fold structures appears related to surface deformation and uplift on the downward-steepening thrust faults that form the structural boundaries of positive flower structures (for example, Dooley and McClay, 1996). One other prominent series of basinward-convex, arcuate, fault-propagation fold scarps has formed on the piedmont adjacent to and south of the eastern Garlock Fault Zone where it bounds the central Quail Mountains (figs. 2, 5). These fault-related fold scarps are located opposite the zone where both the southern Panamint Valley and Owl Lake Fault Zones intersect with and terminate against the eastern Garlock Fault. The fault-related folds in this area probably represent localized secondary transpressive deformation of the eastern Garlock Fault Zone as it passes through, and is possibly distorted and deformed within, this zone of interference with the two major fault zones to the northwest and northeast. A series of middle Pleistocene to early Holocene surficial deposits (ranging from units Qia to Qyao) are directly deformed by the folding on most of these boundary structures to the zones of transpressive uplift.

Anticlinal Uplifts

Alluvial surficial deposits are warped and uplifted by anticlinal folds in the interior of several basins in the Owlshead Mountains quadrangle. Several prominent examples, including the Celestite hills anticline (CHa, fig. 5; Brady, 1984, 1986) and Owls Hole Springs anticlines (within OHSfd, fig. 5), are most prominently developed in the triangular alluvial embayment located between the southeastern Owlshead Mountains, northwestern Avawatz Mountains, and southwestern Noble hills (figs. 2, 5). Two other anticlines occur in the western Owlshead Mountains (for example, the Lost Lake Anticline [LLa] fig. 5; Luckow and others, 2005; Pavlis and others, 2012). Most of these anticlines are topographically expressed as linear ridges to broad swells ranging in height from several to tens of meters. These ridges are commonly oriented transverse to local drainages. The topography of these features typically is characterized longitudinally by an elongate ridgecrest that slopes gently away from a central zone of maximum relief and transversely by opposing sets of gently and steeply sloping, dissected, flanking hillslopes. This morphology appears to reflect strongly the structural geometry of the underlying doubly plunging asymmetric anticlines. There is no regional consistency in either the vergence direction or the orientation of the fold axes. Instead, fold-axis patterns tend to mimic the patterns of adjacent uplifted highlands in a manner suggestive of localized contractional closure, uplift, and structural inversion of a given enclosed section of the basin. The axes of many individual, doubly plunging fold ridges are aligned together across intervening gaps of undeformed alluvium in a geometry that topographically mimics successive culminations in an anticlinal fold train. The overall geometry of many of these folds, including the doubly plunging axial crests and marked transverse asymmetry, suggests possible origins as popup folds uplifted above subsurface thrust faults, although no such structures are exposed at the shallow structural levels of the exposed anticlinal cores of these ridges. One exception may be the Lost Lake Anticline, which is oriented transversely atop an uplifted area in a transpressive right step-over in the en echelon system of sinistral faults on that boundary of the Owlshead Mountains.

Several characteristics of the anticlinal ridges indicate development by active late Quaternary uplift and folding. The axes of some low-relief fold-generated ridges are completely traversed, incised into, and even completely bisected by antecedent local piedmont drainages in response to progressive growth of the underlying anticline. Two other indicators include (1) progressive rotation, uplift, and dissection of successive older middle to late Pleistocene units ranging from unit Qia to unit Qyao on the flanks and margins of uplifted areas and (2) the progressive involvement of younger late Pleistocene to early Holocene units (Qia and Qyao) in folding overlying laterally propagating, low-relief, along-strike extensions of the anticlinal ridge axes.

Normal Faults

Many normal faults are present in the Owlshead Mountains quadrangle, but faults of this type with demonstrated late Pliocene to Quaternary activity are a minor component of the neotectonic regime, relative to the major role of normal faults in neotectonic deformation in the regions of the southwestern Basin and Range to the west, north, and east (fig 1; Workman and others, 2002b; Bryant, 2005; Fridrich and Thompson, 2011). Quaternary normal faults in the quadrangle are more spatially restricted, fewer in number, and associated with a variety of tectonic and structural settings, compared to the other types of structures described earlier. The largest concentration of Quaternary normal faults is in the south end of the central Death Valley basin to the north of Shore Line Butte. In addition, a few normal faults with demonstrable neotectonic activity were identified in the northern and eastern part of the quadrangle (fig. 5). The remaining Quaternary normal faults in the study area lie within a few localized sites of secondary deformation along the Southern Death Valley and eastern Garlock Fault Zones.

Southern End, Central Death Valley Area

Several normal faults displace Pleistocene and Holocene surficial units in the southernmost section of the central Death Valley basin located within the quadrangle to the north of Shore Line Butte (Wright and Troxel, 1984; Brogan and others, 1991; Workman and others, 2002b; Sohn and others, 2007). Collectively, these normal faults mark a relatively sharp tectonic transition from the predominantly contractional deformation in southern Death Valley and the mainly extensional tectonic regime of the central Death Valley basin to the north. These faults are concentrated into two discrete sets of faults located on either side of the central basin axis. The first set consists of an aligned system of southwest-dipping normal faults that diverges from the north end of the southern Death Valley Fault on the northeast side of Shore Line Butte. This zone of faults continues obliquely to the north up the eastern piedmont of Death Valley, where it defines the base of a small escarpment developed in middle to lower Pleistocene (unit Qoa) and upper Tertiary sediments. This normal fault zone eventually merges with the southern end of the Black Mountains normal fault that forms the main range-bounding structure along the base of the Black Mountains in central Death Valley to the north (fig. 5; Brogan and others, 1991; Machette and others, 2001). Thus, this fault zone forms the southern end of the Black Mountains Fault Zone and defines an abrupt tectonic transition from transpressional dextral faulting to the south to major normal faulting to the north within the regional Death Valley Fault System (Klinger, 1999; Machette and others, 2001; Fridrich and Thompson, 2011). In detail, the set of normal faults between Shore Line Butte and the range-front Black Mountains Fault consists of a series of subparallel, branching, en echelon fault strands that are confined into a relatively narrow curvilinear zone of surface rupture. These faults structurally define an escarpment in early to middle-early Pleistocene alluvium (unit Qoa) with interbedded ash from the nearby cinder cone at Cinder Hill (unit Qmv) and displace a series of younger late Pleistocene to middle Holocene deposits (units Qia, Qyao, and a middle unit of Qya), which establishes multiple surface ruptures ranging in age from at least middle Pleistocene to middle Holocene (Wright and Troxel, 1984; Troxel and Butler, 1986b; Sohn and others, 2007).

A second set of north- to northwest-trending normal faults in the map area formed in alluvial fans in the western piedmont of the central Death Valley basin, northwest of Shore Line Butte and lower Wingate Wash (fig. 5; Brogan and others, 1991). This zone consists of an extremely complex, dense network of subparallel to branching individual fault strands that dip both southwest and northeast, thereby defining several narrow subparallel grabens within the array. Many of the faults displace older dissected alluvial fans, mapped as upper Tertiary to lower Pleistocene (QToa) and lower to middle Pleistocene (Qoa) units that were deposited in an alluvial-fan assemblage below the outlet of Warm Springs Canyon in the southeastern Panamint Range. These relations only constrain these displacements as early to middle Pleistocene. However, several fault strands offset a younger set of middle to late Pleistocene (unit Qia) fan deposits that are inset below these older and higher fan remnants, and a few fault strands at the southeast margin of the zone apparently cut Holocene (unit Qya) alluvium on the distal piedmont adjacent to the basin floor.

Chicago Valley and Eastern Nopah Range Area

Only a few major tectonically active fault zones have been identified in the area of the northeastern and eastern section of the quadrangle to the east of southern Death Valley and Silurian Valley. The area has experienced complex middle to late Tertiary deformation, characterized by a complex network of interlinked normal and mostly dextral strike-slip faults, that has produced much of the modern basin-and-range topography (Jennings and others, 1962; Thompson and others, 1999; McMackin, 1997, 2001; Wright and Troxel, 1999; Workman, 2002a, b; Pavlis and others, 2014). However, most of these faults have not been active in the late Pliocene to Quaternary. A 15-km-long zone of north- to northeast-oriented, west-dipping fault scarps cut alluvial fans within the southeastern margin of Chicago Valley. These scarps are located at and several kilometers basinward of the southwestern range front of the Nopah Range (fig. 5). The zone of faults is discontinuous, containing several, small, aligned to stepped, subparallel to branching strands developed mainly in fan deposits of middle to late Pleistocene (unit Qia) and locally latest Pleistocene to early Holocene (unit Qyao) ages, with large gaps present across undeformed early to late Holocene unit Qya fans. This suggests surface ruptures on the mostly middle to late Pleistocene and possibly earliest Holocene faults on this segment of the east boundary fault of Chicago Valley. Several short normal faults displace late to middle Pleistocene unit Qia alluvial deposits along the east-central margin of the Nopah Range in the northeast corner of the quadrangle (fig. 5). The structural setting of this fault zone is uncertain, but it may be related to local reactivation of extension on these graben-bounding faults associated with transtensional deformation observed on the nearby Pahrump Valley section of the dextral State Line Fault Zone to the northeast (Blakely and others, 1999; Workman and others, 2002b; Scheirer and others, 2010).

Normal Faults Associated with Major Transcurrent Fault Zones

The remaining normal faults with Quaternary activity in the map area are located at three sites within or adjacent to the complex zone of surface deformation along either the southern Death Valley or eastern Garlock strike-slip faults. Each of these sites involves sets of multiple normal faults that, unlike the normal fault zones described in the two previous subsections on the Southern End, Central Death Valley Area and on the Chicago Valley and Eastern Nopah Range Area, do not appear related to regional patterns of extension but rather reflect local extensional transtensional strain driven by transcurrent distributed shear within or adjacent to the primary surface trace of the fault zone. For example, some very short (0.5–2 km long) subparallel normal faults have formed at one site adjacent to the central section of the Southern Death Valley Fault Zone, on the lowermost east side of the basin floor to the north of the north end of the Noble hills. These faults are locally clustered and display bidirectional east and west dips that define a subparallel series of shallow graben and low scarps. The scarps are developed across the wide crest of a structurally isolated uplifted unit Qia alluvial fan that has been laterally displaced and warped by a doubly plunging broad anticline between the main and subsidiary strands on the east margin of the Southern Death Valley Fault Zone to the north of the Noble hills. The normal faults are interpreted as bending-moment normal faults developed in the local extensional strain regime in the outer axial crest of the anticline. Another small set of mostly subparallel normal faults are mapped along and near the northwest margin of the Avawatz Mountains. These normal faults are interspersed and embedded within a diffuse zone of anticlinal warping interpreted as reflecting fault-generated folding at the northwest edge of the transpressional uplift zone developed on the central section of the eastern Garlock Fault Zone. Like the other examples, these small normal faults within the marginal fold belt are interpreted as local extensional bending-moment structures on the crest of anticlinal folds. The third set of normal faults is located within the eastern Garlock Fault Zone, where it crosses the Leach Lake playa in the center of the Leach Lake basin (fig. 5). These normal faults differ from the two groups described; these structures represent transtensional deformation related to the internal geometry within the actual fault zone, rather than auxiliary faulting on transpressive anticlinal folds. The normal faults are in a transtensional left-stepping stepover deflection in the central trace of the eastern Garlock Fault. The normal faults are subparallel to and surround parts of a well-defined narrow pull-apart graben developed on a series of bounding sinistral normal-oblique stands in the fault zone. Both the normal-oblique graben-bounding fault strands and the surrounding normal faults cut a variety of very young early to late Holocene surficial units (Qap, Qyp, and Qypf) within active or very young parts of the playa, indicative of latest Holocene displacements on this part of the eastern Garlock Fault Zone.

DESCRIPTION OF MAP UNITS

Complete descriptions of all map units are listed from youngest to oldest within each heading. Detailed descriptions of each singular map unit include, where relevant, the following sequence of data: (1) landscape position, any associated landforms, and drainage characteristics; (2) sedimentology, including grain size and textural ranges, lithologic composition (where distinctive), any sedimentary structures, and degree of consolidation; (3) surface morphology, such as microtopography (for example, primary drainage morphology or relict bar and swale), pavement development, amount of varnishing of surface clasts, and physical clast weathering; (4) depth and degree of soil development, including pedogenic horizonation and accumulation of pedogenic materials; and (5) vegetation associations. Many elements of these descriptions are necessarily generalized owing to the amount of variation commonly observed in altitude, landscape position, relief, climate, drainage patterns, source terrain, and parent materials across the large and diverse map area. Composite map units are described briefly; see Singular Map Units for detailed descriptions although some additional specific composite-unit descriptive elements are incorporated where appropriate. Soil-horizon designations are derived from the system summarized in Birkeland (1999). The stages of soil carbonate morphology are based on Gile and others (1966), as modified by Machette (1985).

Ages ranges of Quaternary to Pliocene divisions used in this report are from Cohen and others (2014): Holocene, 0–11,700 years (yrs); late Pleistocene, 11,700–126,000 yrs; middle Pleistocene, 126,000–781,000 yrs; early Pleistocene (Gelasian and Calabrian), 781,000–2.58 Ma yrs; Pliocene, 2.58–5.33 Ma. Several additional informal subdivisions added for select younger time subintervals include: Recent, 0– 500 yrs; latest Holocene, 500–2,000 yrs; late Holocene, 500–4,000 yrs; middle Holocene, 4,000–7,000 yrs; early Holocene to latest Pleistocene, 7,000–11,700 yrs.

SURFICIAL DEPOSITS AND SURFICIAL DEPOSITS PLUS SUBSTRATE

SINGULAR MAP UNITS

Anthropogenic Deposits

ml **Made land (latest Holocene, Recent)**—Material related to human activities, including construction and agricultural disturbance, that significantly modifies natural conditions and impedes reliable identification of surficial geology

Alluvial Deposits

Wash Deposits

Qaw **Active wash deposits (latest Holocene)**—Alluvial deposits associated with discrete washes and channels that have received active discharge and associated deposition within the past several decades to, at most, the last century. In many cases, the geometry of recent deposition is highlighted in one or more aerial photographs and (or) Landsat images acquired within the past several decades. Requires some degree of discrete channelization, generally within incised upland or proximal piedmont areas, or within distinctly integrated reaches of local to regional drainage, including major transverse and axial-wash drainages such as the Amargosa River, Wingate Wash, and the Greenwater, Chicago, California, and Kingston washes. Prone to flooding during locally intense or prolonged precipitation events. Composed of loose, poorly to moderately sorted, subrounded to subangular, intermixed sand and gravel. Common admixtures of fine to coarse sand, pebbles to cobbles, and locally fine boulder gravel, with a general downdrainage fining pattern observed from mountainous highlands to proximal and distal piedmont positions. Some weak to moderate bedding and other fluvial structures (for example, crossbedding) observed in larger more integrated drainage elements. Increased clast rounding and more heterogeneous admixtures in grain size and lithologies occur along axial drainages. Generally distinct flow-morphology remnants, varying from well-defined channels in upland areas to intermixed subchannels and bars in more distributive channel flow on piedmonts. Local relief between bars and subchannels is commonly ≤0.5 m. No discernible pavement or in situ varnish development on surface. No significant soil development, other than very thin (≤1–2 centimeter [cm] thick) crust of fine-grained silt and very fine sand in reaches that have not experienced recent flows. No long-term vegetation in channels or subchannels and only limited vegetation (predominantly creosote bushes, *Larrea tridentata*, and several other bushes, mostly cheesebrush, *Ambrosia salsola*) along channel margins. Less-channelized active deposits are mapped as unit Qaa on unincised piedmonts or as unit Qav along valley axes

Qawg **Active wash deposit composed of grus (latest Holocene)**—Alluvial deposits derived from granitic source terrain that weathers to grus; associated with active to recent deposition in discrete washes and channels. Commonly intermixed coarse to fine sand and cobble to pebble gravel that is generally finer grained than active deposits at equivalent landscape positions; derived from other rock-type provenances. Generally similar, but less pronounced intra-channel microtopography than unit Qaw. Most other characteristics, including lack of pavement, varnish, and soil development and sparse vegetative association, are also equivalent to unit Qaw

Qyw **Young wash deposit (Holocene and latest Pleistocene)**—Alluvial deposits associated with generally inactive washes, typically occurring as low terraces located commonly 50 to 100 cm above most active washes (unit Qaw), but locally increasing to heights of 5–6 m on incised reaches of major drainages such as the Amargosa River. Surfaces have not received discharge or sedimentation in hundreds to thousands of years. Consists of poorly to moderately sorted, subrounded to subangular sand and pebble to cobble to locally boulder gravel, loose to poorly consolidated. Poorly to moderately bedded. Little to minor modification of microtopography (interchannel morphology) and little to no varnish development, with local relief generally <50 cm. Typically, minor to weak soil development, mostly consisting of thin (1–3 cm thick) Av crust of silt and fine sand, no to cambic B horizonation, and stage I calcic accumulations, mostly limited to depths ≤1 m. Moderately vegetated, mostly creosote to various shrubs and bushes, more uniformly distributed across the surface relative to more active drainage surfaces such as unit Qaw. Surfaces receiving less channelized discharge in more poorly defined braided channel systems are mapped as unit Qya. Anderson (2005) reports ^{14}C ages of ~360 to >1,400 thousand years (ka) for low-level fill terraces along the Amargosa Canyon reach of the Amargosa River.

Qywg **Young wash deposit composed of grus (Holocene and latest Pleistocene)**—Alluvial deposits, derived from granitic source terrain that weathers to grus, associated with generally inactive washes. Commonly associated with low terraces located 50–100 cm above the active washes (unit Qawg). Generally similar deposits to unit Qyw except for a greater proportion of sand and granules and finer-grained, pebble to cobble gravel components. Generally, more subdued relict microtopography, relative to unit Qyw, with minor local relief and varnish development. Generally, more poorly developed soil development, mostly evidenced as Av and at most a thin Bw cambic and very weak stage I calcic horizons. Similar vegetative characteristics to unit Qyw

Qiw **Intermediate wash deposit (late and middle Pleistocene)**—Alluvial-wash deposits, inactive over tens to hundreds of thousands of years, commonly associated with intermediate to high-terrace levels above active washes. Moderately to locally well sorted, subangular to subrounded, pebble to cobble, and locally boulder gravel and sand, poorly to moderately indurated. Surfaces typically characterized by moderately developed to well-developed pavement and moderate to strong varnish on surface clasts. Moderate to strong soil development from 1 to >1.5 m depth, with thick (2–7 cm), fine-textured (fine sand, silt, and some clay) Av horizons, weak to strong Bt argillic horizons, and stage I to III+ calcic to petrocalcic horizons. Typically, minor to moderate but, in places, high (0.5–2 m, locally >7 m) local terrace heights above adjacent drainage channels. Generally sparse to no vegetation, typically creosote to small shrubs and bushes, that is concentrated in local drainages. More widely distributed tracts in distal fan positions are mapped as unit Qia

Alluvial-fan Deposits

Qaa **Active alluvial-fan deposit (latest Holocene)**—Active alluvial-fan deposits that have experienced surface runoff and associated deposition within the past few decades to, at most, the past century. In many cases, the geometry of recent deposition is highlighted in one or more aerial photographs and (or) Landsat images acquired in the past several decades. Generally, poorly integrated, complexly braided to anastomosing channel systems with intervening bars, producing distributed-flow microtopography with local relief ≤0.5 m. Prone to flooding during locally intense and (or) prolonged local to regional precipitation events. Composed of loose, poorly to moderately sorted, coarse to fine sand and subangular to subrounded gravel. Textures vary from fine to coarse sand and pebble to cobble and, locally, boulder gravel, with finer textured sediments in interchannel bars and distal fans. Generally textural fining from proximal to distal fans. No significant modification of original depositional surfaces. No soil development, other than very thin (≤1–2 cm thick) crust of finer grained silt and very fine sand in areas that have not experienced recent flows. No long-term establishment of vegetation in channels or subchannels and only limited vegetation (predominantly creosote bushes, *Larrea tridentata*, and several other bushes, mostly cheesebrush, *Ambrosia salsola*) on interchannel areas

Qaag **Active alluvial-fan deposit composed of grus (latest Holocene)**—Active alluvial-fan deposits derived from granitic source terrain that weathers to grus. Generally associated with poorly integrated distributed channels prone to flooding during high-intensity or long-duration precipitation events. Finer textured than unit Qaa deposits, dominated by fine to coarse sand and pebble to cobble gravel. Smoother microtopography with less internal relief (commonly ≤20–30 cm) between bars and distributary channels than unit Qaa. Most other characteristics, including lack of pavement, varnish, soil development, and sparse vegetative association, are equivalent to unit Qaa

Qya **Young alluvial-fan deposit (Holocene and latest Pleistocene)**—Alluvial-fan deposits associated with alluvial surfaces that are inactive or that receive discharge and sedimentation over hundreds to thousands of years. Moderately to poorly sorted sandy gravel and gravelly sand, poorly to moderately consolidated. Distinct fining of coarse fraction from cobble-boulders to pebble-cobbles between proximal range front to distal piedmont positions. Increased modification of original flow microtopography with increasing age into strong to weak bar and swale remnant surfaces. Variable local dissection, ranging from no to minor incision, especially in medial to distal fan positions, but in places moderately dissected (as much as 2–5 m) with progressively inset older to younger subunits in tectonically uplifted alluviated regions or adjacent to persistently incised axial drainages. No to weak varnish and no to moderate pavement development. Weak to moderate soil development ranging in depth from 30 to 100 cm, characterized by 1- to 5-cm-thick Av horizons consisting of fine sand and silt; at most weak cambic Bw horizons marked by reddening, minor textural fining, and (or) weak structure; and Stage I to II– calcic horizon development. Luminescence dating of unit Qya deposits provides ages of ~4 to 17 ka in the Valjean Valley piedmont in the eastern part of the map (Mahan and others, 2007) and in southern Death Valley in the north-central part of the map (Sohn and others, 2007), although the older deposits are also mapped as unit Qyao. Moderately to sparsely vegetated, typically with creosote and shrubs generally distributed across surfaces, but locally concentrated in small rills and minor drainages

Qyao **Older young alluvial-fan deposit (early Holocene and latest Pleistocene)**—Older subunit of alluvial-fan deposits of unit Qya, differentiated mainly in areas with field control. Similar lithologically to unit Qya but generally at least moderately compact. Alluvial surfaces typically modified with very faint gravel concentrations marking highly dispersed relict bars interspersed with vaguely bounded finer-grained and smoother zones of incipient pavement development on scale of several meters. Commonly some internal drainage and (or) shallow dissection (channels commonly 1–3 m deep), locally increasing to >5 m depth in uplifted or persistently dissected piedmonts. Faint to weak varnish development most strongly developed on more susceptible lithologies in finer-textured segregated zones. Moderate soil development consisting of moderately thick Av horizons (1–5 cm thick), cambic to thin weakly developed Bt argillic horizons, and Stage I–II calcic-horizon development generally at maximum depths of 80 to 100 cm. Luminescence dating of deposits in southern Death Valley in the north-central part of the map provides ages of ~11–17 ka (Sohn and others, 2007)

Qyag **Young alluvial-fan deposit composed of grus (Holocene and latest Pleistocene)**—Alluvial-fan deposits derived from granitic source terrain that weathers to grus. Small-scale to muted bar-and-swale microtopography with only minor local relief (generally ≤10–30 cm depth). Generally loose to weakly consolidated, finer-grained sediments dominated by sand and pebble to fine cobble gravel, relative to unit Qya. Weak to moderate local drainage development with minor internal dissection. No to weak pavement and little to no varnish development. Weak soil development dominated by sandy and silty Av horizons, poorly rubified cambic Bw horizons, and stage I–I+ calcic horizons

Qyaog **Older young alluvial-fan deposit composed of grus (early Holocene and latest Pleistocene)**—Older subunit of alluvial-fan deposits (unit Qyag) derived from granitic source terrain that weathers to grus. Finer-grained sediments dominated by coarse to fine sand and pebble to fine cobble gravel, weakly to poorly consolidated, with finer gravel concentrated in distal fan areas. Mapped only where identified in field. Commonly low relief internal drainage with minimal dissection except within uplifted piedmonts or along incised basin drainages. Generally associated with weakly developed pavements marked by faint relict concentrations of gravel with only, at most, very weak varnish accumulations on surface clasts. Soil development generally at stronger end of spectrum for unit Qyag, but typically more weakly formed and shallower in depth than most unit Qyao deposits, with thin Av, cambic Bw, and stage I carbonate horizons

Qia **Intermediate alluvial-fan deposit (late and middle Pleistocene)**—Alluvial-fan deposits characterized by inactive alluvial surfaces that have been abandoned for tens to hundreds of thousands of years. Degree of internal dissection variable, with local relief varying from 0.5 to 2.0 m, in places exceeding 5 m, along narrow incised drainages. Poorly sorted, weakly to moderately consolidated, poorly stratified cobble-pebble to locally boulder gravel, sand, and silt. Generally associated with wide, flat to gently rounded interfluves that possess moderately developed to well-developed desert pavements, strong varnish, and moderately to locally strongly weathered surface clasts. Moderate to strong soil development, commonly 1–2 m in depth, consisting of well-developed platy Av horizons 3–10 cm thick, moderately to strongly developed Bt argillic horizons and stage II–III+, and locally IV–, calcic horizons. Degree of varnish, pavements, and Bt development more subdued and calcic horizons more strongly developed on unit Qia deposits composed largely of clasts with carbonate lithologies. Pavement, varnish, and Av horizons are also less well developed to absent at altitudes exceeding 1,100 m; Bt horizons can be thicker and calcic horizons can be thinner at these altitudes. Luminescence dating of unit Qia deposits in the upper Valjean Valley area, a piedmont south of the map area, and southern Death Valley in the north-central part of the map yield ages of ~25–53 ka (Mahan and others, 2007; Sohn and others, 2007). Cosmogenic ages for unit Qia deposits vary with position on the piedmont, ranging from ~40 to 100 ka on proximal high-altitude fan deposits and 170 ka for lower elevation more distal units in central and northern Death Valley north of the map area (Machette and others, 2008; Frankel and others, 2007). Surfaces sparsely vegetated on smooth, well-varnished interfluve surfaces, with greater local concentrations of creosote bushes and small shrubs within discrete internal drainages

Qiag **Intermediate alluvial-fan deposit composed of grus (late and middle Pleistocene)**—Alluvial-fan deposits derived from granitic source terrain that weathers to grus. Commonly finer grained than unit Qia, consisting of poorly sorted, weakly to moderately consolidated, poorly stratified sand, silt, and pebble-cobble gravel. Variable dissection, but commonly in range of <0.5 to 2 m. Interfluves characterized by poorly developed desert pavements, lacking relict flow features, with poor varnishing and weak to moderate weathering of surface clasts. Moderate to strong soil development with thin, weak Av horizons and, at depth, moderate Bt argillic horizons and stage II–II+ calcic horizons

Qoa **Old alluvial-fan deposit (middle and early Pleistocene)**—Alluvial-fan deposits characterized by variably degraded remnants of former alluvial surfaces abandoned for hundreds of thousands of years marked by accordant series of gravel ridges. Generally located in proximal piedmonts adjacent to or within pedimented range fronts, uplifted fan remnants above tectonically active uplifted range fronts, or locally within uplifted alluvial divides, depending on position relative to active deformation. Poorly sorted, compact to well-cemented, coarse-grained (boulder-cobble-pebble) gravel and sand. Topographically associated with narrow, gently rounded to locally flat, degraded relict surfaces, with little or no preserved depositional morphology, that are separated by drainages incised meters to tens of meters to the level of adjacent younger piedmont surfaces. Surfaces commonly underlain by variable, weak, stripped pavement associated with fragmented, variably varnished clasts and disaggregated reworked fragments of petrocalcic horizons. Soils typically stripped or eroded, generally characterized by thin younger Av or thin Bw cambic or Bt argillic horizons overlying an older thick (as much as 2 to >4 m) stage IV or greater calcic horizons at depth. Moderately vegetated. An ash interbedded near the base of unit Qoa in the upper alluvial embayment between the Saddle Peak Mountains and Ibex Hills has been correlated with the 0.74 Ma Bishop Tuff (D. Miller, U.S. Geological Survey, unpublished data, 2004). Similar relations are reported in correlative fanglomerates to the north in the Amargosa Desert (Whitney and others, 2004) and to the south in the western Providence Mountains (McDonald and others, 1995). An ash interbedded in unit Qoa in Death Valley northeast of Shore Line Butte is correlated with a source vent at nearby Cinder Hill (Troxel and Butler, 1986b), dated originally by K-Ar method as 0.69 ka (R. Drake *in* Wright and Troxel, 1984) but redated by Ar-Ar method as <0.38 ka (T. Pavlis, University of Texas at El Paso, unpublished data, 2005)

Qoag **Old alluvial-fan deposit composed of grus (middle and early Pleistocene)**—Old alluvial-fan deposits composed of clasts derived from granitic source terrain that weathers to grus. Typically characterized by eroded dissected fan remnants located on accordant gently rounded to rounded ridgecrests located on distal piedmonts within or adjacent to pedimented mountain fronts. Sedimentologic characteristics similar to unit Qoa, with a commonly slightly finer grained gravel component. May have weakly eroded pavements with weathered and fractured clasts and disaggregated carbonate-horizon fragments on the surface. Soils eroded at surface, with no Av and rare thin Bt argillic horizons near the surface and stage III+ to IV+ calcic horizons at depth. Moderate vegetation

QToa **Very old alluvial-fan deposit (early Pleistocene and Pliocene)**—Highly eroded alluvial-fan deposits characterized by a complete absence of original depositional surface and no remnants of soil profiles originally associated with these surfaces. Located in proximal piedmonts, commonly within pediment embayments or as tectonically deformed and (or) uplifted fan remnants in actively deforming areas. Cemented to very compact, poorly sorted, poorly stratified cobble-boulder-pebble gravel and sand with some silt. In places, contains some exotic clast lithologies, but generally consistent with derivation from adjacent highlands, particularly in tectonically uplifted areas. Associated with narrow rounded ridge crests in deeply dissected terrain (relief of tens of meters) with no relict pavements or ridge accordancy indicative of original depositional morphology, characteristics that, in conjunction with soils, differentiate these deposits from unit Qoa. Non-slope soils generally absent or limited to much younger superimposed profiles, although buried paleosols may be exposed locally. Moderately to well vegetated

Debris-flow Fan Deposits

Qyad **Young debris-flow fan deposit (Holocene and latest Pleistocene)**—Fan deposits related primarily to debris flows that are associated with inactive fan surfaces or surfaces that receive flows and sedimentation over hundreds to thousands of years. Variable local dissection, ranging from no to minor incision (to 2–3 m), that generally increases with relative age. Poorly sorted, poorly to moderately consolidated, poorly bedded clay, silt, sand, and gravel (mostly pebble to cobble, with some boulders). Gravel clasts supported in pervasive fine-grained matrix that can be compact to consolidated. Some fining of coarse fraction from proximal to distal positions on piedmont fans. Low-relief microtopography generally present that superficially resembles bar and swale but is associated with gravelly levees and finer-grained intervening flat areas. No to weak pavement development concentrated in interlevee flat areas and no to incipient varnish. Thin, very weak to weak soil development, characterized by thin (1–3 cm) Av horizons, no to weak Bw cambic horizons, and at most shallow-depth stage I calcic horizons; soil development weaker than the typical soil development associated with equivalent-aged alluvial deposits of unit Qya. Generally sparse vegetation mostly concentrated in local rills and minor drainages. Mapped only where verified by field mapping. Luminescence age of 5 ka for a middle subunit of Qyad in Valjean Valley (Mahan and others, 2007)

Qyaod **Older young debris-flow fan deposit (early Holocene and latest Pleistocene)**—Older subunit of debris-flow deposits of Qyad. Similar lithologically to unit Qyad but commonly at least moderately consolidated and contains coarser-grained gravels. Mapped only where verified by field mapping. Surfaces contain low relief, in places with faint, relict levee-gravel concentrations between smooth fine-grained flat areas. Minor local channel incision, mostly 2–3 m deep, within and at margins of unit. Weak to moderate varnish and incipient to weak pavement development, typically enhanced in fine-grained flat areas. Weak, thin soil development characterized by thin (2–3 cm) weak Av horizons, weak color-based Bw cambic horizons, and stage I calcic horizons at shallow depths. Generally sparse vegetation concentrated in local rills and gullies

Qiad **Intermediate debris-flow fan deposit (late and middle Pleistocene)**—Fan deposits related primarily to debris flows that are associated with inactive surfaces that have been abandoned for tens to hundreds of thousands of years. Variably dissected, but maximum internal incision may reach 3 to >5 m, in some cases exceeding smaller local heights of 1–3 m above the adjacent alluvial-piedmont deposits. Poorly sorted, poorly bedded, consolidated clay, silt, sand, and gravel that commonly ranges from cobble to boulder size. Gravel clasts supported in pervasive fine-grained matrix that consolidates deposit. Moderate to strong pavement development, with no relict depositional morphology, although some boulder protuberance on older more degraded deposits may represent former highly eroded levees. Moderate to strong varnish and weathering of surface clasts. Moderate to strong soil development, characterized by moderate to strong Av horizons 3–5 cm thick, weak to moderately developed Bt argillic horizons, and stage II–III+ calcic horizons; soil development weaker and shallower in depth than the typical soil development associated with equivalent-aged alluvial-fan deposits of unit Qia. Vegetation absent to very sparse on surfaces, except where locally concentrated within incised gully systems

Eolian Deposits

Qae **Active eolian sand deposit (latest Holocene)**—Eolian sand deposits that are active and subject to dispersal and migration. Composed of loose, moderately sorted to well sorted, poorly to moderately bedded, fine to medium sand. No soil or stabilized surface development. Generally, lacks vegetation, although locally sparsely mantled by small grasses and isolated shrubs. Boundaries with adjacent units are commonly gradational. Most active eolian deposits lie within a diffusely bounded zone or belt extending discontinuously along and to the north of southern Death Valley and northern Valjean Valley from west of the southernmost Black Mountains to the Valjean Hills. Subdivided by morphology into sand-dune, sand-ramp, and sand-sheet deposits

Qaed **Active eolian sand-dune deposit (latest Holocene)**—Eolian deposits forming distinct dunes subject to migration. Commonly form steep-sided slip faces and sharp crests. Primary locations are the Dumont Dunes, the piedmont west of the central Salt Spring Hills, and in lower embayment on southwest side of Saddle Peak Hills

Qaer **Active eolian sand-ramp deposit (latest Holocene)**—Eolian deposits associated with ramps, or inclined sloping surfaces, subject to migration. Ramps typically banked against partially or completely buried bedrock hills or ridges and may form climbing and falling dunes where actively migrating up or down slopes. Especially prominent on lower altitude sections of the Ibex, Saddle Peak, Salt Spring, and Valjean Hills

Qaes **Active eolian sand-sheet deposit (latest Holocene)**—Eolian deposits associated with low-relief, flat to gently sloping sheets of sand subject to active dispersal and migration. Sand sheets commonly develop above distal to medial piedmont surfaces, commonly adjacent to and downwind of wide, complexly braided channels or channel fans dominated by fine to medium sand and silt, such as distal piedmonts north and east of the Amargosa River in the southern Death Valley

Qye **Young eolian sand deposit (Holocene and latest Pleistocene)**—Eolian deposits that generally are not actively migrating or mobilized for hundreds to thousands of years; composed of loose to slightly compact, moderately sorted to well sorted, moderately to weakly bedded, fine to medium sand. No to weak soil development, mostly in more stabilized areas consisting of thin local crusts above a horizon of admixed silt and sand, locally with minor color modification. Variable vegetation, consisting of dispersed to locally concentrated clusters of creosote, mesquite, or grasses, commonly with coppice dunes to larger coalescent mounds developed around individual to clumped bushes or trees

Qier **Intermediate eolian sand-ramp deposit (late and middle Pleistocene)**—Eolian deposits not active over tens of thousands of years. Commonly associated with inactive stabilized ramps, or inclined sloping surfaces, that are not subject to migration. Ramps are banked against the lower to medial flanks of bedrock ridges. Some development of minor shallow rills. Development of stabilized surfaces with partial pavement consisting of crust of sand intermixed with scattered, moderately to strongly varnished, colluvial clasts of pebble to cobble gravel. Moderate soils developed beneath pavement characterized by Av, Bw cambic, and stage II calcic horizons; local exposures in dissected sideslopes of interbedded sloping paleosols. Mostly barren, with local sparse vegetation mostly concentrated along rills

Mixed Wash, Alluvial-fan, and (or) Eolian Deposits

Qawe **Active mixed wash and eolian deposit (latest Holocene)**—Alluvial-wash and eolian deposits that are thoroughly intermixed, with alluvial-wash processes dominant. Loose alluvial sand and gravel in active washes similar to unit Qaw, but with significant additional admixtures of eolian fine and medium sand at surface and shallow depth. Associated with shallow-depth (≤0.5 m) channels with indistinct boundaries and low-relief muted internal fluvial microtopography. No significant soil development or surface stabilization. Generally, sparse to no vegetation; mostly grasses and few isolated small bushes along some channel margins. Boundaries with adjacent units may be ill defined and gradational. Commonly located in discrete washes on distal piedmonts within areas of significant eolian accumulation or transport

Qaae **Active mixed alluvial-fan and eolian deposit (latest Holocene)**—Alluvial-fan and eolian deposits that are thoroughly intermixed, with alluvial-fan depositional processes dominant. Generally associated with poorly defined active drainages with indistinct microtopography due to muting effect of additional eolian sand component. Loose gravelly sand to sandy gravel with poor to indistinct thin bedding, similar to unit Qaa but with significant additional admixtures of eolian fine and medium sand at surface and shallow depth. No significant soil development or surface stabilization. Rare to no long-term vegetation, mainly widely dispersed in interchannel areas. Boundaries with adjacent units may be ill defined and gradational. Commonly located on low-relief distal to medial piedmonts within areas of significant eolian accumulation or transport

Qywe **Young mixed wash and eolian deposit (Holocene and latest Pleistocene)**—Alluvial-wash and eolian deposits that are thoroughly intermixed, with alluvial-wash processes dominant. Generally associated with mostly inactive washes, similar to unit Qyw, containing low terraces adjacent to active washes. Loose to consolidated gravelly sand and sandy gravel similar to unit Qyw, weakly to thinly bedded, with significant additional admixtures of eolian fine and medium sand at surface and shallow depth. Generally little or no soil development; mostly associated with crust of fine sand and silt that is locally weakly vesicular and possibly thin color Bw cambic horizon. No to very weak pavement, mostly consisting of veneer of scattered, noncontiguous gravel with weak to no varnish development. Sparse vegetation, mostly isolated creosote and small bushes, some with small coppice-dune accumulations. Boundaries with adjacent units may be ill defined and gradational. Commonly located in variably incised discrete washes within piedmonts in areas of significant eolian accumulation or transport

Qyae **Young mixed alluvial-fan and eolian deposit (Holocene and latest Pleistocene)**—Alluvial-fan and eolian deposits that are thoroughly intermixed, with alluvial-fan depositional processes dominant. Generally associated with mostly inactive alluvial surfaces with indistinct microtopography, in part enhanced by the muting effect of an additional eolian sand component. Variable local relief, with mostly little or minor dissection, locally increasing to 2–5 m in some medial to proximal piedmonts in sand-rich areas. Loose to consolidated gravelly sand and sandy gravel similar to unit Qya, but with significant additional admixtures of eolian fine and medium sand, especially at the surface and shallow depth. Generally little or no soil development, mostly associated with crust of fine sand and silt that is locally weakly vesicular, possibly thin color Bw cambic horizon, and, in older subunit, possibly thin stage I calcic horizon. No to very weak pavement, mostly consisting of veneer of isolated noncontiguous gravel, with weak to no varnish development. Sparse vegetation, mostly isolated creosote and small bushes, some with small coppice-dune accumulations. Boundaries with adjacent units may be ill defined and gradational. Commonly located in mostly low-relief piedmonts in areas of significant eolian accumulation or transport

Qyea **Young mixed eolian and alluvial-fan deposit (Holocene and latest Pleistocene)**—Eolian and alluvial-fan deposits that are thoroughly intermixed, with eolian depositional processes dominant. Generally associated with mostly inactive alluvial surfaces that have a very significant, even dominant, eolian fine and medium sand component that discontinuously mantles but is intermixed with alluvium, especially at the surface and shallow depths. Mostly flat and undissected with, at most, shallow local drainage, typically vaguely defined to cryptic due to masking effect of eolian sand component on surface. Loose to poorly consolidated sand and gravelly sand, with sparse scattered to poorly interbedded pebble to cobble gravel. Little or no soil development, mostly consisting of poorly defined thin horizon of textural fining and possible color change, with little or no secondary carbonate. No to very weak pavement, defined by layer of widely scattered isolated surface gravels with weak to no varnish development. Sparse vegetation, mostly grasses, small bushes, and locally mesquite bosque plant association, but no creosote bush. Vegetation commonly associated with large prominent single to coalescent coppice dunes and mounds. Boundaries with adjacent units may be ill defined and gradational. Located in mostly low relief piedmonts in areas of major eolian-sand accumulation and transport, commonly adjacent to potential source areas (for example, Silurian and Valjean Valleys)

Qiwe **Intermediate mixed wash and eolian deposit (late and middle Pleistocene)**—Alluvial-wash and eolian deposits that are thoroughly intermixed, with alluvial-wash processes dominant. Commonly poorly to moderately consolidated gravelly sand, with a cobble, pebble, to local boulder gravel component, associated with intermediate to high terrace levels above active channels and (or) lower terraces, similar to unit Qiw but with significant additional admixtures of eolian fine and medium sand. Generally low internal relief but developed along drainages with low to moderate incision commonly in range of 2 to >7 m. Variable, weak to moderate pavement, with loosely packed layer of moderately to weakly varnished surface clasts. Variable, weak to moderate to locally strong soil development consisting of Bt argillic and stage II–III calcic horizon development. Moderate to sparse vegetation. Typically located along incised reaches of major axial or transverse drainage such as the Amargosa River or Kingston Wash in areas of significant accumulation and transport of eolian sand

Qiae **Intermediate mixed alluvial-fan and eolian deposit (late and middle Pleistocene)**—Alluvial-fan and eolian deposits that are thoroughly intermixed, with alluvial-fan depositional processes dominant. Generally associated with abandoned inactive alluvial surfaces with very low relief and widely spaced incised drainages (depths of 2 to >7 m). Commonly poorly to moderately consolidated gravelly sand, with cobble, pebble, to local boulder gravel; similar to unit Qia but with significant additional admixtures of eolian fine and medium sand. Variable, weak to moderate pavement, with scattered to loosely packed surface layer of moderately to weakly varnished surface clasts. Variable, weak to moderate to locally strong soil development consisting of Bt argillic and stage II–III calcic-horizon development that is generally weaker and more inconsistent than observed in unit Qia. Generally sparse vegetation, especially absent in interdrainage areas, in places associated with small to moderately sized coppice-dune formation. Typically located on dissected proximal to medial piedmonts and range fronts in areas of significant accumulation and transport of eolian sand such as the southeastern margin of Tecopa Basin, the southern piedmonts of the Sperry and Dumont Hills, and the central and southeastern Silurian Valley

Qoae **Old mixed alluvial-fan and eolian deposit (middle and early Pleistocene)**—Alluvial-fan and eolian deposits that are thoroughly intermixed, with alluvial-fan depositional processes dominant. Generally associated with abandoned inactive alluvial surfaces with very low relief on narrow interfluves between moderately to deeply incised drainages (depths of 5 to >10 m). Commonly poorly to moderately consolidated gravelly sand, with cobble, pebble, to local boulder gravel, similar to unit Qoa, but with significant admixtures of eolian fine and medium sand. Variable, weak to moderate pavement, with scattered to loosely packed surface layer of moderately to weakly varnished surface clasts and disaggregated reworked fragments of petrocalcic horizons. Variable, weak to moderate to locally strong soil development consisting of Bt argillic and stage III–IV calcic-horizon development that is generally weaker and more inconsistently developed than observed in unit Qoa. Generally sparse vegetation, especially absent in interdrainage areas, in places associated with small to moderate coppice dune formation. Typically located on dissected proximal to medial piedmonts in areas of significant accumulation and transport of eolian sand such as piedmonts in southeastern California Valley and locally in upper Silurian Valley

QToae **Very old mixed alluvial-fan and eolian deposit (early Pleistocene and Pliocene)**—Alluvial-fan and eolian deposits that are thoroughly intermixed, with alluvial-fan depositional processes dominant. Generally associated with highly eroded and dissected alluvial-fan deposits characterized by a complete absence of original depositional surfaces. Cemented to very compact gravel sand to sandy gravel with some silt, similar to unit QToa but with additional eolian fine and medium sand intermixed at surface and in upper section. Associated with deeply dissected terrain (relief of tens of meters) with no preserved relict pavements. Non-slope soils generally absent or limited to much younger superimposed profiles. Sparsely to moderately vegetated. Occurs mostly in highly dissected terrain at basin margins or within adjacent highlands in areas of significant long-term accumulation and transport of eolian sand, such as the southeastern margin of Tecopa Basin

Playa Deposits

Qap **Active playa deposit (latest Holocene)**—Deposits associated with dry playas that actively receive water and sediment from surface runoff derived from adjoining piedmonts and highlands, and locally axial valley washes, over years to decades. Prone to flooding, with ephemeral standing water present following single large or prolonged series of runoff-generating precipitation events. Mainly weakly bedded, poorly sorted silt, clay, and sand, with evaporative salt in some cases. Bedding thin to thick and subhorizontal. Compact. Flat to very gently undulating surfaces, in places mud cracked with salt encrustations; in places cut by linear to polygonal fissures that support similarly oriented vegetation arrays. No soil development. Subject to eolian deposition and erosion during windstorms. Sparse or no vegetation across primary surfaces actively receiving runoff and sediment accumulation. Typically located in several physiographic and geologic settings, including (1) the center of basins with closed internal drainage (for example, Owl Lake and Lost Lake playas), (2) very low gradient reaches of axial drainages (for example, Silurian Lake playa and playa in upper Wingate Wash), and (3) small, closed depressions developed in deformation zones along active fault systems (for example, the central section of the Southern Death Valley and southern Panamint Valley Fault Zones)

Qyp **Young playa deposit (Holocene and latest Pleistocene)**—Deposits associated with dry mostly inactive playas that are rarely or not flooded within decades or longer. Mostly weakly bedded, poorly sorted silt, clay, and sand, commonly compact. Generally flat to gently undulating surfaces, with no to sparse vegetation. May have some weak soil formation in areas that have not received recent discharge or sedimentation. Located along margins of Leach Lake playa that have been uplifted along active traces of the eastern Garlock Fault and are isolated from topographically lower and more active areas of the playa (unit Qap)

Qypf **Young playa-fringe deposit (Holocene and latest Pleistocene)**—Deposits along the margins or fringes of playas that exhibit characteristics of multiple depositional processes. Associated with areas that do not receive sediment or discharge except in rare, exceptionally large rainfall events over tens to hundreds of years. Composed of silt, clay, and sand, commonly compact. Forms low-gradient surface with sparse to moderate vegetation, mostly grasses and isolated creosote to salt-tolerant bushes, some with low coppice-dune accumulations. Genetically associated with complex intermixture of eolian, playa, lacustrine, alluvial, and groundwater-discharge deposits. Commonly located along margins of larger playas such as Silurian Lake, as well as inactive Holocene (unit Qyp) sections of Leach Lake playa. Luminescence dating along the margins of Silurian Lake playa establishes a complex, mostly late to locally middle Holocene age (0.85 to 6.5 ka; Mahan and others, 2007), suggesting that the sections of the playa within this map unit have been inactive since at least this time period.

Qip **Intermediate playa deposit (late and middle Pleistocene)**—Deposits associated with inactive playas that have not received discharge or sediments in tens to hundreds of thousands of years. Composed of silt, clay, and sand, commonly compact to weakly consolidated. Forms low-gradient to gently undulating surfaces with no to sparse vegetation consisting mostly of grasses and isolated creosote to salt-tolerant bushes, some with low coppice-dune accumulations. May support some incipient development of local, low-relief rills and drainage. Located along margins of Leach Lake playa that have been uplifted along active traces of the eastern Garlock Fault

Valley-axis Deposits

Qav **Active valley-axis deposit (latest Holocene)**—Fine-grained deposits along valley axes in the center of alluvial basins that actively receive discharge and sediment on at least decadal scales. Most commonly associated with margins of unincised channel reaches and (or) the margins of valley lowlands of axial drainages or basin-axis reaches of interbasin regional drainages such as the Amargosa River. Low-relief, gently sloping to undulating surfaces characterized by small, indistinct anastomosing washes, low diffuse interfluves, and complexly interfingering wash, alluvial, and eolian sediments. Composed of loose, moderately to poorly sorted fine gravel, sand, silt, and clay. Prone to flooding during large or sustained precipitation events. Little or no soil development, at most consisting of a thin crust and upper texturally defined horizons with increased fine sand and silt. Active channels commonly lack vegetation, but older interfluves and low terraces host moderately dense vegetation consisting of creosote bushes, small shrubs, and annual grasses. Low coppice dunes may form on single or clustered vegetation on more inactive surfaces. Contacts with adjacent wash or alluvial-fan deposits commonly gradational and somewhat arbitrary

Qyv **Young valley-axis deposit (Holocene and latest Pleistocene)**—Fine-grained deposits along mostly inactive valley axes in the center of alluvial basins that have not received discharge or sediments for hundreds to thousands of years. Most commonly associated with older and more elevated margins of slightly incised to unincised channel reaches and (or) the margins of valley lowlands of axial drainages or basin-axis reaches of interbasin regional drainages such as the Amargosa River. Low-relief, gently sloping to undulating surface characterized by small, indistinct anastomosing washes, low diffuse interfluves, and complexly interfingering wash, alluvial, and eolian sediments. Composed of loose, moderately to poorly sorted, fine gravel, sand, silt, and clay. Weak soil development consisting of thin to moderate Av, Bw cambic, and stage I calcic horizons generally equivalent to younger to middle subunits of Qya deposits. Moderately vegetated by creosote bushes, small desert shrubs, and eolian-related grasses, commonly with low coppice dunes forming at the base of single to clustered vegetation. Contacts with adjacent wash or alluvial-fan deposits commonly gradational and somewhat arbitrary

Lacustrine Deposits

Qil **Intermediate lacustrine deposit (late and middle Pleistocene)**—Pluvial-lake sediments deposited along the margin of southern Death Valley that formed in association with preserved stands of late Pleistocene pluvial Lake Manley. Poorly to moderately consolidated, moderately sorted to well-sorted, moderately bedded to well-bedded sand, silt, and rounded to subrounded pebble-cobble gravel. Local foreset crossbedding. Mainly occur as discontinuous, thin capping veneers, commonly on sloping to locally benched sections of dissected broad interfluves (2 to >5 m height). Associated with moderate to strongly varnished pavement and moderate to strong soil development in upper part of preserved deposit, consisting of Bt argillic and stage II–III calcic soils similar to unit Qia. No to sparse vegetation on capping surfaces. Commonly located as moderately deformed capping and inset deposits above older, more deformed sediments of unit QToal along and adjacent to the Southern Death Valley Fault Zone in and north of the Noble hills. Existing age constraints consist of tufa deposits within the sediments yielding uranium-series ages of ~130–140 ka (J. Caskey, San Francisco State University, unpublished data, 2011)

Qilg **Intermediate lacustrine gravel deposit (late and middle Pleistocene)**—Pluvial-lake sediments, deposited along the margin of southern Death Valley, that formed in association with preserved stands of late Pleistocene pluvial Lake Manley. Similar to unit Qil, except consisting of coarser-grained facies of lacustrine sediments dominated by pebble to cobble gravel and sand textures. Similar surface and soil development characteristics to unit Qil. Commonly occurring as moderately deformed capping and inset deposits above older, more deformed sediments of unit QToal along and adjacent to the Southern Death Valley Fault Zone in and north of the Noble hills

Mixed Alluvial and Lacustrine Deposits

QToal **Quaternary old and Quaternary to upper Tertiary mixed alluvial and lacustrine deposit (middle and early Pleistocene to Pliocene)**—Interstratified sequence of alluvial and lacustrine deposits, with alluvial processes dominant. Consists of (1) poorly to moderately consolidated, moderately bedded to well-bedded, coarse to fine sand; (2) pebble to cobble, subrounded to rounded gravel; (3) fine-grained sequences of moderately indurated to well-indurated, moderately bedded to well-bedded, fine-grained silt and clay; and (4) single or multiple layers of indurated, thinly bedded to massive evaporites, mainly gypsum, halite, and anhydrite, that are interbedded within some fine-grained strata. Deposits located primarily in two areas along and adjacent to the Southern Death Valley Fault Zone within southern Death Valley, including variably deformed strata within a series of low-relief dissected ridges, hills, and intervening planated surfaces that are discontinuously exposed beneath younger capping to inset middle to late Quaternary alluvial deposits in the central part of the valley northwest of the Noble hills and complexly deformed and uplifted deposits of the Confidence Hills Formation of Beratan and others (1999) extensively exposed throughout the Confidence Hills. Fine-grained mudstones and evaporite beds are more common lower in the section and particularly prominent in the Confidence Hills section, with coarse sand and gravel components increasing upsection and some gravels high in the section of the central valley deposits. Several discrete subunits are differentiable, based both on lithologic variations and degree of deformation locally indicated by angular unconformities. Age control consists of (1) numerous interbedded tephra layers in the central valley locality that include the Mesquite Lake tephra (~3.4 Ma) in lower, more deformed strata and tephras of upper Glass Mountain (~1.2 Ma); an overlying series of newly identified ashes, including the Amargosa ash (~1.3 Ma) and the Bailey bed (~1.2 Ma); and the Lava Creek B ash (~640 ka) in the overlying upper sequence (Green, 2009; Knott and others, 2018) and (2) the Huckleberry Ridge tephra (~2.0 Ma) in the lower section and a paleomagnetic chronology that extends from below the Re´union event in the lower Matuyama reverse chron to well above the Olduvai event in the Brunhes normal chron in the Confidence Hills Formation (Troxel and others, 1986; Beratan and others, 1999)

Groundwater-discharge Deposits

Qag **Active groundwater-discharge deposit (latest Holocene)**—Deposits in moist to wet zones of active groundwater discharge. Commonly located at seeps on bedrock-alluvial contacts where the water table intersects the surface. Composed of loose to compact fine sand and silt, generally pale gray, light brown, and white. Abundant, locally dense vegetation dominated by mesquite bosque associations, grasses, and (or) reed thickets commonly concentrated in seepage areas that act as traps for the significant fine-grained eolian component of sediments. Generally modified to varying degrees by anthropogenic water development, including formation of artificially impounded pools and (or) enhanced water entrapment around small natural seepage zones. Associated with Saratoga Springs, springs at Ibex Hills, Resting Spring, Salt Spring Hills, and Owl Hole Springs. Larger spring deposits locally subdivided into spring-mound and wetland subunits

Qags **Active spring-mound groundwater-discharge deposit (latest Holocene)**—Active groundwater-discharge deposits that form distinct mounds or elevated areas. Fine-grained sediments may be, locally, very compact to weakly cemented by carbonate. Commonly associated with abundant vegetation dominated by mesquite bosque associations, grasses, and (or) reed thickets across mounds (for example springs near Shoshone)

Qagw **Active wetland groundwater-discharge deposit (latest Holocene)**—Active groundwater-discharge deposits located in very moist low-relief zones of seepage. Commonly associated with wet, in places muddy, organic-rich fine-grained sediments. Locally dense, abundant grassland to marsh-like saturated-zone vegetation. Mainly associated with springs adjacent to the Amargosa River channel north of Shoshone, in lower Tecopa basin near Tecopa and Tecopa Hot Springs, and in lowland areas around and upslope from Saratoga Springs

Qyg **Young groundwater-discharge deposit (Holocene and latest Pleistocene)**—Deposits in zones of former groundwater discharge inactive over hundreds to thousands of years. Forms in flat to dissected badland areas that, in places, surround and enclose more spatially restricted and localized zones of active seepage. Composed of light-colored, loose to compact, massive to poorly bedded silt and fine sand. May include variable amounts of calcium-carbonate materials, including diffusely disseminated matrix accumulations, capping ledges, and popcorn-like nodules as surface litter fragments and in localized zones in near-surface sediments. Soil development similar to unit Qya but with increased carbonate accumulations distributed over shallower depth range. Generally limited to sparse vegetation, especially relative to unit Qag in actively discharging springs

Qig **Intermediate groundwater-discharge deposit (late and middle Pleistocene)**—Deposits in zones of former groundwater discharge inactive over periods of tens to hundreds of thousands of years. Occurs locally in flat unincised zones within undissected interior parts of basins (for example, southern Death Valley floor between Saddle Peak Hills and Ibex Hills) but more commonly exposed as badlands or in valley walls of dissected terrain (for example, lower California Valley, southwestern Tecopa basin, central Chicago Valley, Silurian creek in the Salt Spring Hills area, and Denning Spring area between the western Avawatz and eastern Granite Mountains). Light-colored, loose to moderately indurated, massive to poorly bedded silt and fine sand with some clay. Variably but ubiquitously associated with secondary calcium carbonate morphologically distributed as nodules, diffuse to well indurated matrix cement, and carbonate-replaced casts of organic materials (rhizoliths). Soil development generally similar to unit Qia deposits but with typically stronger carbonate morphology (commonly stage II+ to IV calcic horizons) distributed in dense pods, lenses, and ledge-like stratal zones over a shallower depth range. May include one or more carbonate-dominated paleosols in thicker sections. Generally sparse to very limited vegetation. Yielded luminescence ages of ~20–50 ka and ~150–185 ka in several adjacent sections in lower California Valley (Mahan and others, 2007) and ^{14}C ages of 18–28 ka B.P. from shallow cores in the Salt Spring Hills area (Anderson and Wells, 2003b)

Qigs **Intermediate spring-mound groundwater-discharge deposit (late and middle Pleistocene)**—Groundwater-discharge deposits in areas of formerly active surface discharge that form distinct spring-fed mounds, ledges, or elevated areas. Commonly well cemented secondary carbonate and (or) opaline silica precipitates, locally laminated, that are intermixed with dispersed fine-grained sand or silt grains. Uranium-series dating of unit Qigs in eastern Tecopa basin yields ages of ~72, ~160, and ~280 ka (Nelson and others, 2001)

Mixed Lacustrine and Groundwater-discharge Deposits

QTolg **Quaternary intermediate, old, and Quaternary to upper Tertiary very old mixed lacustrine and groundwater-discharge deposits (Pleistocene and Pliocene)**—Intermixed sequence of lacustrine, groundwater-discharge, and local alluvial and fluvial deposits. These deposits were formed by a former series of shallow lakes and (or) spring-fed zones of surface groundwater discharge that were locally interspersed with fluvial and alluvial deposits of the ancestral Amargosa River and coeval tributary drainages within the basin. Exposed extensively in badland areas and valley walls throughout dissected sections of Tecopa basin and southern Chicago Valley. Consists predominantly of poorly bedded alternating sequences of light-colored, compact to weakly consolidated, fine-grained sediments (mudstones, claystones, siltstones, and fine-grained sandstone). Also contains local interbedded concentrations of sandy, subrounded to subangular, pebble to cobble gravels that locally exhibit fluvial to alluvial crossbedding and pebble imbrications. The fine-grained sediments locally contain interbedded, discontinuous to lenticular beds of fine-grained gravel, mostly in upper and northern parts of the section, and a series of at least 15 tephra layers that commonly form prominent widespread marker horizons. Many of the fine-grained sediments contain secondary authigenic alteration products including a variety of clays, zeolites, and other precipitates such as calcite, dolomite, halite, and gypsum (Starkey and Blackmon, 1979), as well as numerous sedimentary structures and recrystallized biotic casts (mudcracks, calcified root casts, and leaf mats) and microfossils (mostly ostracods) consistent with formation in shallow-depth lakes and (or) wetland areas. Some local intraformational fault and soft-sediment deformation (too small to map) also locally observed. Recovery of abundant vertebrate macrofossils of mostly Blancan, Irvingtonian, and Rancholabrean ages also reported (for example, Woodbourne and Whistler, 1991; Reynolds, 1991; Whistler and Webb, 2000). Geochronologic control establishes an age range of ~0.2 to >2.4 Ma from (1) tephrochronologic correlations of four of the interbedded ash layers, including the Wadsworth (~200 ka), Lava Creek B (~665 ka), Bishop (~760 ka), and Huckleberry Ridge (~2.1 Ma) ashes and (2) paleomagnetic stratigraphy of the entire section that includes Gauss, Matuyama, and Brunhes chrons (Hillhouse, 1987; Morrison, 1999)

Mass-wasting Deposits

Hillslope Deposits

Qha **Young to old colluvial hillslope deposits, undifferentiated (Holocene and Pleistocene)**—Discontinuous surficial mantle or veneer restricted to relatively thin irregular but areally significant local accumulations of hillslope deposits representing ≤4 percent coverage area above topographically irregular substrate bedrock surface. Generally, too small and irregular to be mapped individually, and unit has been mapped as surficial component of composite colluvial-veneer substrate map units. Includes mixtures of colluvium, talus, weathering residuum, and small landslides. Typically, thin (≤2m thick) and very patchy and irregularly distributed. Primarily consists of loose to weakly consolidated mixtures of angular to subangular pebble to cobble gravel with variable, but generally low amounts of fine-grained sand, silt, and locally clay matrix that compositionally reflects underlying or adjacent bedrock substrate material. Variable soil development, mainly ranging from no to weak thin soils, with some stronger soils (Bt argillic and Bk calcic soil horizons) on local areas of greater slope stability.

Colluvial Deposits

Qmc **Young to old mass-movement colluvial deposit, undifferentiated (Holocene and Pleistocene)**—Colluvial materials generally thicker than 2 m and covering a wide area. Consists of rocky, loose, angular, and poorly sorted material, with little matrix and open spaces between clasts. Variable soil development, ranging from very weak to strongly developed soils, with Bt argillic and Bk calcic horizons within any interstitial fine matrix. May be associated with locally varnished geomorphic surfaces completely mantling underlying rock substrate where deposits are sufficiently thick and continuous

Landslide Deposits

Qml **Young to old mass-movement landslide deposit, undifferentiated (Holocene and Pleistocene)**—Mass-wasting deposits generally thicker than 2 m associated with landslides covering a wide area. Generally, exhibit irregular hummocky surfaces. May be associated with discernible breakaway scarps and lobate internal features. Composed of variably consolidated, loose to cemented, angular, coarse to fine, and poorly sorted rocky debris; may include a fine-grained matrix supporting a network of framework clasts. Surfaces of older stabilized landslides may be associated with weak to moderate pavement, varnish, and soil development

COMPOSITE MAP UNITS

Veneered Map Units

[Veneers or covering mantles of a given surficial deposit that overlie older geologic units (surficial or substrate). Veneers are commonly thin (≤2–3 m) and generally or nearly continuous. Veneers are indicated to left of slash (/) above underlying older substrate material, to right and below slash. Refer to descriptions of singular units in Singular Map Units section for each component of composite map unit. Major undifferentiated bedrock substrate materials are described at end of Description of Map Units. Descriptions include additional details for each veneered composite unit]

Surficial-Deposit Veneers Overlying Older Geologic Units (Surficial or Substrate)

Qye/Qyw **Young eolian sand deposit *overlying* young wash deposit (Holocene and latest Pleistocene *overlying* Holocene and latest Pleistocene)**—Unit Qye forms a thin (<2 m) but nearly continuous eolian mantle overlying moderately to mostly inactive wash deposits within a zone of extensive active eolian accumulation

Qye/Qya **Young eolian sand deposit *overlying* young alluvial-fan deposit (Holocene and latest Pleistocene *overlying* Holocene and latest Pleistocene)**—Unit Qye forms a thin (<2 m), but nearly continuous eolian mantle overlying moderately to mostly inactive alluvial-fan deposits on piedmonts within a zone of extensive active eolian accumulation

Qye/Qiw **Young eolian sand deposit *overlying* intermediate wash deposit (Holocene and latest Pleistocene *overlying* late and middle Pleistocene)**—Unit Qye forms a thin (<2 m), but nearly continuous eolian mantle overlying older Pleistocene terrace deposits adjacent to a wash within a zone of extensive active eolian accumulation

Qye/Qia **Young eolian sand deposit *overlying* intermediate alluvial-fan deposit (Holocene and latest Pleistocene *overlying* late and middle Pleistocene)**—Unit Qye forms a thin (<2 m) but nearly continuous eolian mantle overlying older alluvial-fan deposits on older inactive piedmont areas within a zone of extensive active eolian accumulation

Qye/Qoa **Young eolian sand deposit *overlying* old alluvial-fan deposit (Holocene and latest Pleistocene *overlying* middle and early Pleistocene)**—Unit Qye forms a thin (<2 m) but nearly continuous eolian mantle overlying old dissected alluvial-fan deposits along range fronts within a zone of extensive active eolian accumulation

Qye/QToa Young eolian sand deposit *overlying* Quaternary to upper Tertiary very old alluvial-fan deposit **(Holocene and latest Pleistocene *overlying* early Pleistocene and Pliocene)**—Unit Qye forms a thin (<2 m) but nearly continuous eolian mantle overlying very old dissected alluvial-fan deposits along range fronts within a zone of extensive active eolian accumulation

Qye/ca+sl **Young eolian sand deposit *overlying* carbonate and siliciclastic rocks (Holocene and latest Pleistocene *overlying* pre-Quaternary)**—Unit Qye forms a thin (<2 m), but nearly continuous, eolian mantle overlying mixed rock substrate within low bedrock hills and lower slopes of bedrock ranges within a zone of extensive active eolian accumulation

Qye/fp **Young eolian sand deposit *overlying* felsic plutonic rocks (Holocene and latest Pleistocene *overlying* pre-Quaternary)**—Unit Qye forms a thin (<2 m), but nearly continuous, eolian mantle overlying rock substrate within low bedrock hills and lower slopes of bedrock ranges within a zone of extensive active eolian accumulation

Qye/fv **Young eolian sand deposit *overlying* felsic volcanic rocks (Holocene and latest Pleistocene *overlying* pre-Quaternary)**—Unit Qye forms a thin (<2 m), but nearly continuous, eolian mantle overlying rock substrate within low bedrock hills and lower slopes of bedrock ranges within a zone of extensive active eolian accumulation

Qye/mr **Young eolian sand deposit *overlying* metamorphic rocks (Holocene and latest Pleistocene *overlying* pre-Quaternary)**—Unit Qye forms a thin (<2 m), but nearly continuous, eolian mantle overlying rock substrate within low bedrock hills and lower slopes of bedrock ranges within a zone of extensive active eolian accumulation

Qye/pc **Young eolian sand deposit *overlying* partly consolidated deposits and rocks (Holocene and latest Pleistocene *overlying* pre-Quaternary, locally lower Quaternary)**—Unit Qye forms a thin (<2 m), but nearly continuous, eolian mantle overlying partially consolidated rock substrate within low bedrock hills and lower slopes of bedrock ranges within a zone of extensive active eolian accumulation

Qye/sl **Young eolian sand deposit *overlying* siliciclastic rocks (Holocene and latest Pleistocene *overlying* pre-Quaternary)**—Unit Qye forms a thin (<2 m) but nearly continuous eolian mantle overlying rock substrate within low bedrock hills and lower slopes of bedrock ranges within a zone of extensive active eolian accumulation

Qyae/Qia **Young mixed alluvial-fan and eolian deposit *overlying* intermediate alluvial-fan deposit (Holocene and latest Pleistocene *overlying* late and middle Pleistocene)**—Unit Qyae is a generally continuous and thin (<2 m) veneer above older, mostly inactive, alluvial fans located in an upper piedmont area with significant eolian accumulation

Qia/QToa **Intermediate alluvial-fan deposit *overlying* Quaternary to upper Tertiary very old alluvial-fan deposit (late and middle Pleistocene *overlying* early Pleistocene and Pliocene)**—Unit Qia is a generally continuous and thin (<2 m) surface veneer above very old alluvial-fan deposits. Commonly located in areas of dissected fans within a canyon embayment

Colluvial Veneers Overlying Bedrock Substrate Units

[Surficial veneer restricted to relatively thin and generally discontinuous, but areally significant, mantle of colluvium representing at least ≥40 percent coverage area above topographically irregular bedrock surface. Refer to descriptions of singular units in Singular Map Units section for each surficial-unit component. Bedrock substrate materials described individually at end of Description of Map Units]

Qha/ca **Hillslope deposits *overlying* carbonate rock (Holocene and Pleistocene *overlying* pre-Quaternary)**—Abundant unit Qha consists of colluvium, weathered debris, and local landslide deposits. Veneer thin (<2 m), discontinuous, and patchy above a topographically irregular rock surface consisting of undifferentiated assemblage of carbonate rocks

Qha/ca+sl **Hillslope deposits *overlying* carbonate and siliciclastic rocks (Holocene and Pleistocene *overlying* pre-Quaternary)**—Unit Qha consists of colluvium, weathered debris, and local landslide deposits. Veneer thin (<2 m thick), discontinuous, and patchy above a topographically irregular rock surface consisting of undifferentiated, variably intermixed assemblages of clastic carbonate and siliceous rocks

Qha/fp **Hillslope deposits *overlying* felsic plutonic rocks (Holocene and Pleistocene *overlying* pre-Quaternary)**—Unit Qha consists of colluvium, weathered debris, and local landslide deposits. Veneer thin (<2 m thick), discontinuous, and patchy above a topographically irregular rock surface. Substrate consists of undifferentiated felsic plutonic rocks

Qha/fv **Hillslope deposits *overlying* felsic volcanic rocks (Holocene and Pleistocene *overlying* pre-Quaternary)**—Unit Qha consists of colluvium, weathered debris, and local landslide deposits. Veneer thin (<2 m thick), discontinuous, and patchy above a topographically irregular rock surface. Substrate consists of undifferentiated felsic volcanic rocks

Qha/mp **Hillslope deposits *overlying* mafic plutonic rocks (Holocene and Pleistocene *overlying* pre-Quaternary)**—Unit Qha consists of colluvium, weathered debris, and local landslide deposits. Veneer thin (<2 m thick), discontinuous, and patchy above topographically irregular rock surface. Substrate consists of undifferentiated mafic plutonic rocks

Qha/mr **Hillslope deposits *overlying* metamorphic rocks (Holocene and Pleistocene *overlying* pre-Quaternary)**—Unit Qha consists of colluvium, weathered debris, and local landslide deposits. Veneer thin (<2 m thick), discontinuous, and patchy above a topographically irregular rock surface. Substrate consists of undifferentiated metamorphic rocks with complexly mixed lithologies

Qha/mv **Hillslope deposits *overlying* mafic volcanic rocks (Holocene and Pleistocene *overlying* pre-Quaternary)**—Unit Qha consists of colluvium, weathered debris, and local landslide deposits. Veneer thin (<2 m thick), discontinuous, and patchy above a topographically irregular rock surface of undifferentiated mafic volcanic rocks

Qha/pc **Hillslope deposits *overlying* partly consolidated deposits and rocks (Holocene and Pleistocene *overlying* pre-Quaternary, locally lower Quaternary)**—Unit Qha consists of colluvium, weathered debris, and local landslide deposits. Veneer thin (<2 m thick), discontinuous, and patchy above topographically irregular rock surface. Substrate consists of moderately to weakly consolidated sedimentary rocks that are mostly Tertiary to, locally, lower Quaternary

Qha/sl **Hillslope deposits *overlying* siliciclastic rocks (Holocene and Pleistocene *overlying* pre-Quaternary)**—Unit Qha consists of colluvium, weathered debris, and local landslide deposits. Veneer thin (<2 m thick), discontinuous, and patchy above topographically irregular rock surface of undifferentiated silicic sedimentary and metamorphic clastic rocks

Combined Map Units

Combined Surficial Units that have Approximately Similar Age Ranges

[Combined unit label represents two closely spatially intermingled singular surficial units with approximately similar age ranges. Spatially dominant unit listed first, to left of plus sign (+). Refer to descriptions of singular units in Singular Map Units section; following descriptions include additional details for each combined composite unit]

Qya+Qyad **Young alluvial-fan deposit *and* young debris-flow fan deposit (Holocene and latest Pleistocene *and* Holocene and latest Pleistocene)**—Located in areas of complexly intermingled, mixed-mode, relatively young alluvial and debris-flow fan deposits (for example, the piedmonts north and east of the Avawatz Mountains)

Qya+Qye **Young alluvial-fan deposit *and* young eolian sand deposit (Holocene and latest Pleistocene *and* Holocene and latest Pleistocene)**—Located in areas of young alluvial-fan deposits within zones of significant, and commonly localized, young influx and accumulation of eolian deposits (for example, the southeastern Tecopa basin)

Qia+Qip **Intermediate alluvial-fan deposit *and* intermediate playa deposit (late and middle Pleistocene *and* late and middle Pleistocene)**—Located where intermediate alluvial-fan deposits adjoin dissected intermediate playa deposits (for example, southern Crystal Hills)

Qia+Qig **Intermediate alluvial-fan deposit *and* intermediate groundwater-discharge deposit (late and middle Pleistocene *and* late and middle Pleistocene)**—Located where intermediate alluvial-fan deposition adjoins and (or) overlaps inactive zones of intermediate former groundwater discharge in axial parts of dissected basins (for example, lower California Valley)

Qiae+Qig **Intermediate mixed alluvial-fan and eolian deposit *and* intermediate groundwater-discharge deposit (late and middle Pleistocene *and* late and middle Pleistocene)**—Located where intermediate alluvial-fan deposition adjoins and (or) overlaps inactive zones of intermediate former groundwater discharge in parts of dissected basins with localized eolian influx

Qig+Qia **Intermediate groundwater-discharge deposit *and* intermediate alluvial-fan deposit (late and middle Pleistocene *and* late and middle Pleistocene)**—Located where inactive zones of intermediate former groundwater-discharge deposits locally adjoin and (or) are overlapped by intermediate alluvial fan deposition in dissected basins (for example, lower California Valley)

Combined Surficial Units that have Approximately Sequential Age Ranges With No Discernible Age Gaps

[Combined unit label represents two tightly intermingled singular surficial units that have approximately sequential age ranges with no discernible age gaps between component units. Spatially dominant unit listed first, to left of plus sign (+); ages of singular-unit components listed in same order of relative spatial dominance. Refer to descriptions of singular units in Singular Map Units section; following descriptions include additional details for each combined composite unit]

Qaw+Qya **Active wash deposit *and* young alluvial-fan deposit (latest Holocene *and* Holocene and latest Pleistocene)**—Located in narrow alluvial basins, commonly in or near highland areas, where active wash deposits traverse the distal margins of young alluvial-fan deposits

Qaw+Qyad **Active wash deposit *and* young debris-flow fan deposit (latest Holocene *and* Holocene and latest Pleistocene)**—Located where deposits along active washes adjoin and intermix with young debris-flow fan deposits (for example, eastern and northern piedmonts of Avawatz Mountains)

Qyw+Qaw **Young wash deposit *and* active wash deposit (Holocene *and* latest Holocene)**—Located where deposits along active washes adjoin and intermix with larger young wash deposits, commonly associated with low terraces and bars, commonly located within broad but areally restricted valleys

Qyw+Qiw **Young wash deposit *and* intermediate wash deposit (Holocene *and* late and middle Pleistocene)**—Located in canyons and narrow areally restricted valleys, commonly in highlands, floored with deposits along large young washes adjacent to intermediate wash deposits associated with terraces along incised drainages

Qyw+Qia **Young wash deposit *and* intermediate alluvial-fan deposit (Holocene *and* late and middle Pleistocene)**—Located in canyons and narrow areally restricted valleys, commonly in highlands or in dissected basins, floored with deposits along large young washes adjacent to intermediate alluvial-fan deposits

Qiw+Qyw **Intermediate wash deposit *and* young wash deposit (late and middle Pleistocene *and* Holocene)**—Located in canyons and narrow restricted valleys, commonly in highlands, flanked by extensive tracts of intermediate wash deposits associates with terraces along incised drainages adjacent to young wash deposits within relatively narrow but distinct valley floors

Qiw+Qyag **Intermediate wash deposit *and* young alluvial-fan deposit composed of grus (late and middle Pleistocene *and* Holocene and latest Pleistocene)**—Located where extensive tracts of intermediate wash deposits associated with terraces adjacent to large, incised drainages that adjoin the distal area of young alluvial-fan deposits with clastic component dominated by grus

Qaa+Qya **Active alluvial-fan deposit *and* young alluvial-fan deposit (latest Holocene *and* Holocene and latest Pleistocene)**—Located in areas with tightly, spatially intermingled deposition of active and young alluvial-fan sediments

Qaa+Qyad **Active alluvial-fan deposit *and* young debris-flow fan deposit (latest Holocene *and* Holocene and latest Pleistocene)**—Located where active alluvial-fan deposits adjoin and spatially intermix with young debris-flow fan deposits, near major distributed drainages on undissected to slightly dissected portions of piedmonts with mixed-mode fan deposition (for example, eastern Avawatz Mountains piedmont)

Qya+Qia **Young alluvial-fan deposit *and* intermediate alluvial-fan deposit (Holocene and latest Pleistocene *and* late and middle Pleistocene)**—Located in areas with tightly intermingled sedimentation of young and intermediate alluvial-fan deposits, generally concentrated in broad upland valleys and proximal to medial positions on highly to slightly dissected piedmonts

Qya+Qiad **Young alluvial-fan deposit *and* intermediate debris-flow deposit (Holocene and latest Pleistocene *and* late and middle Pleistocene)**—Located where young alluvial-fan deposits adjoin and tightly intermingle with intermediate debris-flow fan deposits; concentrated at proximal to medial positions on slightly to moderately dissected piedmonts with mixed-mode fan deposition (for example, Avawatz Mountains and southeastern Owlshead Mountains piedmonts)

Qya+Qap **Young alluvial-fan deposit *and* active playa deposit (Holocene and latest Pleistocene *and* latest Holocene)**—Located in small intramontane basins, commonly fault controlled, dominated by young alluvial-fan deposition enclosing areas of accumulation of young playa deposits within very small, but discrete, active lowland playas (for example, central Quail Mountains)

Qya+Qilg **Young alluvial-fan deposit *and* intermediate lacustrine-gravel deposit (Holocene and latest Pleistocene *and* late and middle Pleistocene)**—Located in areas where young alluvial-fan deposits are spatially interspersed with local inactive zones of former intermediate lacustrine deposits on the distal piedmonts of closed basins (for example, south-central part of southern Death Valley, north of the Noble hills)

Qya+Qig **Young alluvial-fan deposit *and* intermediate groundwater-discharge deposit (Holocene and latest Pleistocene *and* late and middle Pleistocene)**—Located where young alluvial-fan deposits adjoin and (or) overlap intermediate deposits from inactive zones of former groundwater discharge in axial parts of dissected basins (for example, lower California Valley and along Salt Creek west of the Salt Spring Hills)

Qyag+Qilg **Young alluvial-fan deposit composed of grus *and* intermediate lacustrine-gravel deposit (Holocene and latest Pleistocene *and* late and middle Pleistocene)**—Located in areas where young grus-dominated alluvial-fan deposits are interspersed with local intermediate lacustrine deposits on the distal piedmonts of closed basins (for example, south-central part of southern Death Valley, north of Noble hills)

Qia+Qyw **Intermediate alluvial-fan deposit *and* young wash deposit (late and middle Pleistocene *and* Holocene)**—Located in wide canyons and broad valleys, commonly in highlands or in dissected basins, containing intermediate alluvial-fan deposits adjacent to large drainages with young fluvial wash deposits

Qia+Qya **Intermediate alluvial-fan deposit *and* young alluvial-fan deposit (late and middle Pleistocene *and* Holocene and latest Pleistocene)**—Located in area with tightly intermingled deposition of intermediate and young alluvial-fan deposits; concentrated in broad canyon floors and on moderately to slightly dissected piedmonts

Qia+Qoa **Intermediate alluvial-fan deposit *and* old alluvial-fan deposit (late and middle Pleistocene *and* middle and early Pleistocene)**—Located in areas with tightly intermingled deposition of intermediate and old alluvial-fan deposits; concentrated in canyon mouths and within embayments of pedimented range fronts

Qia+Qye **Intermediate alluvial-fan deposit *and* young eolian-sand deposit (late and middle Pleistocene *and* Holocene and latest Pleistocene)**—Located in areas of intermediate alluvial-fan deposition within zones of significant, and commonly localized, influx and accumulation of young eolian deposits in moderately to highly dissected basin margins, (for example, the southeastern Tecopa basin)

Qiag+Qyaog **Intermediate alluvial-fan deposit composed of grus *and* older young alluvial-fan deposit composed of grus (late and middle Pleistocene *and* early Holocene and latest Pleistocene)**—Located in areas with tightly intermingled deposition of intermediate and older young subunits of alluvial-fan deposits on piedmonts dominated by grus fan deposition (for example, eastern piedmont of Owlshead Mountains)

Qoa+Qia **Old alluvial-fan deposit *and* intermediate alluvial-fan deposit (middle and early Pleistocene *and* late and middle Pleistocene)**—Located in area with tightly intermingled deposition of old and intermediate alluvial-fan deposits. Concentrated in fault-uplifted older fan deposits or within embayments and the most proximal piedmonts of pedimented range fronts

Qoa+QToa **Old alluvial-fan deposit *and* Quaternary to upper Tertiary very old alluvial-fan deposit (middle and early Pleistocene *and* early Pleistocene and Pliocene)**—Located in areas with tightly intermingled deposition of old and very old alluvial-fan deposits commonly within faulted and uplifted fan remnants on tectonically active range fronts (for example, along front of northeastern Avawatz Mountains)

Qyad+Qiad **Young debris-flow fan deposit *and* intermediate debris-flow fan deposit (Holocene and latest Pleistocene *and* late and middle Pleistocene)**—Located in areas with tightly intermingled deposition of young and intermediate debris-fan deposits on piedmonts with significant accumulation of variously aged debris flows (for example, the northern and eastern piedmonts of the Avawatz Mountains)

Qiad+Qyad **Intermediate debris-flow fan deposit *and* young debris-flow fan deposit (late and middle Pleistocene *and* Holocene and latest Pleistocene)**—Located in areas with tightly intermingled deposition of intermediate and young debris-fan deposits on piedmonts with significant accumulation of variously aged debris flows (for example, the northern and eastern piedmonts of the Avawatz Mountains)

Qaae+Qyae **Active mixed alluvial-fan and eolian deposit *and* young mixed alluvial-fan and eolian deposit (latest Holocene *and* Holocene and latest Pleistocene)**—Located in areas with tightly intermingled deposition of active and young alluvial-fan deposits intermixed with eolian deposits on active to young piedmonts with significant influx and admixture of young eolian materials into surface units

Qyae+Qiae **Young mixed alluvial-fan and eolian deposit *and* intermediate mixed alluvial-fan and eolian deposit (Holocene and latest Pleistocene *and* late and middle Pleistocene)**—Located in areas with tightly intermingled deposition of young and intermediate alluvial-fan deposits intermixed with eolian deposits on piedmonts with significant influx and admixture of eolian materials into surface units

Qyae+Qig **Young mixed alluvial-fan and eolian deposit *and* intermediate groundwater-discharge deposit (Holocene and latest Pleistocene *and* late and middle Pleistocene)**—Located where young alluvial-fan deposits intermixed with young eolian deposits adjoin and (or) overlap intermediate deposits from inactive zones of former groundwater discharge along basin axes with significant influx and admixture of young eolian materials into surface units (for example, lower California Valley and central Chicago Valley)

Qiae+Qyae **Intermediate mixed alluvial-fan and eolian deposit *and* young mixed alluvial-fan and eolian deposit (late and middle Pleistocene *and* Holocene and latest Pleistocene)**—Located in areas with tightly intermingled sedimentation of intermediate and young alluvial-fan deposits intermingled with young eolian deposits on piedmonts with significant influx and admixture of young eolian materials into surface units (for example, eastern Silurian Valley)

Qig+Qya **Intermediate groundwater-discharge deposit *and* young alluvial-fan deposit (late and middle Pleistocene *and* Holocene and latest Pleistocene)**—Located where intermediate deposits from inactive zones of former groundwater discharge are adjoined by and (or) overlapped by young alluvial-fan deposits in axial parts of dissected basins (for example, lower California Valley and along Salt Creek east of Salt Spring Hills)

Qig+Qyae **Intermediate groundwater-discharge deposit *and* young mixed alluvial-fan and eolian deposit (late and middle Pleistocene *and* Holocene and latest Pleistocene)**—Located where intermediate deposits from inactive zones of former groundwater discharge are adjoined by and (or) overlapped by sedimentation of young alluvial-fan deposits intermixed with young eolian deposits in basins with significant influx and admixture of eolian materials into surface units (for example, central Chicago Valley and southwestern piedmont of Saddle Peak Hills)

Combined Surficial Units that have Different Age Ranges With Discernible Age Gaps

[Combined unit label represents two tightly intermingled singular surficial units that have different age ranges with discernible age gaps in component units. Spatially dominant unit listed first, to left of plus sign (+). Refer to descriptions of individual units in Singular Map Units section; following descriptions include additional details for each combined composite unit]

Qaw+Qiw **Active wash deposit *and* intermediate wash deposit (latest Holocene *and* late and middle Pleistocene)**—Located in canyon lowlands of large washes floored with active wash deposits in channels and associated low terraces adjacent to flanking intermediate wash deposits on higher-level terrace deposits

Qaw+Qig **Active wash deposit *and* intermediate groundwater-discharge deposit (latest Holocene *and* late and middle Pleistocene)**—Located where active wash deposits are developed adjacent to intermediate deposits from inactive zones of former groundwater discharge (for example, along north margin of Amargosa River in southern Death Valley adjacent to lower valley between Ibex and Saddle Peak Hills)

Qiw+QToa **Intermediate wash deposit *and* Quaternary to upper Tertiary very old alluvial-fan deposit (late and middle Pleistocene *and* early Pleistocene and Pliocene)**—Located in areas of localized uplift along major drainages where intermediate wash deposits associated with terraces are eroded into and deposited against very old dissected alluvial-fan deposits (for example, south-central part of southern Death Valley to north of Noble hills)

Qiw+QTolg **Intermediate wash deposit *and* Quaternary to upper Tertiary very old mixed lacustrine and groundwater-discharge deposit (late and middle Pleistocene *and* Pleistocene and Pliocene)**—Located in areas where intermediate wash deposits associated with terraces of major drainages are eroded into and deposited against old and very old mixed lacustrine and groundwater-discharge deposits along axial portions of dissected basins (for example, central Tecopa basin and southern Chicago Valley)

Qaa+QTolg **Active alluvial-fan deposit *and* Quaternary to upper Tertiary very old mixed lacustrine and groundwater-discharge deposit (latest Holocene *and* Pleistocene and Pliocene)**—Located in areas of active alluvial-fan deposits on tributaries adjacent to the valley floors of major axial drainages within a dissected basin with exposures of old and very old mixed lacustrine and groundwater-discharge deposits (for example, central and lower Tecopa basin)

Qya+Qoa **Young alluvial-fan deposit *and* old alluvial-fan deposit (Holocene and latest Pleistocene *and* middle and early Pleistocene)**—Located in areas with tight intermingling of young and old alluvial-fan deposits, mainly occurring within canyon mouths and embayments of pedimented range fronts (for example, the eastern Resting Spring Range and Sperry Hills

Qya+QToa **Young alluvial-fan deposit *and* Quaternary to upper Tertiary very old alluvial-fan deposit (Holocene and latest Pleistocene *and* early Pleistocene and Pliocene)**—Located in areas with tight intermingling of deposition of young and very old alluvial-fan deposits, particularly along the dissected margins of topographic escarpments where very old alluvial-fan deposits are deformed and uplifted within young zones of deposition along tectonically active fault zones (for example, southwestern Avawatz Mountains)

Qya+QToal **Young alluvial-fan deposit *and* Quaternary to upper Tertiary very old mixed alluvial and lacustrine deposit (Holocene and latest Pleistocene *and* middle and early Pleistocene and Pliocene)**—Located in area with tightly intermingled sedimentation of young alluvial-fan deposit and old and very old mixed alluvial and lacustrine deposits, particularly along the dissected margins of topographic escarpments where old and very old basin sediments are deformed and uplifted near active zones of deposition along tectonically active fault zones (for example, north of the Noble hills and eastern Confidence Hills)

Qya+QTolg **Young alluvial-fan deposit *and* Quaternary to upper Tertiary very old mixed lacustrine and groundwater-discharge deposit (Holocene and latest Pleistocene *and* Pleistocene and Pliocene)**—Located in areas of young alluvial-fan deposits along and within valleys of incised tributaries of major axial drainages within dissected basins with exposures of old and very old inactive mixed lacustrine and groundwater-discharge deposits (for example, lower Tecopa basin and southern Chicago Valley)

Qia+Qaw **Intermediate alluvial-fan deposit *and* active wash deposit (late and middle Pleistocene *and* latest Holocene)**—Located in wide canyons and broad valleys, commonly in highlands or in dissected basins, containing flanking intermediate alluvial-fan deposits adjacent to active wash deposits in large drainages

Qia+QToa **Intermediate alluvial-fan deposit *and* Quaternary to upper Tertiary very old alluvial-fan deposit (late and middle Pleistocene *and* early Pleistocene and Pliocene)**—Located in area with close spatially intermingled sedimentation of intermediate and very old alluvial-fan deposits on the margins of highly dissected basins (for example, the northern and southern Tecopa basin) or on tectonically active uplifted highlands or range fronts (for example, the eastern Owlshead Mountains, Confidence Hills, and Celestite hills)

Qia+QTolg **Intermediate alluvial-fan deposit *and* Quaternary to upper Tertiary very old mixed lacustrine and groundwater-discharge deposit (late and middle Pleistocene *and* Pleistocene and Pliocene)**—Located in areas of intermediate alluvial-fan deposits along valleys of incised tributaries of major axial drainages within a dissected basin with exposures of inactive old and very old mixed lacustrine and groundwater-discharge deposits (for example, Tecopa basin and southern Chicago Valley)

QToa+Qia **Quaternary to upper Tertiary Very old alluvial-fan deposit *and* intermediate alluvial-fan deposit (early Pleistocene and Pliocene *and* late and middle Pleistocene)**—Located in areas with closely intermingled sedimentation of very old and intermediate alluvial-fan deposits on the margins of highly dissected basins (for example, southeastern Chicago Valley)

Qyae+Qoae **Young mixed alluvial-fan and eolian deposit *and* old mixed alluvial-fan and eolian deposit (Holocene and latest Pleistocene *and* middle and early Pleistocene)**—Located in areas with closely intermingled deposition of young and old alluvial-fan deposits intermixed with eolian deposits on piedmonts with significant influx and admixture of eolian materials into surface units (for example, southeastern California Valley)

Qyae+QTolg **Young mixed alluvial-fan and eolian deposit *and* Quaternary to upper Tertiary very old mixed lacustrine and groundwater-discharge deposit (Holocene and latest Pleistocene *and* Pleistocene and Pliocene)**—Located in areas of young fan deposits intermixed with eolian deposits with significant influx and admixture of eolian materials into surface units, commonly along incised drainages within parts of dissected basins with exposures of inactive zones of old and very old mixed lacustrine and groundwater-discharge deposits (for example, southern Tecopa basin)

Qiae+QToae **Intermediate mixed alluvial-fan and eolian deposit *and* Quaternary to upper Tertiary very old mixed alluvial-fan and eolian deposit (late and middle Pleistocene *and* early Pleistocene and Pliocene)**—Located in areas with tightly intermingled zones of intermediate and very old alluvial-fan deposits intermixed with eolian deposits on the margins of highly dissected basins with significant influx of eolian materials into surface units (for example, the southeastern Tecopa basin)

Qilg+QToal **Intermediate lacustrine gravel deposit *and* Quaternary to upper Tertiary very old mixed alluvial and lacustrine deposit (late and middle Pleistocene *and* middle and early Pleistocene and Pliocene)**—Located in areas where inactive zones of intermediate lacustrine deposits are interspersed with old and very old mixed alluvial and lacustrine deposits in basins that are deformed and uplifted along active fault zones (for example, north of Noble hills)

Qig+QToa **Intermediate groundwater-discharge deposit *and* Quaternary to upper Tertiary very old alluvial-fan deposit (late and middle Pleistocene *and* early Pleistocene and Pliocene)**—Located where inactive zones of intermediate former groundwater discharge occur within areas of very old alluvial fan deposits along the margins of dissected basins (for example, southeastern Chicago Valley)

QTolg+Qya **Quaternary to upper Tertiary very old mixed lacustrine and groundwater-discharge deposit *and* young alluvial-fan deposit (Pleistocene and Pliocene *and* Holocene and latest Pleistocene)**—Located in areas of young fan deposits along and within valleys of incised tributaries of major axial drainages in dissected basin with exposures of inactive very old mixed lacustrine and groundwater-discharge deposits (for example, lower Tecopa basin and southern Chicago Valley)

QTolg+Qye **Quaternary to upper Tertiary very old mixed lacustrine and groundwater-discharge deposit *and* young eolian sand deposit (Pleistocene and Pliocene *and* Holocene and latest Pleistocene)**—Located in the margins of moderately to highly dissected basins in areas of young alluvial-fan deposits and inactive zones of significant old and very old lacustrine and groundwater-discharge deposits that are intermixed with young eolian deposits in areas associated with commonly localized influx and accumulation of eolian materials (for example, southeastern Tecopa basin)

Combined Surficial Deposits With Exposed Bedrock Substrates

[Combined unit label represents surficial deposits tightly intermingled with mostly pre-Quaternary exposed bedrock substrate. Spatially dominant unit listed first, to left of plus sign (+). Refer to descriptions of singular units in the Singular Map Units section for surficial-unit component; descriptions of generalized bedrock substrate materials described at end of Description of Map Units. Following descriptions include additional details for each combined composite unit]

Qyw+fp **Young wash deposit *and* felsic plutonic rocks (Holocene and latest Pleistocene *and* pre-Quaternary)**—Located in broad canyons with young wash deposits developed in highland areas with discontinuous exposures of felsic plutonic bedrock (for example, southern Granite Mountains)

Qiw+pc **Intermediate wash deposit *and* partly consolidated deposits (late and middle Pleistocene *and* pre-Quaternary, locally lower Quaternary)**—Located where intermediate terrace deposits overlie discontinuously exposed bedrock consisting mainly of weakly to moderately consolidated Tertiary sedimentary rocks in canyons or adjacent to major drainages

Qya+fp **Young alluvial-fan deposit *and* felsic plutonic rocks (Holocene and latest Pleistocene *and* pre-Quaternary)**—Located in proximal-piedmont areas near eroded uplands and range fronts where young fan deposits are spatially interspersed with discontinuous exposures of felsic plutonic bedrock (for example, southern Dumont Hills, eastern Noble hills, and southern Quail Mountains)

Qya+fv **Young alluvial-fan deposit *and* felsic volcanic rocks (Holocene and latest Pleistocene *and* pre-Quaternary)**—Located in proximal-piedmont areas near eroded uplands and range fronts where young fan deposits are interspersed with discontinuous exposures of felsic volcanic bedrock (for example, southern Sperry Hills and southwestern Avawatz Mountains)

Qya+mv **Young alluvial-fan deposit *and* mafic volcanic rocks (Holocene and latest Pleistocene *and* pre-Quaternary)**—Located in proximal-piedmont areas near eroded uplands and range fronts where young fan deposits are interspersed with discontinuous exposures of mafic volcanic bedrock (for example, southwestern Owlshead Mountains)

Qya+pc **Young alluvial-fan deposit *and* partly consolidated deposits and rocks (Holocene and latest Pleistocene *and* pre-Quaternary, locally lower Quaternary)**—Located in proximal-piedmont areas near eroded uplands and range fronts where young fan deposits are interspersed with discontinuous exposures consisting mainly of weakly to moderately consolidated Tertiary sedimentary rocks (for example southern Dumont Hills, eastern Noble hills, and southern Quail Mountains)

Qya+sl **Young alluvial-fan deposit *and* siliciclastic rocks (Holocene and latest Pleistocene *and* pre-Quaternary)**—Located in proximal-piedmont areas near eroded uplands and range fronts where young fan deposits are spatially interspersed with discontinuous exposures of siliciclastic bedrock (for example western Saddle Peak Hills)

Qyag+fp **Young alluvial-fan deposit composed of grus *and* felsic plutonic rocks (Holocene and latest Pleistocene *and* pre-Quaternary)**—Located in proximal-piedmont areas near eroded uplands and range fronts where young fan deposits composed of grus are spatially interspersed with discontinuous exposures of felsic plutonic bedrock (for example, eastern Owlshead and southern Quail Mountains)

Qia+fp **Intermediate alluvial-fan deposit *and* felsic plutonic rocks (late and middle Pleistocene *and* pre-Quaternary)**—Located in proximal-piedmont areas near eroded uplands, dissected range fronts, and (or) interior mountain valleys where intermediate fan deposits are interspersed with discontinuous exposures of felsic plutonic bedrock (for example, southwestern Sperry Hills, northwestern Owlshead Mountains, and southern Granite Mountains)

Qia+fv **Intermediate alluvial-fan deposit *and* felsic volcanic rocks (late and middle Pleistocene *and* pre-Quaternary)**—Located in proximal-piedmont areas near eroded uplands, dissected range fronts, and (or) interior mountain valleys where intermediate fan deposits are interspersed with discontinuous exposures of felsic volcanic bedrock (for example, southwestern Sperry Hills, southwestern Avawatz Mountains, and southeastern Granite and Quail Mountains)

Qia+mp **Intermediate alluvial-fan deposit *and* mafic plutonic rocks (late and middle Pleistocene *and* pre-Quaternary)**—Located in proximal-piedmont areas near eroded upland, dissected range fronts, and (or) interior mountain valleys where intermediate fan deposits are interspersed with discontinuous exposures of mafic plutonic bedrock (for example, northeastern Granite Mountains)

Qia+mr **Intermediate alluvial-fan deposit *and* metamorphic rocks (late and middle Pleistocene *and* pre-Quaternary)**—Located in proximal-piedmont areas near eroded uplands and (or) interior mountain valleys where intermediate fan deposits are interspersed with discontinuous exposures of metamorphic bedrock (for example, northeastern Avawatz Mountains, southern Quail Mountains, and western Black Mountains)

Qia+mv **Intermediate alluvial-fan deposit *and* mafic volcanic rocks (late and middle Pleistocene *and* pre-Quaternary)**—Located in proximal-piedmont areas near eroded uplands, dissected range fronts, and (or) interior mountain valleys where intermediate fan deposits are interspersed with discontinuous exposures of mafic volcanic bedrock (for example, western Granite Mountains, Quail Mountains, and southeastern Panamint Range)

Qia+pc **Intermediate alluvial-fan deposit *and* partly consolidated deposits and rocks (late and middle Pleistocene *and* pre-Quaternary, locally lower Quaternary)**—Located in proximal-piedmont areas near eroded uplands, dissected range fronts, and (or) interior mountain valleys where intermediate fan deposits are interspersed with discontinuous exposures of bedrock consisting mainly of weakly to moderately consolidated Tertiary sedimentary rocks (for example, southern and northern Sperry Hills, northeastern and western Avawatz Mountains, Noble hills, and southern Quail Mountains)

Qia+sl **Intermediate alluvial-fan deposit *and* siliciclastic rocks (late and middle Pleistocene *and* pre-Quaternary)**—Located in proximal-piedmont areas near eroded uplands, dissected range fronts, and (or) interior mountain valleys where intermediate fan deposits are spatially interspersed with discontinuous exposures of siliciclastic bedrock (for example, southwestern Sperry Hills and southern Black Mountains)

Qiag+fp **Intermediate alluvial-fan deposit composed of grus *and* felsic plutonic rocks (late and middle Pleistocene *and* pre-Quaternary)**—Located in proximal-piedmont areas near eroded uplands, dissected range fronts, and (or) interior mountain valleys where intermediate fan deposits composed of grus are interspersed with discontinuous exposures of felsic plutonic bedrock (for example, eastern Owlshead Mountains and western Granite Mountains)

Qoa+mr **Old alluvial-fan deposit *and* metamorphic rocks (middle and early Pleistocene *and* pre-Quaternary)**—Located in proximal-piedmont areas near eroded uplands, dissected range fronts, and (or) interior mountain valleys where old fan deposits are interspersed with discontinuous exposures of metamorphic bedrock (for example, valley embayments of central Black Mountains)

Qoa+pc **Old alluvial-fan deposit *and* partly consolidated deposits (middle and early Pleistocene *and* pre-Quaternary, locally lower Quaternary)**—Located in proximal-piedmont areas near eroded uplands and dissected range fronts where old fan deposits are interspersed with discontinuous exposures of bedrock consisting mainly of weakly to moderately consolidated Tertiary sedimentary rocks (for example, southern range front of Dumont Hills)

Qig+pc **Intermediate groundwater-discharge deposit *and* partly consolidated deposits and rocks (late and middle Pleistocene *and* pre-Quaternary, locally lower Quaternary)**—Located in interior mountain valleys where intermediate groundwater-discharge deposits are interspersed with discontinuous exposures of bedrock consisting mainly of weakly to moderately consolidated Tertiary sedimentary rocks (for example, paleogroundwater-discharge deposits near Denning Spring in the west-central Avawatz Mountains)

pc+Qya **Partly consolidated deposits and rocks *and* young alluvial-fan deposit (Pre-Quaternary, locally lower Quaternary *and* Holocene and latest Pleistocene)**—Located in proximal-piedmont areas near eroded uplands and range fronts where discontinuous exposures of bedrock consisting mainly of weakly to moderately consolidated Tertiary sedimentary rocks are interspersed with young fan deposits (for example southern Dumont Hills)

VOLCANIC ROCKS

[Volcanic rocks consisting of lava flows, cinder cones, and ash deposits emplaced during the Quaternary are identified because they commonly overlie, are interstratified with, or are buried by adjoining surficial deposits and affect geomorphic processes and landscape development]

Qmv **Mafic volcanic rock (Quaternary)**—Lava flows, cinder cones, and thin ash deposits of basaltic and andesitic composition. Occurs in the northwestern part of the map where it underlies Shore Line Butte, Cinder Hill, and all or basal sections of several adjacent low hills in the eastern part of Death Valley below the Black Mountains (Wright and Troxel, 1984; Troxel and Butler, 1986b). Consists primarily of (1) basaltic lava flows at Shore Line Butte and low hills to the east and northeast (K-Ar age of 1.5 Ma from R.E. Drake *in* Wright and Troxel, 1984); (2) andesitic cinder cone of Cinder Hill dated originally by K-Ar as 0.69 Ma (R. Drake *in* Wright and Troxel, 1984) but redated by Ar-Ar as 0.38 Ma (T. Pavlis, University of Texas at El Paso, unpublished data, 2005); and (3) thin beds of basaltic to andesitic scoriaceous tephra layers interbedded with gravel deposits of unit Qoa in eastern Death Valley interpreted as derived from Cinder Hill (Wright and Troxel, 1984; Troxel and Butler, 1986b)

PEDIMENT SURFACES (EROSIONAL)

[Pediment surfaces are gently sloping erosional surfaces in various stages of burial or erosional dissection. Commonly developed on proximal piedmonts adjoining the flanks of bedrock mountain fronts or escarpments that have experienced significant erosional modification and (or) lateral mountainward retreat. Pediment surfaces form on many substrates, indicated by unit to right of hyphen (-), including units ca+sl, fp, fv, mv, and sl. Variable geomorphic and stratigraphic characteristics, including (1) veneered pediment (Qpv) associated with thin (typically ≤2 m thick) mantles of surficial deposits with variable, but typically young to intermediate Quaternary ages and (2) incised pediment (Qpi) with general absence of any associated surficial-deposit mantles and persistent incision into underlying substrate that may range from 2 to >5 m in depth. Individual pediment surfaces erosionally develop within long protracted variable intervals of time that are commonly difficult to precisely constrain other than they must postdate the age of the subjacent substrate that they form across and precede and (or) coincide with the ages of any overlying post-formational surficial-deposit units. Subdivided by surficial characteristics and substrate type]

SINGULAR MAP UNITS

Qpv **Veneered pediment (age unknown)**—Erosional surface consisting of a fairly smooth, mostly undissected or weakly dissected surficial sediment veneer that overlies an underlying, mostly buried, gently sloping substrate pediment surface. Exposed surficial veneer is generally thin (≤2 m thick) and composed of alluvial or wash deposits of varying age, lithology, surface morphology, and degree of soil development. Planated pediments are mostly covered but may be identified and mapped by local exposures of substrate in small trimmed outcrops, knobs, road cuts, and washes. Located on the minimally dissected range fronts or internal valleys of pedimented mountain ranges. Differentiated by type of substrate in pediment

Qpi **Incised pediment (age unknown)**—Erosional surface consisting of incised pediment surfaces expressed by accordant interfluves of exposed planated substrate, with only localized and patchily preserved veneers of surficial deposits with variable ages, lithologies, surface morphologies, and degrees of soil development. Significant incision through any localized remnant surficial veneer into planated substrate pediments by channels commonly associated with transport of locally eroded detritus. Located on dissected flanks of pedimented range fronts. Differentiated by type of substrate in pediment.

COMPOSITE MAP UNITS

Qpi-ca+sl **Incised pediment *developed on* carbonate and siliciclastic rocks (age unknown developed on pre-Quaternary)**—Most of the surface expressed by accordant interfluves of exposed substrate, with only a localized and patchily preserved surficial-deposit veneer. Significant incision into substrate by channels commonly associated with transport of locally eroded detritus. Located on dissected flanks of pedimented range fronts underlain by carbonate and siliciclastic rocks (for example, northern Silurian Hills)

Qpi-fp **Incised pediment *developed on* felsic plutonic rocks (age unknown *developed on* pre-Quaternary)**—Most of the surface expressed by accordant interfluves of exposed substrate, with only a localized and patchily preserved surficial-deposit veneer. Significant incision into substrate by channels commonly associated with transport of locally eroded grus-dominated detritus. Located on dissected flanks of pedimented range fronts underlain by felsic plutonic rocks (for example, northwestern, central, and eastern Owlshead Mountains and northern Granite Mountains)

Qpi-fv **Incised pediment *developed on* felsic volcanic rocks (age unknown *developed on* pre-Quaternary)**—Most of the surface expressed by accordant interfluves of exposed substrate, with only a localized and patchily preserved surficial-deposit veneer. Significant incision into substrate by channels commonly associated with transport of locally eroded detritus. Located on dissected flanks of pedimented range fronts underlain by felsic volcanic rocks (for example, northern Ibex Hills and south-central Granite Mountains)

Qpi-mv **Incised pediment *developed on* mafic volcanic rocks (age unknown *developed on* pre-Quaternary)**—Incised pediment developed on a substrate of metamorphic rocks. Most of the surface expressed by accordant interfluves of exposed substrate, with only a localized and patchily preserved surficial-deposit veneer. Significant incision into substrate by channels commonly associated with transport of locally eroded detritus. Located on dissected flanks of pedimented range fronts underlain by mafic volcanic rocks (for example, southwestern Owlshead Mountains)

Qpv-fp **Veneered pediment *developed on* felsic plutonic rocks (age unknown *developed on* pre-Quaternary)**—Forms fairly smooth, mostly undissected or weakly dissected sediment veneer that is composed of alluvial or wash deposits of varying age and degree of soil development. Located on the minimally dissected range fronts or internal valleys of pedimented mountains ranges underlain by felsic plutonic rocks (for example, Valjean Hills)

Qpv-sl **Veneered pediment *developed on* siliciclastic rocks (age unknown *developed on* pre-Quaternary)**—Forms fairly smooth, mostly undissected or weakly dissected sediment veneer that is composed of alluvial or wash deposits of varying age and degree of soil development. Mapped above underlying substrate of siliciclastic pediment that may be identified by local exposures in small knobs, road cuts, and washes. Located on the minimally dissected range fronts or internal valleys of pedimented mountain ranges underlain by siliciclastic rocks (for example, southeastern Granite Mountains)

SUBSTRATE MATERIALS (PRE-QUATERNARY)

[Substrate materials are shallowly buried or exposed rock or partly consolidated materials that underlie surficial deposits and (or) pediment erosional surfaces or veneers. Units defined according to generic rock types of potential significance to the weathering and production of sediments for surficial deposits. Undifferentiated ages range from Pliocene, and locally lower Quaternary, to Proterozoic within the unmapped specific lithostratigraphic formational units included in each of these general rock types. Mapped substrate units are labeled with associated overlying hillslope deposits (for example, unit Qha-fp). Substrate units are not mapped individually and do not have individual map unit colors or labels. They are differentiated on the map as part of specific composite units that contain a given substrate component]

ca **Carbonate rocks (pre-Quaternary)**—Undifferentiated assemblage of carbonate rock. Includes variably textured clastic to crystalline mineralogic assemblages of limestone, dolomites, and marble. Commonly susceptible to dissolution weathering with a clastic weathering residual of silt

ca+sl **Carbonate and siliciclastic rocks (pre-Quaternary)**—Lithologically variable intermixed components of clastic, carbonate, and siliceous clastic rock. Includes sequences of limestones, dolomites, marbles, sandstones, siltstones, shale, conglomerates, and quartzites with a range of textures and compositions. Weathered materials include variable admixtures of quartz, feldspar pebbles, sand, silt, and clay

fp **Felsic plutonic rocks (pre-Quaternary)**—Undifferentiated assemblages of felsic plutonic rocks typically >68 percent silica. Includes intrusives and ejecta composed of granites, quartz monzonites, granodiorites, and aplites. Weathered materials variable depending on the specific intrusive bodies, ranging from fine-grained grussy sand and fine gravel composed predominantly of quartz and feldspar with some clay (for example, the northern and northeastern Owlshead Mountains and Granite Mountains) to sand, coarse-grained gravel, and clay that may provide sources for debris-flow deposits on adjacent piedmont fans (for example, southeastern Owlshead Mountains)

fv **Felsic volcanic rocks (pre-Quaternary)**—Undifferentiated felsic volcanic rocks typically >68 percent silica. Includes flows, dikes, and ejecta composed of rhyolite, rhyodacite, and felsite. Weathered materials include clastic material and feldspar, quartz, and clays

mp **Mafic plutonic rocks (pre-Quaternary)**—Undifferentiated mafic plutonic rocks typically <68 percent silica. Includes intrusives and dikes composed of monzonite, diorite, monzodiorite, gabbro, epidotized dikes, and peridotite. Weathered materials include clastic materials plus feldspar, amphiboles, and micas. May produce debris-flow deposits on adjacent fans, especially below tectonically active range fronts, such as the northeastern and eastern Avawatz Mountains

mr **Metamorphic rocks (pre-Quaternary)**—Undifferentiated metamorphic rocks of complexly mixed lithology and textures. Includes structurally and lithologically intermixed rocks composed of gneiss, schist, slate, migmatite, and structurally mixed rocks. Weathered materials variable

mv **Mafic volcanic rocks (pre-Quaternary)**—Undifferentiated mafic volcanic rocks contain <68 percent silica. Includes flows, ejecta, and dikes composed of andesite, dacite, basalt, and mafic dikes. Some metasomatic altered rock types especially susceptible to weathering. Weathered materials include common clay. Unaltered rocks may produce bouldery gravel detritus on adjacent alluvial fans

pc **Partly consolidated deposits (pre-Quaternary, locally lower Quaternary)**—Moderately to weakly consolidated sedimentary deposits with varying textures and compositions. May include volcanic or highly altered rocks. May form badlands topography where especially susceptible to erosion and dissection. Weathered materials commonly include silt and clay. Typically, Tertiary; may include older portions of unit QToa where age control is especially poor or absent

sl **Siliciclastic rock (pre-Quaternary)**—Undifferentiated silicic sedimentary and metamorphic clastic rocks. Includes shales, siltstones, sandstones, quartzites, and conglomerates of varying textures and compositions. Weathered materials include quartz, silt, and clay

References Cited

Anderson, D.E., 2005, Holocene fluvial geomorphology of the Amargosa River through Amargosa Canyon, California, *in* Calzia, J.P., ed., Fifty years of Death Valley research—A volume in honor of Lauren A. Wright and Bennie Troxel: Earth Sciences Review Special Issue, v. 73, p. 291–307, https://doi.org/10.1016/j.earscirev.2005.04.010.

Anderson, D.E., and Wells, S.G., 2003a, Late Pleistocene lake highstands in Death Valley, *in* Enzel, Y., Wells, S.G., and Lancaster, N., eds., Paleoenvironments and paleohydrology of the Mojave and southern Great Basin Deserts: Boulder, Colorado, Geological Society of America Special Paper 368, p. 115–128.

Anderson, K.C., and Wells, S.G., 2003b, Latest Quaternary paleohydrology of Silurian Lake and Salt Spring basin, Silurian Valley, California, *in* Enzel, Y., Wells, S.G., and Lancaster, N., eds., Paleoenvironments and paleohydrology of the Mojave and southern Great Basin Deserts: Boulder, Colorado, Geological Society of America Special Paper 368, p. 129–141.

Andrew, J.E., 2000, The Mesozoic and Tertiary tectonic history of the Panamint Range and Quail Mountains, California: Lawrence, Kansas, University of Kansas, Ph.D. dissertation, 64 p.

Andrew, J.E., 2007, Western Quail Mountains geologic map: Geological Society of America, Digital Map and Chart Series DMCH005, scale 1:12,000, accessed January 14, 2021 at https://doi.org/10.1130/2007.DMCH005.

Andrew, J.E., Walker, J.D., and Monestero, F.C., 2015, Evolution of the central Garlock Fault Zone—A major sinistral fault embedded in a dextral plate margin: Geological Society of America Bulletin, v. 127, no. 1–2, p. 227–249, https://doi.org/10.1130/B31027.1.

Bedford, D.R., 2003, Surficial and bedrock geologic map database of the Kelso 7.5-minute quadrangle, San Bernardino County, California: U.S. Geological Survey Open-File Report 03–501, scale 1:24,000, pamphlet 27 p., https://doi.org/10.3133/ofr03501.

Bedford, D.R., Miller, D.M., and Phelps, G.A., 2010, Surficial geologic map of the Amboy 30' x 60' quadrangle, San Bernardino County, California: U.S. Geological Survey Scientific Investigations Map 3109, scale 1:100,000, pamphlet 26 p., https://doi.org/10.3133/sim3109.

Beratan, K.K., Hsieh, J., and Murray, B., 1999, Pliocene–Pleistocene stratigraphy and depositional environments, southern Death Valley, California, *in* Wright, L.A., and Troxel, B.W., eds., Cenozoic basins of the Death Valley region: Boulder, Colorado, Geological Society of America Special Paper 333, p. 289–300, https://doi.org/10.1130/0-8137-2333-7.289.

Birkeland, P.W., 1999, Soils and geomorphology: New York, Oxford University Press, 430 p.

Blakely, R.J., Jachens, R.C., Calzia, J.P., and Langenheim, V.E., 1999, Cenozoic basins of the Death Valley extended terrane as reflected in regional-scale gravity anomalies, *in* Wright, L.A., and Troxel, B.W., eds., Cenozoic basins of the Death Valley region: Boulder, Colorado, Geological Society of America Special Paper 333, p. 1–16.

Blakely, R.J., and Ponce, D.A., 2001, Map showing depth to pre-Cenozoic basement in the Death Valley ground-water model area, Nevada and California: U.S. Geological Survey Miscellaneous Field Studies MF–2381–E, scale 1:250,000, pamphlet 7 p, https://doi.org/10.3133/mf2381E.

Brady, R.H., III, 1984, Cenozoic geology of the northeastern Avawatz Mountains in relation to the intersection of the Garlock and Death Valley Fault Zones, San Bernardino County, California: Davis, University of California, Ph.D. dissertation, 292 p.

Brady, R.H., III, 1986, Stratigraphy and tectonics of the northern Avawatz Mountains at the intersection of the Garlock and Death Valley Fault Zones, San Bernardino County, California—A field guide, *in* Troxel, B.W., ed., Guidebook, Quaternary tectonics of southern Death Valley: Friends of the Pleistocene, Pacific Cell, p. 1–12.

Bright, J., and Anderson, K.C., 2007, Re-interpretation of Pleistocene Lake Dumont, Salt Spring basin, California, based on faunal analyses, *in* Miller, D.M., and Valin, Z.C., eds., Geomorphology and tectonics at the intersection of Silurian and Death Valleys, southern California—2005 Guidebook Pacific Cell, Friends of the Pleistocene: U.S. Geological Survey Open-File Report 2007–1424, p. 51–61, https://doi.org/10.3133/ofr20071424.

Brogan, G.B., Kellogg, K.S., Slemmons, D.B., and Terhune, C.L., 1991, Late Quaternary faulting along the Death Valley-Furnace Creek Fault system, California and Nevada: U.S. Geological Survey Bulletin 1991, 23 p., 4 plates, https://doi.org/10.3133/b1991.

Bull, W.B, 1991, Geomorphic responses to climate change: New York, Oxford University Press, 326 p.

Butler, P.R., 1984, Fluvial response to on-going tectonism and base-level changes, lower Amargosa River, southern Death Valley, California: Sedimentary Geology, v. 38, p. 107–125, https://doi.org/10.1016/0037-0738(84)90076-9.

Butler, P.R., Troxel, B.W., and Verosub, K.L., 1988, Late Cenozoic history and styles of deformation along the Southern Death Valley Fault Zone, California: Geological Society of America Bulletin, v. 100, p. 402–410, https://doi.org/10.1130/0016-7606(1988)100%3C0402:LCHASO%3E2.3.CO;2.

Bryant, W.A., 2005, Digital database of Quaternary and younger faults from the Fault Activity Map of California, version 2.0: California Geological Survey Web Page, accessed January 13, 2010 at https://www.conservation.ca.gov/cgs/Pages/Publications/QuaternaryFaults_ver2.aspx.

California Geological Survey, 2000a, Official map of the Alquist-Priolo earthquake fault zones, Old Ibex Pass quadrangle (1990): California Geological Survey, CD-ROM 2000-003.

California Geological Survey, 2000b, Official map of the Alquist-Priolo earthquake fault zones, East of Owl Lake quadrangle (1990): California Geological Survey CD-ROM 2000-003.

California Geological Survey, 2000c, Official map of the Alquist-Priolo earthquake fault zones, Confidence Hills East quadrangle (1990): California Geological Survey CD-ROM 2000-005.

California Geological Survey, 2000d, Official map of the Alquist-Priolo earthquake fault zones, Confidence Hills West quadrangle (1990): California Geological Survey CD-ROM 2000-005.

California Geological Survey, 2000e, Official map of the Alquist-Priolo earthquake fault zones, Shore Line Butte quadrangle (1990): California Geological Survey CD-ROM 2000-005.

California Geological Survey, 2000f, Official map of the Alquist-Priolo earthquake fault zones, Avawatz Pass SW quadrangle (1976): California Geological Survey CD-ROM 2000-003.

California Geological Survey, 2000g, Official map of the Alquist-Priolo earthquake fault zones, Leach Lake SE quadrangle (1976): California Geological Survey CD-ROM 2000-003.

California Geological Survey, 2000h, Official map of the Alquist-Priolo earthquake fault zones, Leach Lake SW quadrangle (1976): California Geological Survey CD-ROM 2000-003.

California Geological Survey, 2000i, Official map of the Alquist-Priolo earthquake fault zones, Quail Mountains SE quadrangle (1976): California Geological Survey CD-ROM 2000-003.

California Geological Survey, 2000j, Official map of the Alquist-Priolo earthquake fault zones, Quail Mountains SW quadrangle (1976 California Geological Survey CD-ROM 2000-003.

California Geological Survey, 2000k, Official map of the Alquist-Priolo earthquake fault zones, Hidden Spring quadrangle (1976): California Geological Survey CD-ROM 2000-003.

Caskey, J.M., Goodman, J.T., Green, H.L., Niles, J.H., Wan, E., Wahl, D.B., and Olsen, Holly, 2010, Constraints on post-middle-Pleistocene offsets and new perspectives on Plio-Pleistocene tectonism along the Southern Death Valley Fault Zones [abs.]: Geological Society of America, Abstract with Programs, v. 42, no. 4, p. 55.

Clark, M.M., 1972, Map showing recently active breaks along the Garlock and associated faults, California: U.S. Geological Survey Miscellaneous Geologic Investigations Map I–741, scale 1:24,000, 5 sheets, https://doi.org/10.3133/i741.

Cohen, K.M., Finney, S.C., Gibbard, P.L., and Fan, J.-X., 2014, The ICS International Chronostratigraphic Chart, v. 2014-10: Episodes, v. 36, no. 3, p. 199–204, accessed February 25, 2015, at http://www.stratigraphy.org/ICSchart/ChronostratChart2014-10.pdf.

Davis, G.A., 2018, Revisiting the Garlock Fault—More to it than meets the eye [abs.]: Geological Society of America Abstracts with Programs, v. 50, no. 5, https://doi: 10.1130/abs/2018RM-313564.

Davis, G.A., and Burchfiel, B.C., 1973, Garlock Fault—An intracontinental transform structure, southern California: Geological Society of America Bulletin, v. 84, https://doi.org/10.1130/0016-7606(1973)84%3C1407:GFAITS%3E2.0.CO;2.

Dixon, T.H., Norabuena, E., and Hotaling, L., 2003, Paleoseismology and global positioning system—Earthquake-cycle effects and geodetic versus geologic fault slip rates in the eastern California Shear Zone: Geology, v. 31, no. 1, p. 55–58, https://doi.org/10.1130/0091-7613(2003)031%3C0055:PAGPSE%3E2.0.CO;2.

Dokka, R.K., and Travis, C.J., 1990, Late Cenozoic strike-slip faulting in the Mojave Desert, California: Tectonics, v. 9, no. 2, p. 311–340, https://doi.org/10.1029/TC009i002p00311.

Dooley, T., and McClay, K., 1996, Pleistocene strike-slip deformation in the Confidence Hills, Southern Death Valley Fault Zone, eastern California, USA: London, Journal of Geological Society, v. 153, p. 375–387, https://doi.org/10.1144/gsjgs.153.3.0375.

Dohrenwend, J., 2001, Satellite image map of Death Valley, Chapter D, *in*, Machette, M.N., Johnson, M.L., and Slate, J.L., eds., Quaternary and late Pliocene geology of the Death Valley region—Recent observations on tectonics, stratigraphy, and lake cycles (Guidebook for Pacific Cell-Friends of the Pleistocene Field-trip): U.S. Geological Survey Open-File Report 2001–51, p D117–D119, https://doi.org/10.3133/ofr0151.

Earthscope Southern & Eastern California LiDAR Project, 2009, Distributed by OpenTopography, https://doi.org/10.5069/G9G44N6Q.

Environmental Systems Research Institute [ESRI], 2009, Arc GIS ArcMAP system, ver. 9.3.1. https://esri.com.

Frankel, K.L., Brantley, K.S., Dolan, J.F., Finkel, R.C., Klinger, R.E., Knott, J.R., Machette, M.N., Owen, L.A., Phillips, F.M., Slate, J.L., and Wernicke, B.P, 2007, Cosmogenic ^{10}Be and ^{36}Cl geochronology of offset alluvial fans along the northern Death Valley Fault Zone—Implications for transient strain in the eastern California shear zone: Journal of Geophysical Research, v. 112, no. B06407, 18 p, https://doi.org/10.1029/2006JB004350.

Frankel, K.L., Owens, L.A., Dolan, J.F., Knott, J.R., Lifton, Z.M., Finkel, R.C., and Wasklewicz, T., 2015, Timing and rates of Holocene normal faulting along the Black Mountains Fault Zone, Death Valley, USA: Lithosphere, v. 8, p. 3–22, https://doi.org/10.1130/L464.1.

Fridrich, C.J., and Thompson, R.A., 2011, Cenozoic tectonic reorganizations of the Death Valley region, southeastern California and southwestern Nevada: U.S. Geological Survey Professional Paper 1783, 36 p., 1 plate, https://doi.org/10.3133/pp1783.

Ganev, P.N., Dolan, J.F., McGill, S.F., and Frankel, K.L., 2012, Constancy of geologic slip rate along the central Garlock Fault—Implications for strain rate accumulation and release in southern California: Geophysical Journal International, v. 190, p. 745–760, https://doi.org/10.1111/j.1365-246X.2012.05494.x.

Gile, L.H., Peterson, F.F., and Grossman, R.B., 1966, Morphological and genetic sequences of carbonate accumulations in desert soils: Soil Science, v. 101, no. 5, p. 347–360.

Green, H.L, 2009, Neotectonic investigation of the Southern Death Valley Fault Zone, southeastern California: California, San Francisco State University, M.S. thesis, 133 p., 1 plate, scale 1:12,000.

Green, H.L., Redwine, J.L., and Miller, D.M., 2007, Reconnaissance studies of soils-geomorphic correlations and late Quaternary deformation of alluvial fan deposits east of the Avawatz Mountains, Mojave Desert, California, *in* Miller, D.M., and Valin, Z.C., eds., Geomorphology and tectonics at the intersection of Silurian and Death Valleys, southern California—2005 Guidebook, Pacific Cell, Friends of the Pleistocene: U.S. Geological Survey Open-File Report 2007–1424, p. 113–139, https://doi.org/10.3133/ofr20071424.

Guest, B., Pavlis, T.L., Golding, H., and Sherpa, L., 2003, Chasing the Garlock—A study of tectonic response to vertical axis rotation: Geology, v. 31, no. 6, p. 553–556, https://doi.org/10.1130/0091-7613(2003)031%3C0553:CTGASO%3E2.0.CO;2.

Hatem, A.E., and Dolan, J.F., 2018, A model for the initiation, evolution, and controls on seismic behavior of the Garlock Fault, California: Geochemistry, Geophysics, Geosystems, v. 19, p. 2166–2178, https://doi.org/10.1029/2017GC007349.

Hereford, R., Webb, R.H., and Longpré, C.I., 2003, Precipitation history of the Mojave Desert region, 1893–2001: U.S. Geological Survey Fact Sheet 117–03, 4 p, https://doi.org/10.3133/fs11703.

Hereford, R., Webb, R.H., and Longpré, C.I., 2006, Precipitation history and ecosystem response to multidecadal precipitation variability in the Mojave Desert region, 1893–2001: Journal of

Arid Environments, v. 67, p. 13–34, https://doi.org/10.1016/j.jaridenv.2006.09.019.

Hillhouse, J.W., 1987, Late Tertiary and Quaternary geology of the Tecopa basin, southeastern California: U.S. Geological Survey Miscellaneous Investigations Map I–1728, scale 1:48,000, pamphlet 16 p, https://doi.org/10.3133/i1728.

Jayko, A.S., 2005, Late Quaternary denudation, Death and Panamint Valleys, eastern California: Earth Science Reviews, v. 73, p. 271–289, https://doi.org/10.1016/j.earscirev.2005.04.009.

Jayko, A.S., 2009, Surficial geologic map of the Darwin Hills 30' X 60' quadrangle, Inyo County, California: U.S. Geological Survey Scientific Investigations Map 3040, scale 1:100,000, pamphlet 19 p, https://doi.org/10.3133/sim3040.

Jayko, A.S., Forester, R.M., Kaufman, D.S., Phillips, F.M., Yount, J.C., McGeehin, J., and Mahan, S.A., 2008, Late Pleistocene lakes and wetlands, Panamint Valley, Inyo County, California, *in* Reheis, M.C., Hershler, R., and Miller, D.M., eds., Late Cenozoic drainage history of the southwestern Great Basin and lower Colorado River Region—Geologic and biotic perspectives: Geological Society of America Special Paper 439, p. 151–184.

Jennings, C.W., Burnett, J.L., and Troxel, B.W., 1962, Geologic map of California—Trona sheet: California Division of Mines and Geology, scale 1:250,000.

Klinger, R.E., 1999, Tectonic geomorphology along the Death Valley Fault system—Evidence of recurrent late Quaternary activity in Death Valley National Park, *in* Slate, J.L., ed., Proceedings of conference on status of geologic research and mapping, Death Valley National Park: U.S. Geological Survey Open-File Report 99–153, p. 132–140, https://doi.org/10.3133/ofr99153.

Knott, J.R., 1999, Quaternary stratigraphy and geomorphology of Death Valley, *in* Slate, J.L., ed., Proceedings of conference on status of geologic research and mapping, Death Valley National Park: U.S. Geological Survey Open-File Report 99–153, p. 90–96, https://doi.org/10.3133/ofr99153.

Knott, J.R., Machette, M.N., Wan, E., Klinger, R.E., Liddicoat, J.C., Sarna-Wojcicki, A.M., Fleck, R.J., Deino, A.L, Geissman, J.W., Slate, J.L., Wahl, D.B., Wernicke, B.P., Wells, S.G., Tinsley, JC., III, Hathaway, J.C, and Weamer, V.M., 2018, Late Neogene–Quaternary tephrochronology, stratigraphy, and paleoclimate of Death Valley, California, USA: Geological Society of America Bulletin, v. 130, no. 7/8, p. 1231–1255, https://doi.org/10.1130/B31690.1.

Knott, J.R, Sarna-Wojcicki, A.M., Machette, M.N., and Klinger, R.E, 2005, Upper Neogene stratigraphy and tectonics of Death Valley—A review, *in* Calzia, J.P., ed., Fifty years of Death Valley research—A volume in honor of Lauren A. Wright and Bennie Troxel: Earth Sciences Review Special Issue, v. 73, p. 245–270, https://doi.org/10.1016/j.earscirev.2005.07.004.

Luckow, H.G., Pavlis, T.L., Serpa, L.F., Guest, B., Wagner, D.L., Snee, L., Hensley, T.M., and Korjenkov, A., 2005, Late Cenozoic sedimentation and volcanism during transtensional deformation in Wingate Wash and the Owlshead Mountains, Death Valley, *in* Calzia, J.P., ed., Fifty years of Death Valley research—A volume in honor of Lauren A. Wright and Bennie Troxel: Earth Sciences Review Special Issue, v. 73, p. 177–219, https://doi.org/10.1016/j.earscirev.2005.07.013.

Machette, M.N., 1985, Calcic soils of the southwestern United States, *in* Weide, D.L., ed., Soils and Quaternary geology of the southwestern United States: Geological Society of America Special Paper 203, p. 1–21, https://doi.org/10.1130/SPE203-p1.

Machette, M.N., Klinger, R.E., Knott, J.R., Wills, C.J., Bryant, W.A., and Reheis, M.C., 2001, A proposed nomenclature for the Death Valley Fault system, *in* Machettte, M.N., Johnson, M.L., and Slate, J.L, eds., Quaternary and late Pliocene geology of the Death Valley region—Recent observations on tectonics, stratigraphy, and lake cycles, Pacific Cell, Friends of the Pleistocene field trip, February 17–19, 2001: U.S. Geological Survey Open-File Report 01–51, p. J173–J183, https://doi.org/10.3133/ofr0151.

Machette, M.N., Slate, J.L., and Phillips, F.M., 2008, Terrestrial cosmogenic-nuclide dating of alluvial fans in Death Valley, California: U.S. Geological Survey Professional Paper 1755, 44 p, https://doi.org/10.3133/pp1755.

Mahan, S.A., Miller, D.M., Menges, C.M., and Yount, J.C., 2007, Late Quaternary stratigraphy and luminescence geochronology of the northeastern Mojave Desert: Quaternary International, v. 166, p. 61–78, https://doi.org/10.1016/j.quaint.2006.12.010.

McDonald, E.V., McFadden, L.D., and Wells, S.G., 1995, The relative influences of climate change, desert dust, and lithologic control on soil-geomorphic processes on alluvial fans, Mojave Desert, California—Summary of results: San Bernardino County Museum Association Quarterly, v. 42, no. 3, p. 35–42.

McGill, S.F., 1994a, Holocene slip rate of the easternmost Garlock Fault, Avawatz Mountains, California: San Bernardino County Museum Association Quarterly, v. 41, no. 3, p. 24.

McGill, S.F., 1994b, Neotectonics of the easternmost Garlock Fault in the Avawatz Mountains, *in* Reynolds, R.E, ed., Off limits in the Mojave Desert: San Bernardino County Museum Association Special Publication 94-1, p. 96–100.

McGill, S.F., and Sieh, K.E., 1991, Surficial offsets on the eastern and central Garlock Fault associated with prehistoric earthquakes: Journal of Geophysical Research, v. 96, p. 21,597–21,621, https://doi.org/10.1029/91JB02030.

McKittrick, M.A., 1988, Surficial geologic map of the Resting Spring and Nopah Ranges, Inyo County, California, and Nye County, Nevada: U.S. Geological Survey Miscellaneous Field Studies Map MF–1941, scale 1:62,500, https://doi.org/10.3133/mf1941.

McMackin, M.R., 1997, Late Tertiary evolution of the Southern Death Valley Fault system—The origin of the Tecopa hump, a tectonic dam on the Amargosa River: San Bernardino County Museum Association Quarterly, v. 44, no. 2, p. 37–41.

McMackin, M.R., 2001, Regional deformation by strike-slip faulting—The eastern California shear zone meets the Garlock Fault Zone, *in* Dunne, G., and Cooper, J., comps., Geologic excursions in the California deserts and adjacent Transverse Ranges: Pacific Section, Society of Sedimentary Geology, Book 88, p. 1–16.

Mendonca, J., 2007, Preliminary results on neotectonic and geomorphic evolution of the northeastern Avawatz Mountains, southern Death Valley, California, *in* Miller, D.M., and Valin, Z.C., eds., Geomorphology and tectonics at the intersection of Silurian and Death Valleys, southern California, 2005 Guidebook, Pacific Cell, Friends of the Pleistocene: U.S. Geological Survey Open-File Report 2007–1424, p. 51–61, https://doi.org/10.3133/ofr20071424.

Menges, C.M., 2008, Multistage late Cenozoic evolution of the Amargosa River drainage, southwestern Nevada and eastern California, *in* Reheis, M.C., Hershler, R., and Miller, D.M., eds., Late Cenozoic drainage history of the southwestern Great Basin and lower Colorado River region—Geologic and biotic perspectives: Geological Society of America Special Paper 439, p. 39–90, https://doi.org/10.1130/2008.2439(03).

Menges, C.M., and Cossette, P.M., 2023, Digital database for surficial geologic map of the Owlshead Mountains quadrangle, Inyo and San Bernardino Counties, California: U.S. Geological Survey data release, https://doi.org/10.5066/P9LSW65B.

Menges, C.M., and Miller, D.M., 2007, Introduction, *in* Miller, D.M., and Valin, Z.C., eds., Geomorphology and tectonics at the intersection of Silurian and Death Valleys, southern California, 2005 Guidebook, Pacific Cell, Friends of the Pleistocene: U.S. Geological Survey Open-File Report 2007–1424, p. 1–6, https://doi.org/10.3133/ofr20071424.

Menges, C.M., Pavlis, T.L., McMackin, M.R., and Serpa, L., 2006, Contractional strain related to interference of intersecting sets of strike-slip faults in the southern Death Valley region, California [abs.]: EOS, Transactions of the American Geophysical Union, v. 87, no. 52, Fall Meeting Supplement, Abstract T21B-0411.

Menges, C.M., Pavlis, T.L., McMackin, M.R., Serpa, L., and Bennett, R.A., 2005, Geomorphic and structural evidence for significant neotectonic contractional strain within southern Death Valley and bordering areas, eastern California [abs.]: Geological Society of America, Abstracts with Programs, v. 37, no. 7, p. 69.

Menges, C.M., Taylor, E.M., Workman, J.B., and Jayko, A.S., 2001, Regional surficial-deposit mapping in the Death Valley area of California and Nevada in support of ground-water modeling, *in* Machettte, M.N., Johnson, M.L., and Slate, J.L, eds., Quaternary and late Pliocene geology of the Death Valley region—Recent observations on tectonics, stratigraphy, and lake cycles, Pacific Cell, Friends of the Pleistocene field trip, February 17–19, 2001: U.S. Geological Survey Open-File Report 01–51, p. H151–H166, https://doi.org/10.3133/ofr0151.

Miller, D.M, Menges, C.M., and Likke, D.J., 2014, Generalized surficial geologic map of the Fort Irwin area, San Bernardino County, California, *chap. B of* Buesch, D.C., ed., Geology and geophysics applied to groundwater hydrology at Fort Irwin California: U.S. Geological Survey Open-File Report 2013–1024, pamphlet 11 p., scale 1:100,000, https://doi.org/10.3133/ofr20131024B.

Miller, D.M., Menges, C.M., and McMackin, M.R., 2007, Geomorphology and tectonics at the intersection of Silurian and Death Valleys—Field Trip road log, *in* Miller, D.M., and Valin, Z.C., eds., Geomorphology and tectonics at the intersection of Silurian and Death Valleys, southern California, 2005 Guidebook, Pacific Cell, Friends of the Pleistocene: U.S. Geological Survey Open-File Report 2007–1424, p. 7–49, https://doi.org/10.3133/ofr20071424.

Miller, D.M., and Yount, J.L., 2002, Late Cenozoic tectonic evolution of the north-central Mojave Desert inferred from fault history and physiographic evolution of the Fort Irwin area, California, *in* Glazner, A.F., Walker, J.D., and Bartley, J.M., eds., Geologic evolution of the Mojave Desert and southwestern Basin and Range: Geological Society of America Memoir, 195, p. 173–197.

Miller, M.B., 2005, Geological landscapes of the Death Valley region, *in* Calzia, J.P., ed., Fifty years of Death Valley research—A volume in honor of Lauren A. Wright and Bennie Troxel: Earth Sciences Review Special Issue, v. 73, p. 17–30, https://doi.org/10.1016/j.earscirev.2005.07.010.

Miller, M.M., Johnson, D.J., Dixon, T.H., and Dokka, R.K., 2001, Refined kinematics of the eastern California shear zone from GPS observations, 1993–1998: Journal of Geophysical Research, v. 106, no. B2, p. 2245–2263, https://doi.org/10.1029/2000JB900328.

Monastero, M.F., Sabin, A.E., and Walker, J.D., 1997, Evidence for post-early-Miocene initiation of movement on the Garlock Fault from offset of the Cudahy Camp Formation, east-central California: Geology, v. 25, p. 247–250, https://doi.org/10.1130/0091-7613(1997)025%3C0247:EFPEMI%3E2.3.CO;2.

Morrison, R.B, 1999, Lake Tecopa—Quaternary geology of Tecopa Valley, California, a multimillion-year record and its relevance to the proposed nuclear-waste repository at Yucca Mountain, Nevada, *in* Wright, L.A., and Troxel, B.W., eds., Cenozoic basins of the Death Valley region: Boulder, Colorado, Geological Society of America Special Paper 333, p. 301–344.

Muehlberger, W.R., 1954, Geology of the Quail Mountains, San Bernardino County: California Division of Mines and Geology Bulletin 170, Map Sheet 16, scale 1:48,000.

Nelson, S.T., Karlsson, H.R., Paces, J.B., Tingey, D.G., Ward, S., and Petera, M.T., 2001, Paleohydrologic record of spring deposits in and around Pleistocene pluvial Lake Tecopa, southeastern California: Geological Society of America Bulletin 113, no. 5, p. 659–670, https://doi.org/10.1130/0016-7606(2001)113%3C0659:PROSDI%3E2.0.CO;2.

Noble, L.F., and Wright, L.A., 1954, Geology of the central and southern Death Valley region, California, *in* Jahns, R.H., ed., Geology of southern California: California Division of Mines and Geology Bulletin 170, chap. II, p. 59–74.

Noble, L.F, Wright, L.A., and Troxel, B.W., 1963, Fault pattern of the southern Death Valley region, eastern California: Geological Society of America Special Paper 73, p. 55.

Page, W.R., Lundstrom, S.C., Harris, A.G., Langenheim, V.E., Workman, J.B., Mahan, S.A., Paces, J.B., Dixon, G.L., Rowley, P.D., Burchfiel, B.C., Bell, J.W., and Smith, E.I., 2005, Geologic and geophysical maps of the Las Vegas 30’ x 60’ quadrangle, Clark and Nye Counties, Nevada, and Inyo County, California: U.S. Geological Survey Scientific Investigations Map 2814, scale 1:100,000, text 54 p., 2 plates, https://doi.org/10.3133/sim2814.

Pavlis, T.L., Guest, B., Golding-Luckow, H., Serpa, L., and Wagner, D., 2012, Geologic map of the Wingate Wash area, Death Valley National Park, California and Nevada: Geological Society of America Digital Map, 1:25,000 scale, accessed 3/16/2018 at https://www.geosociety.org/maps/2012-DMCH011/.

Pavlis, T.L., Rutkofske, J., Guerrero, F., and Serpa, L.F., 2014, Structural overprinting of Mesozoic thrust systems in eastern California and its importance to reconstruction of Neogene extension in the southern Basin and Range: Geosphere, v. 10, no. 4, p. 732–756, https://doi.org/10.1130/GES00993.1.

Pavlis, T.L., Serpa, L., Troxel, B., Dean, M., Hartman, T., and Rodesta, T., 1998, Late Cenozoic deformation in eastern Fort Irwin and its significance for the tectonic history of the Garlock

Fault system, *in* Calzia, J.P., and Reynolds, R.E. eds., Finding faults in the Mojave: 1998 Mojave Desert Quaternary Research Center Field Trip Guide and Volume, San Bernardino County Museum Association Quarterly, v. 45, no. 2, p. 77–83.

Pavlis, T.L., and Trullenque, G., 2021, Evidence for 40–41 km of dextral slip on the southern Death Valley fault—Implications for the eastern California shear zone and extensional tectonics: Geology, v. 49, p. 767–772, https://doi.org/10.1130/G48528.1.

Reheis, M.C., Hardin, J.W., McFadden, L.D., and Shroba, R.R., 1989, Development rates of late Quaternary soils, Silver Lake playa, California: Soil Science Society of America Journal, v. 53, no. 4, p. 1127–1140, https://doi.org/10.2136/sssaj1989.03615995005300040024x.

Reynolds, R.E., 1991, The Shoshone Zoo—A Rancholabrean assemblage from Tecopa, *in* Reynolds, R.E., ed., Crossing the borders—Quaternary studies in eastern California and southwestern Nevada: San Bernardino County Museum Association, Special Publication, p. 159–162.

Ries, K.G, III, Newson, J.K., Smith, M.J., Guthrie, J.D. Steeves, P.A., Haluska, T.L., Kolb, K.R., Thompson, R.F., Santoro, R.D., and Vraga, H.W., 2017, Streamstats, version 4: U.S. Geological Survey Fact 2017-3046, 4 p., https://doi.org/10.3133/fs20173046.

Sarna-Wojcicki, A.M., Bowerman, H.R., Meyer, C.E., Russell, P.C., Woodward, M.J, McCoy, G., Rowe, J.J., Baedeker, P.A., Asaro, F., and Michael, H., 1984, Chemical analyses, correlations, and ages of Upper Pliocene and Pleistocene ash layers of east-central and southern California: U.S. Geological Survey Professional Paper 1293, p. 1–40, https://doi.org/10.3133/pp1293.

Scheirer, D.S., Sweetkind, D.S., and Miller, J.J., 2010, Multiple phases of basin formation along the State Line Fault system in the Pahrump and Mesquite Valleys, Nevada and California: Geosphere, v. 6, no. 2, p. 93–129, https://doi.org/10.1130/GES00520.1.

Schermer, E.R., Luyendyk, B.P., and Cisowski, S., 1996, Late Cenozoic structure and tectonics of the northern Mojave Desert: Tectonics, v. 15, no. 5, p. 905–932, https://doi.org/10.1029/96TC00131.

Schmidt, K.M., and McMackin, M., 2006, Preliminary surficial geologic map of the Mesquite Lake 30’ x 60’ quadrangle, California and Nevada: U.S. Geological Survey Open-File Report 2006–1035, scale 1:100,000, pamphlet 89 p, https://doi.org/10.3133/ofr20061035.

Schmidt, K.M., and Menges, C.M., 2007, Debris-flow deposits and watershed erosion rates from the Kingston Range, California, *in* Miller, D.M., and Valin, Z.C., eds., Geomorphology and tectonics at the intersection of Silurian and Death Valleys, 2005 Guidebook, Pacific Cell, Friends of the Pleistocene: U.S. Geological Survey Open-File Report 2007–1424, p. 51–61, https://doi.org/10.3133/ofr20071424.

Serpa, L., deVoogs, B., Wright, L., Willemin, J., Oliver, J., Houser, E., and Troxel, B., 1988, Structure of the central Death Valley pull-apart basin and vicinity from COCORP seismic data: Geological Society of America Bulletin, v. 1900, no. 9, p 1437–1450, https://doi.org/10.1130/0016-7606(1988)100%3C1437:SOTCDV%3E2.3.CO;2.

Serpa, L., and Pavlis, T.L., 1996, Three-dimensional model of the late Cenozoic history of the Death Valley region, southeastern California: Tectonics, v. 15, no. 6, p. 1113–1128, https://doi.org/10.1029/96TC01633.

Slate, J.L., Berry, M.E., and Menges, C.M., 2009, Surficial geologic map of the Death Valley Junction 30’ x 60’ quadrangle, California and Nevada: U.S. Geological Survey Scientific Investigations Map 3013, scale 1:100,000, https://doi.org/10.3133/sim3013.

Slate, J.L., Berry, M.E., Rowley, P.D., Fridrich, C.J., Morgan, K.S., Workman, J.B., Young, O.D., Dixon, G.L., Williams, V.S., McKee, E.H., Ponce, D.A., Hildenbrand, T.G., Swadley, W.C., Lundstrom, S.C., Ekren, E.B., Warren, R.G., Cole, J.C., Fleck, R.J., Lanphere, M.A., Sawyer, D.A., Minor, S.A., Grunwald, D.J., Laczniak, R.J., Menges, C.M., Yount, J.C., and Jayko, A.S., 2000, Digital geologic map of the Nevada Test Site and vicinity, Nye, Lincoln, and Clark Counties, Nevada, and Inyo County, California: U.S. Geological Survey Open-File Report 99–554–A, scale 1:100,000, pamphlet 53 p, https://doi.org/10.3133/ofr99554A.

Smith, R.S.U., 2007, Dumont Dunes, *in* Miller, D.M., and Valin, Z.C., eds., Geomorphology and tectonics at the intersection of Silurian and Death Valleys, 2005 Guidebook, Pacific Cell, Friends of the Pleistocene: U.S. Geological Survey Open-File Report 2007–1424, p. 149–156, https://doi.org/10.3133/ofr20071424.

Sohn, M.F., Mahan, S.A., Knott, J.R., and Bowman, D.D., 2007, Luminescence ages for alluvial-fan deposits in southern Death Valley—Implications for climate-driven sedimentation along a tectonically active mountain front: Quaternary International, v. 166, p. 49–60, https://doi.org/10.1016/j.quaint.2007.01.002.

Spencer, J.E., 1981, Geology and geochronology of the Avawatz Mountains, San Bernardino County, California: Massachusetts Institute of Technology, Ph.D. dissertation, 183 p.

Spencer, J.E., 1990a, Geologic map of the southern Avawatz Mountains, northeastern Mohave Desert region, San Bernardino County, California: U.S. Geological Survey Miscellaneous Field Studies Map MF–2117, scale 1:24,000, https://doi.org/10.3133/mf2117.

Spencer, J.E., 1990b, Late Cenozoic extensional and compressional tectonism in the southern and western Avawatz Mountains, southeastern California, *in* Wernicke, B.P., ed., Basin and Range extensional tectonics near the latitude of Las Vegas, Nevada: Geological Society of America Memoir 176, p. 317–333.

Starkey, H.C., and Blackmon, P.D., 1979, Clay mineralogy of Pleistocene Lake Tecopa, Inyo County, California: U.S. Geological Survey Professional Paper 1061, 34 p, https://doi.org/10.3133/pp1061.

Stroud, J.R., and McGill, S.F., 1994, Late Quaternary activity on a thrust fault in the northeastern Avawatz Mountains, Mojave Desert, California: San Bernardino County Museum Association Quarterly, v. 41, no. 3, p. 30–31.

Thompson, R.A., Wright, L.A., Johnson, C.M., and Fleck, R.J., 1999, Temporal, spatial, and compositional constraints on extension-related volcanism in central Death Valley, California, *in* Slate, J.L., ed., Proceedings of conference on status of geologic research and mapping, Death Valley National Park: U.S. Geological Survey Open-File Report 99–153, p. 27–28, https://doi.org/10.3133/ofr99153.

Troxel, B.W., 1986a, ed., Guidebook, Quaternary tectonics of southern Death Valley: Friends of the Pleistocene Pacific Cell, privately published, 44 p.

Troxel, B.W., 1986b, Pleistocene and Holocene deformation on a segment of the Southern Death Valley Fault Zone, California, *in* Troxel, B.W., ed., Guidebook, Quaternary tectonics of southern Death Valley: Friends of the Pleistocene Pacific Cell, privately published, p. 13–16.

Troxel, B.W., and Butler, P.R., 1986a, Multiple Quaternary deformation, central part of the Confidence Hills, Death Valley, California—An example of folding along a strike-slip fault zone, *in* Troxel, B.W., ed., Guidebook, Quaternary tectonics of southern Death Valley: Friends of the Pleistocene Pacific Cell, privately published, p. 25–28.

Troxel, B.W., and Butler, P.R., 1986b, The relations between Quaternary faulting, volcanism, and fan development, southern Death Valley, California, *in* Troxel, B.W., ed., Guidebook, Quaternary tectonics of southern Death Valley: Friends of the Pleistocene Pacific Cell, privately published, p. 31–35.

Troxel, B.W., Sarna-Wojcicki, A. M., and Meyers, C.E., 1986, Ages, correlations, and sources of three ash beds in deformed Pleistocene beds, Confidence Hills, Death Valley, California, *in* Troxel, B.W., ed., Guidebook, Quaternary tectonics of southern Death Valley: Friends of the Pleistocene Pacific Cell, privately published, p. 29–30.

Wells, S.G., Brown, W.J., Enzel, Y., Anderson, R.Y., and McFadden, L.D., 2003, Late Quaternary geology and paleohydrology of pluvial Lake Mojave, southern California, *in* Enzel, Y., Wells, S.G., and Lancaster, N., eds., Paleoenvironments and paleohydrology of the Mojave and southern Great Basin Deserts: Boulder, Colorado, Geological Society of America Special Paper 368, p. 79–114.

Wells, S.G., McFadden, L.D., and Harden, J., 1990, Preliminary results of age estimations and regional correlations of Quaternary alluvial fans within the Mojave Desert of southern California, *in* Reynolds, R.E., Wells, S.G., and Brady, R.H., comps., At the end of the Mojave—Desert studies in the eastern Mojave Desert: Redlands, California, San Bernardino County Museum Association, p. 45–54.

Whistler, D.P., and Webb, S.D., 2000, Fossil vertebrates of the Plio/Pleistocene Tecopa Lake beds, Inyo County, California: San Bernardino County Museum Association Quarterly, v. 47, no. 2, p. 63–64.

Whitney, J.W., Taylor, E.M., and Wesling, J.R., 2004, Quaternary stratigraphy and mapping in the Yucca Mountain area, *in* Keefer, W.R., Whitney, J.W., and Taylor, E.M., eds., Quaternary paleoseismology and stratigraphy of the Yucca Mountain area: U.S. Geological Survey Professional Paper 1689, p. 11–21, https://doi.org/10.3133/pp1689.

Wills, C.J., 1989a, Death Valley Fault Zone, Inyo and San Bernardino Counties, California: California Division of Mines and Geology Fault Evaluation Report FER–204, 17 p.

Wills, C.J., 1989b, A neotectonic tour of the Death Valley Fault Zone, Inyo County, California: Geology, v. 42, no. 9, p. 195–200.

Woodbourne, M.O., and Whistler, D.P., 1991, The Tecopa Lake beds, *in* Reynolds, R.E., ed., Crossing the borders—Quaternary studies in eastern California and southwestern Nevada: San Bernardino County Museum Association Special Publication, p. 155–177.

Workman, J.B., Menges, C.M., Page, W.R., Ekren, E.B., Rowley, P.D., and Dixon, G.L., 2002a, Tectonic map of the Death Valley groundwater model area, Nevada and California: U.S. Geological Survey Miscellaneous Field Studies MF–2381–B, 1:250,000 scale, pamphlet 54 p, https://doi.org/10.3133/mf2381B.

Workman, J.B., Menges, C.M., Page, W.R., Taylor, E.M., Ekren, E.B., Rowley, P.D., Dixon, G.L., Thompson, R.A., and Wright, L.A., 2002b, Geologic map of the Death Valley ground-water model area, Nevada and California: U.S. Geological Survey Miscellaneous Field Studies MF–2381–A, 1:250,000 scale, 47 p, https://doi.org/10.3133/mf2381A.

Wright, L.A., 1954, Geology of the Alexander Hills area, Inyo and San Bernardino Counties, *in* Jahns, R.H., ed., Geology of southern California: California Division of Mines and Geology Bulletin 170, Map Sheet 17.

Wright, L.A., 1976a, Geologic map of the region of central and southern Death Valley, eastern California and southwestern Nevada, *in* Troxel, B.W., and Wright, L.A., eds., Geological features, Death Valley, California: California Division of Mines Special Report 106, p. 16.

Wright, L.A., 1976b, Fault map of the region of central and southern Death Valley, eastern California and southwestern Nevada, *in* Troxel, B.W., and Wright, L.A., eds., Geological features, Death Valley, California: California Division of Mines Special Report 106, p. 17.

Wright, L.A., and Troxel, B.W., 1954, Geologic guide to the western Mojave Desert and Death Valley regions, *in* Jahns, R.H., ed., Geology of southern California: California Division of Mines and Geology Bulletin 170, Geologic Guide I, 50 p.

Wright, L.A, and Troxel, B.W., 1967, Limitations on right-lateral strike-slip displacement, Death Valley and Furnace Creek Fault Zones, California: Geological Society of America Bulletin, v. 78, p. 933–949, https://doi.org/10.1130/0016-7606(1967)78[933:LORSDD]2.0.CO;2.

Wright, L.A., and Troxel, B.W., 1973, Shallow-fault interpretation of Basin and Range structure, *in* DeJong, K.A., and Scholten, Robert, eds., Gravity and tectonics: New York, John Wiley and Sons, p. 397–407.

Wright, L.A., and Troxel, B.W., 1984, Geology of the northern half of the Confidence Hills 15-minute quadrangle, Inyo County, California: California Division of Mines and Geology, Map Sheet 34, scale 1:24,000, 31 p.

Wright, L.A., and Troxel, B.W., eds., 1999, Cenozoic basins of the Death Valley region: Geological Society of America Special Paper 333, 381 p.

Yount, J.C., Schermer, E.R., Felger, T.J., Miller, D.M., and Stephens, K.A., 1994, Preliminary geologic map of Fort Irwin basin, north-central Mojave Desert, California: U.S. Geological Survey Open-File Report 94–173, 25 p, https://doi.org/10.3133/ofr94173.